NASA Contractor Report -172438

DESIGN, FABRICATION AND TEST OF COMPOSITE CURVED FRAMES FOR HELICOPTER FUSELAGE STRUCTURE

D.W. Lowry, N.E. Krebs and A.L. Dobyns

SIKORSKY AIRCRAFT
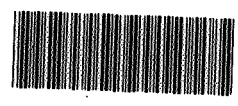DIVISION OF UNITED TECHNOLOGIES CORPORATION
Stratford, Conn.

NASA

National Aeronautics and
Space Administration

Langley Research Center
Hampton, Virginia 23665

LM101893E

DESIGN, FABRICATION AND TEST OF COMPOSITE CURVED FRAMES FOR HELICOPTER FUSELAGE STRUCTURE

By

D.W. Lowry, N.E. Krebs and A.L. Dobyns

October 1984

by

**SIKORSKY AIRCRAFT
DIVISION OF UNITED TECHNOLOGIES CORPORATION
Stratford, Connecticut**

for

NASA

National Aeronautics and
Space Administration

Langley Research Center
Hampton, Virginia 23665

1. Report No. NASA CR - 172438	2. Government Accession No.	3. Recipient's Catalog No.
4. Title and Subtitle Design, Fabrication and Test of Composite Curved Frames for Helicopter Fuselage Structure		5. Report Date October 1984
		6. Performing Organization Code
7. Author(s) D.W. Lowry, N. E. Krebs and A.L. Dobyns		8. Performing Organization Report No. SER-510145
		10. Work Unit No.
9. Performing Organization Name and Address Sikorsky Aircraft Div. United Technologies Corp. N. Main Street, Stratford, CT 06602		11. Contract or Grant No. NAS1-16B26
		13. Type of Report and Period Covered
12. Sponsoring Agency Name and Address National Aeronautics and Space Administration Washington D.C. 20546		14. Sponsoring Agency Code

15. Supplementary Notes

Langley technical monitor : Mr. Donald Baker

16. Abstract

This report discusses aspsects of curved beam effects and their importance in designing composite frame structures. The curved beam effect induces radial flange loadings which in turn causes flange curling. This curling increases the axial flange stresses and induces transverse bending. These effects are more important in composite structures due to their general inability to redistribute stresses by general yielding, such as in metal structures. A detailed finite element analysis was conducted and used in the design of composite curved frame specimens. Five specimens were statically tested and comparisons made of predicted and test strains. The study showed the curved frame effects must be accurately accounted for to avoid premature fracture; finite element methods can accurately predict most of the stresses and no elastic relief from curved beam effects occurred in the composite frames tested. Finite element studies are presented for comparative curved beam effects on composite and metal frames.

17. Key Words (Suggested by Author(s)) crushing peel curved beam radius curved frame transverse strain flange bending graphite epoxy	18. Distribution Statement Subject to category 24

19. Security Classif. (of this report) unclassified	20. Security Classif. (of this page) unclassified	21. No. of Pages 121	22. Price

FOREWORD

Page intentionally left blank

TABLE OF CONTENTS

LIST OF FIGURES

LIST OF FIGURES (Cont'd)

LIST OF FIGURES (Cont'd)

LIST OF TABLES

LIST OF SYMBOLS

A   Area of cross section, square inches

b   Flange free length, inches

$\bar{b}$ Average flange free length, inches

b'   Effective free flange length, inches

d   Beam depth, distance between midpoints of flanges, inches

E   Modulus of elasticity, msi

F   Allowable stresses, subscript indicates direction, ksi

G   Shear modulus, msi

P   Applied load, lb.

p   Induced radial (flange) load, lb./in.

r   Radius of curvature (distance) to mid-point of flange, subscript (o) for convex and (i) for concave side, inches

R   Radius of curvature (distance) to geometric axis, inches

t   Flange thickness, inches

w   Width of flange, inches

x   Axial stress direction

y   Distance from geometric axis for curved beam, from neutral axis for straight beam, inches

z   Beam section property non-dimensional

α Bleich's ratio of effective to actual free flange length, non-dimensional

LIST OF SYMBOLS (Cont'd)

β Ratio of maximum transverse to average axial flange stress, non-dimensional

ε Strain, in./in., or noted as micro-inches, μ in./in., subscript c for compressions, and t for tension

ν_{12} Poissons Ratio, major direction, non-dimensional

σ Applied stress, psi

σ_x Axial (circumferential) flange stress, psi

σ_y Flange bending stress; psi

DESIGN, FABRICATION AND TEST OF COMPOSITE CURVED FRAMES FOR HELICOPTER FUSELAGE STRUCTURES

By

D.W. Lowry

Sikorsky Aircraft
Division of United Technologies
Stratford, Connecticut

SUMMARY

This report discusses aspects of curved beam effects and their importance in designing composite frame structures. The curved beam effect induces radial flange loadings which in turn causes flange curling. This curling increases the axial flange stresses and induces transverse bending. These effects are more important in composite structures due to their general inability to redistribute stresses by general yielding, such as in metal structures. A detailed finite element analysis was conducted and used in the design of composite curved frame specimens. Five specimens were statically tested and comparisons made of predicted and test strains. The study showed the curved frame effects must be accurately accounted for to avoid premature fracture; finite element methods can accurately predict most of the stresses and no elastic relief from curved beam effects occurred in the composite frames tested. Finite element studies are presented for comparative curved beam effects on composite and metal frames.

1.0 INTRODUCTION

This application of advanced composite materials has been extended to helicopter airframe structures. These structures are generally of light gage construction which amplifies the importance of stability and stiffness effects in their design. A specific type affected are beams or frames, particularly the curved portion, where the stress field is more complex.

The curved frame study was initiated because of previous problems with premature fractures of curved composite airframe type structures. Under NASA Contract NAS1-16826 "Design, Fabrication and Test of Composite Curved Frames for Helicopter Fuselage Structure" Sikorsky Aircraft investigated specific problems involved with using advanced composite materials.

The work included reviewing curved beam effects, analysis and design of composite curved frames, fabrication and static test to fracture.

The study started with reviewing available analytical methods and effects on curved beams, particularly with thin flanges that would be representative of light gage helicopter airframe construction. This background was used to initially size curved frame structures for a detailed finite element (FE) analysis. Design loads for the curved portion of the frame, are those of a typical helicopter airframe. In this study seven different designs were investigated to assess the weight/cost of each design. The bead stiffened design was selected.

Thereafter the curved frame specimens were fabricated and static tested. Strain gage results are compared with FE analysis to evaluate curved beam effects and assess stress analysis capabilities. In this report an assessment is made using finite element studies to compare analytical methods and test data.

2.0 PRELIMINARY ANALYSIS AND DESIGN

2.1 Curved Beam Effects

Most metal aircraft beams and frames are analyzed without con-
sidering curvature effects, except where induced web crushing is
important. The effects of curvature in the flanges, which in-
crease axial stress and induces transverse flange bending, are
generally considered to be relieved due to material yielding. In
essence, the curvature effects may be considered as an early yield
load condition but do not affect the ultimate (static) strength of
the structure. However, it can be expected that the current
advanced composite materials, with their low strain capability,
will not provide such plastic relief and the curved beam effects
may be retained to fracture. It is important to understand the
effects of curvature and the parameters affecting the stresses for
composite structures in general.

The effects of curvature are illustrated in Figure 1a. For solid
beams there is a shift of the neutral axis and an increase of the
axial stress (σ_x) on the concave side. For a two flange beam,
representative of aircraft frames, the flange axial load is
approximately the applied moment divided by the distance between
flanges. The applied loading, as illustrated, induces radial
forces in the web (crushing in this case) and curling of flanges.
The flange curling increases the maximum axial stress and induces
transverse bending.

The methods of analysis for the basic effects of curvature are
well documented and result in using the Winkler-Bach formula:

$$\sigma_x = \frac{M}{AR} \left[1 + \frac{1}{Z} \frac{y}{R+y} \right]$$

The symbols are defined in the List of Symbols and Z is a property
of the area.

$$Z = -\frac{1}{A} \int \frac{y}{R+y} \, dA$$

3

The Z solutions have been tabulated in Reference 1 and the axial stresses can be calculated for various geometries. Tests have shown that there is an additional stress induced in thick flanges of I-beams due to rotation about their own neutral axis, (Reference 2). However, a more significant increase in stress in I-beams is due to the radial forces and depends on the flange flexibility parameter of b^2/tr.

For most aircraft beams and frames, the web contributes only a small bending resistance. Neglecting the web contribution, the average axial stress is:

$$\bar{\sigma}_x = \frac{M}{dwt}$$

and for very thin webs the flange free length is:

$$b \cong \frac{w}{2}$$

With thin flanges the curling effect distorts the cross section so that plane sections do not remain plane and the axial stress varies along the flange width.

Approximate solutions have been made for isotropic materials (Reference 1) and Bleich's solution was used. Bleich determined an effective half width as:

$$\alpha = \frac{b'}{b}$$

so that the ratio of the average to peak circumferential stress can be determined.

$$\bar{\sigma}_x b = \sigma_{x,MAX} b' \quad \text{and} \quad \frac{\sigma_{x,MAX}}{\bar{\sigma}_x} = \frac{1}{\alpha}$$

Correspondingly Bleich defined the maximum induced transverse bending to average axial stress ratio as:

$$\frac{\sigma_{y,MAX}}{\bar{\sigma}_x} = \beta$$

4

Values of α and β are available (Reference 1) as a function of the flange flexibility parameter b^2/tr. Thus, once the average flange stress is determined, the peak σ_x and σ_y can be calculated.

As stated, the Bleich analysis is approximate and for an isotropic material. It can be expected that curvature/flange flexibility effects will differ for a composite beam. However, the Bleich solution does offer a rapid assessment of the expected effects. A non-dimensional plot of the flange axial and bending stresses is presented in Figure 1b to be used as a guideline for curvature effects.

5
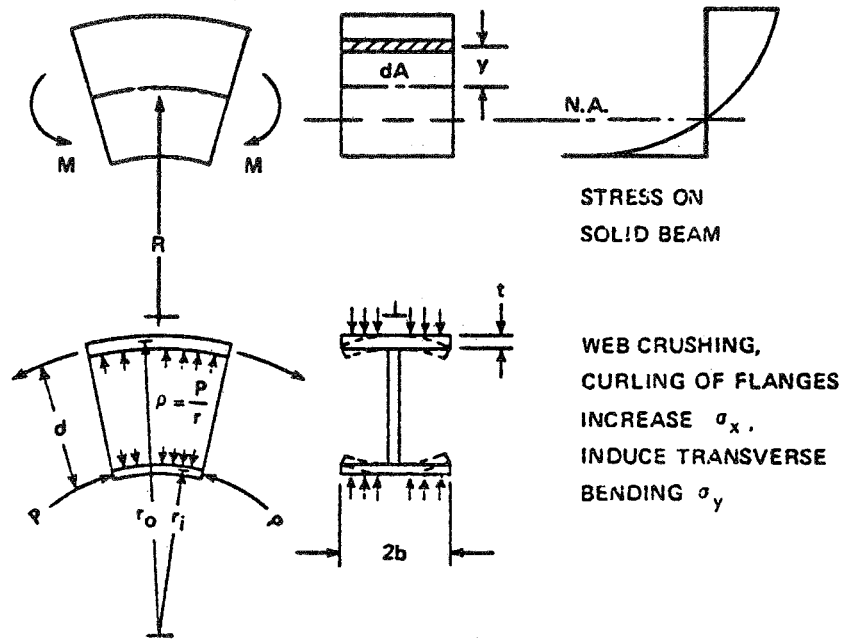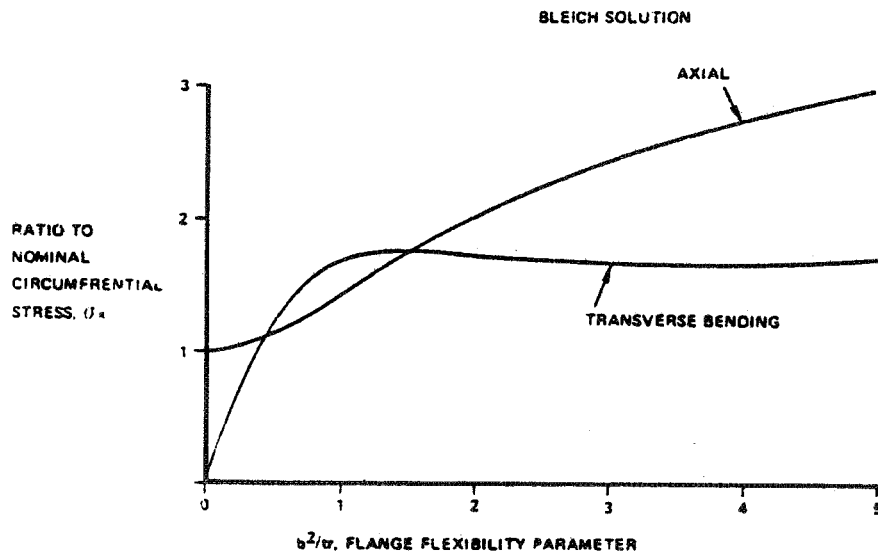
Figure 1A.

Figure 1B.

Figure 1. Curvature Effects and Increased Induced
Stress From Flange Flexibility

2.2 UH-60A Frame Station 379 Loads

Design loads for the composite curved frame were obtained from the BLACK HAWK loads analysis report, Reference 3. Crash condition 64 subcase 500 was determined to be the most severe loading in the upper curved portion of the frame at Sta. 379 (rear frame supporting the roof structures, Figure 2). The bending moment, axial load and shear distributions are presented in Figures 3, 4 and 5 respectively.

The most severe combination of loads affecting the inner cap (compression) are 7.23 kNm (64,000 in lb.) bending moment with an axial (compression) load of 53.8 kN (12,100 lb.) The shear at the peak bending moment is zero. The maximum shear is 36.0 kN (8,100 lbs.).

2.3 Composite Curved Frame Geometry and Design Loads

The configuration that best represents the most severe loading condition for stability/strength of the curved portion of the composite frame is illustrated in Figure 6. The criteria is to represent the combined compression load at the inner cap from the bending moment and axial load and also to retain two, constant 20 inch long, straight frame sections beyond the curved portion.

To satisfy the preceding criteria and assure fracture would occur in the curved portion, a preliminary load analysis resulted in a specific load offset, as shown in Figure 6.
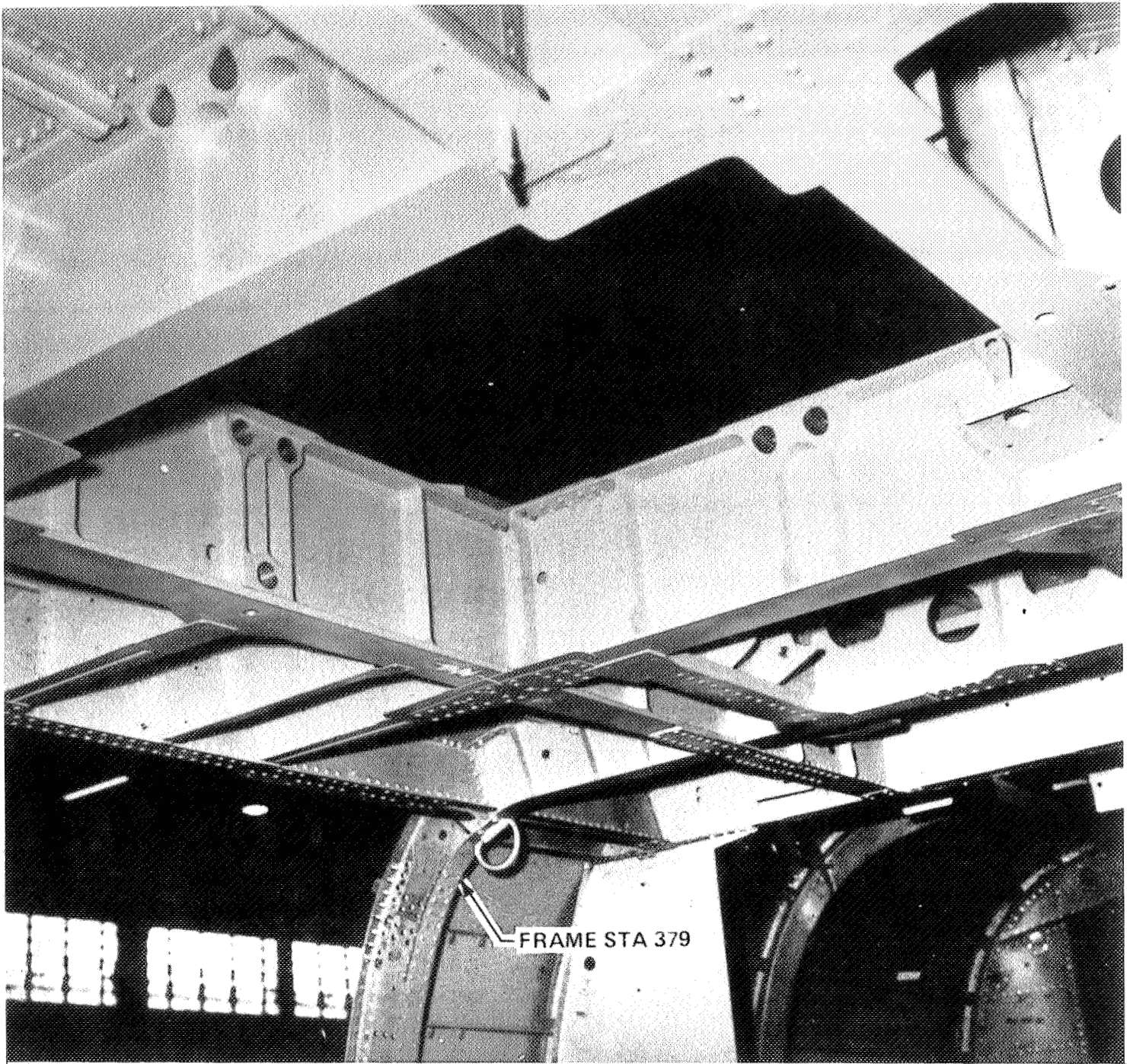
Figure 2. UH-60 Roof Structure and Frame Station 379

CBAR FINITE ELEMENTS

11.78 (104,280)

(42,670) 4.82

CRASH CONDITION
SUB—CASE 500

7.83 (69,360)

6.20 (54,900)

1.39 (12,370)

982

980   981

979   1055 1056 1057

978   1054

977   1053

1052   (-18,440) -2.08

CBAR ELEMENT NOS.

976   1051   (-55,510) -6.27

975   1050   (-64,000) -7.23

974   1049   (-46,000) -5.19

1048   (-31,780) -3.59

973   1047   (-11,630) -1.31

BENDING MOMENT DIAGRAM   kNm   (IN. - LB)
(+ B.M. CAUSES TENSION IN THE OUTER CAP)

POSITIVE BENDING IS PLOTTED OUTSIDE THE FRAME

Figure 3.   Bending Moment Diagram — UH—60A —
Frame Station 379

9

CBAR FINITE ELEMENTS

68.4
(15,400)

39.1
(8,800)

36.7
(8,240)

40.6
(9,130)

(11,900)
52.9

(8,550)
38.0

23.4
(5,260)

53.8
(12,100)

41.2
(9,270)

1056

1055

1054

1053

29.5
(6,630)

26.6
(5,980)

1052

1051

15.7
(3,520)

17.9
(4,020)

1050

CRASH CONDITION
SUB-CASE 500

(-230) 1.0

1049

(-640) 2.8

1048

(-1,800) 8.0
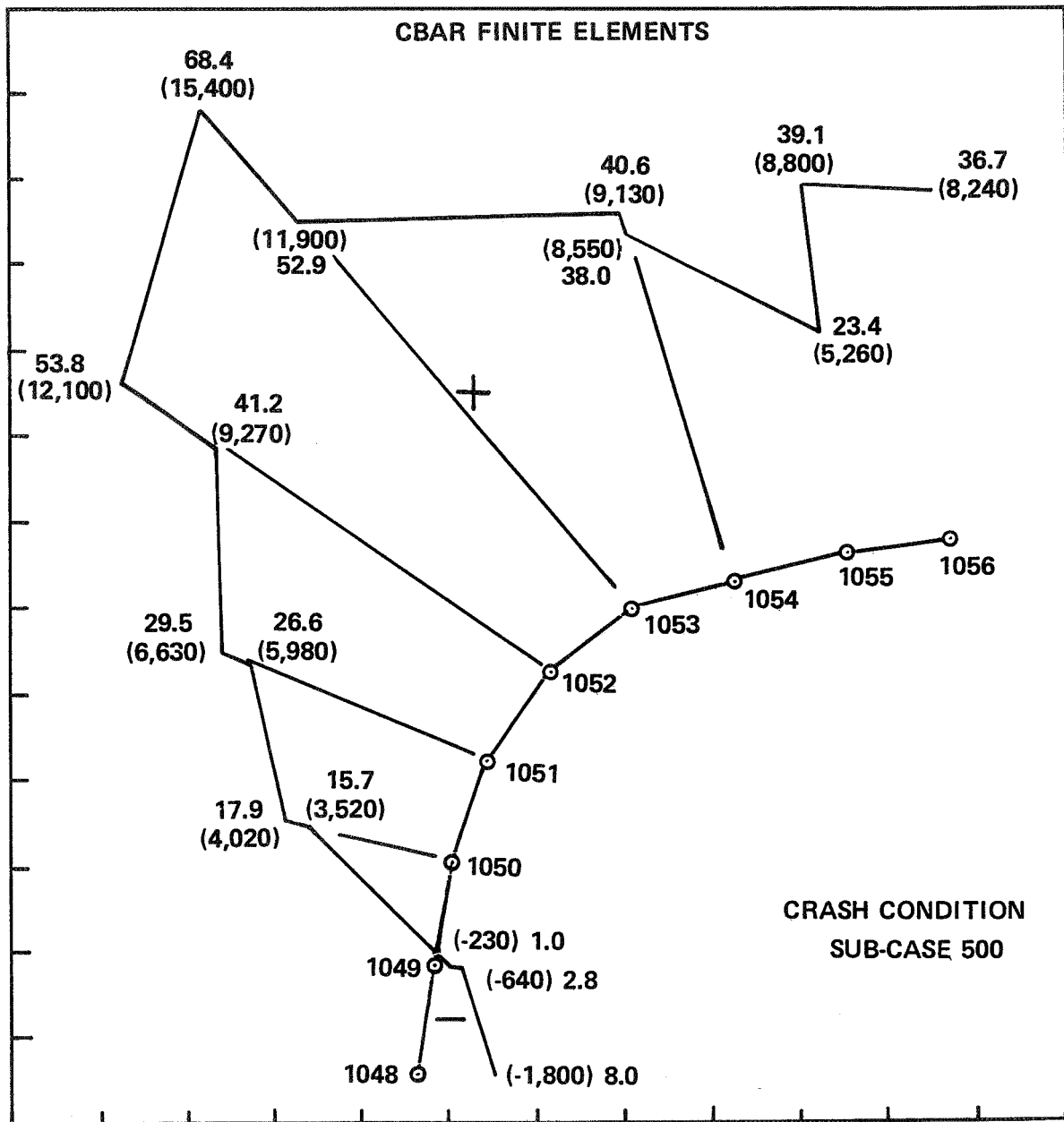
AXIAL LOAD DIAGRAM kN (LB)

(+ AXIAL LOAD PLOTTED ON OUTSIDE OF FRAME)

POSITIVE AXIAL LOAD CAUSES TENSION ON CBAR CROSS-SECTION

Figure 4. Axial Load Diagram - UH-60A -
Frame Station 379

10
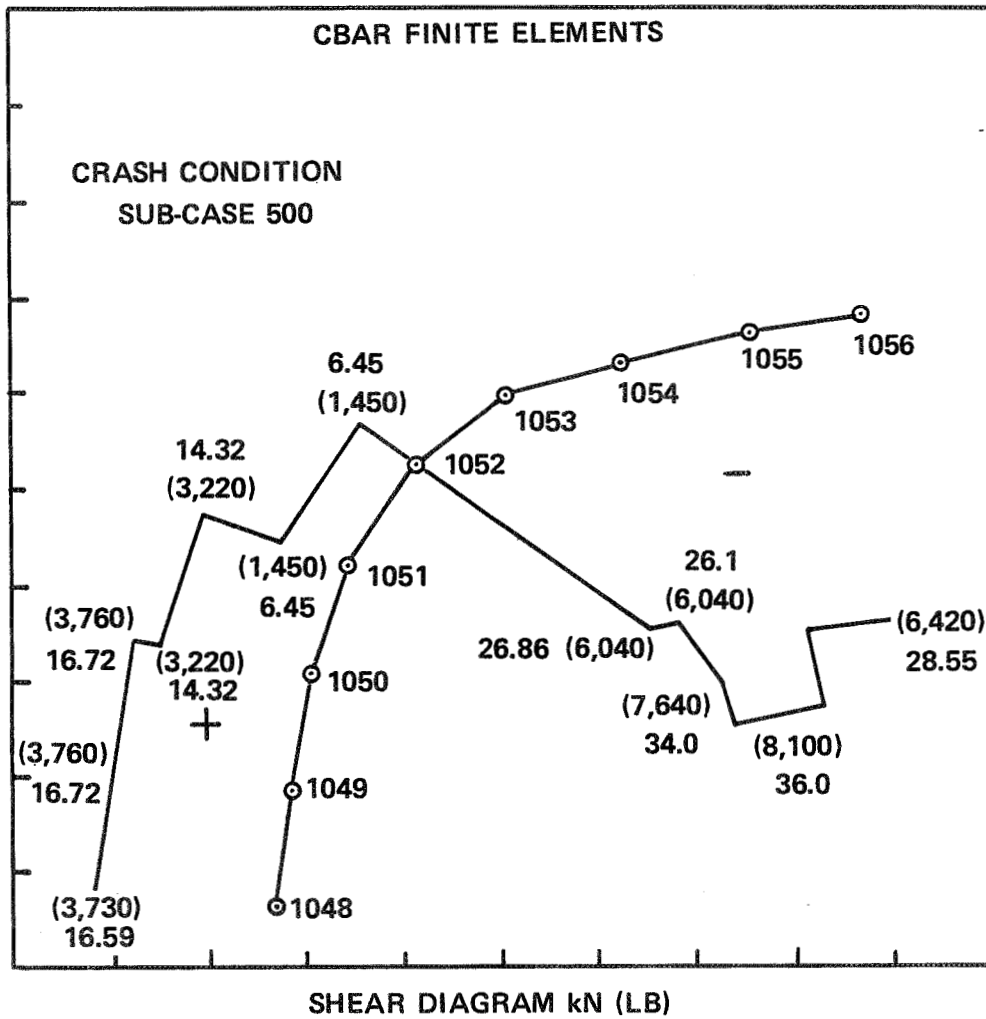
Figure 5. Shear Diagram — UH-60A — Frame Station 379

R = 20.3 CM
(8.0")

LOADING PAD

11.4cm
(4.5")

12.7cm
(5")

B   50.8cm
(20")

50.8cm
(20")

B

16cm
(6.30")

N.A.

60°

47.4 kN
(10,650 LB)

47.4kN
(10,650 LB)

16.1cm
(6.32")

B

OUTER CAP

A

B

LOADING FIXTURE

0° 10° 20°   30° 20° 10°   0°

A

12
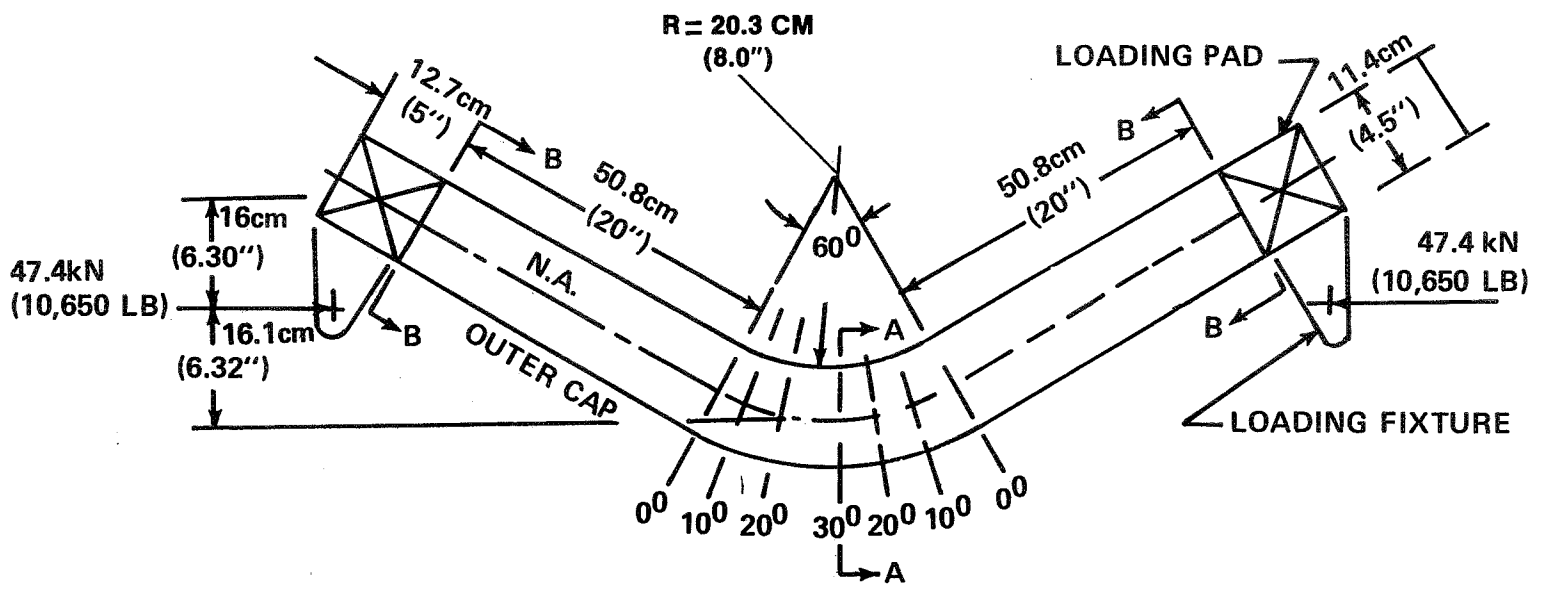
Figure 6.   Composite Curved Frame Geometry and Design Loads

AXIAL LOAD (LB) kN

30° 0° 30°

0   0

(COMPRESSION)

(9220) 41.01   (9220) 41.01

(10,650) 47.37

SHEAR (LB) kN

23.66 (5320)

(3640) 16.19

SIGN CONVENTION: POSITIVE SHEAR

+

−

(5320) 23.66
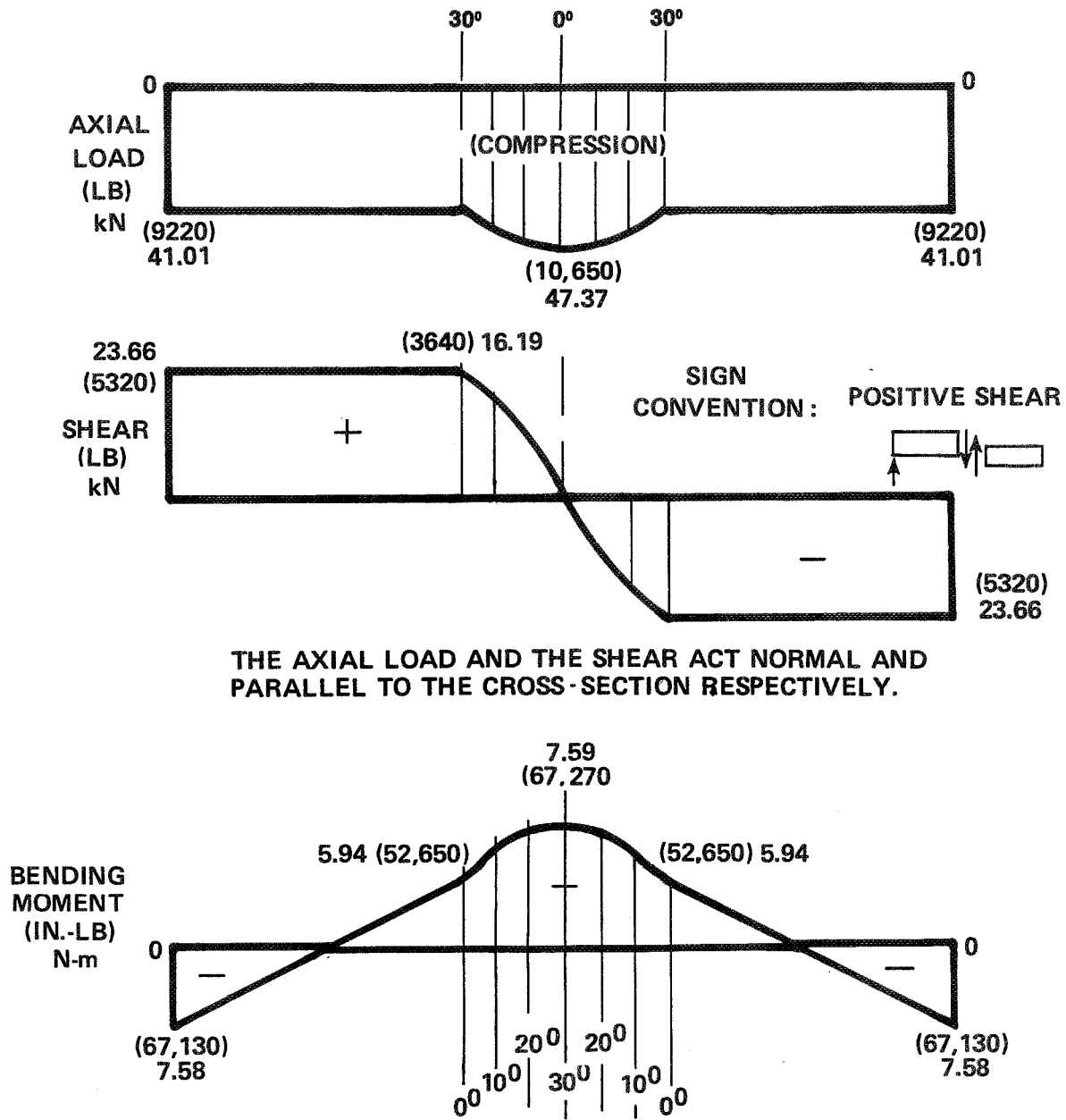
THE AXIAL LOAD AND THE SHEAR ACT NORMAL AND
PARALLEL TO THE CROSS-SECTION RESPECTIVELY.

BENDING MOMENT (IN.-LB) N-m

7.59 (67,270)

5.94 (52,650)   (52,650) 5.94

−

0   0

(67,130) 7.58   (67,130) 7.58

20° 20°
0° 10° 30° 10° 0°

(+ B.M. CAUSES
TENSION IN THE
OUTER CAP)

Figure 7.   Composite Curved Frame − Axial Load, Shear,
and Bending Moment Diagram

13

2.3.1 Loads Analysis of Composite Curved Frame

M_{max} = 7.23 kNm (64,000 in. lbf)   (Reference Figure 3) (Node 1051)

P (Axial Load) = 53.28 kN (12,100)   (Reference Figure 4) (Node 1052)

For the composite frame the centroidal distance (d) between frame caps is 11.43 cm (4.5 in.)

Maximum Compression Cap Load is then

$$P_i = \frac{M}{d} + \frac{P}{2}$$

$$= \frac{7.23}{11.43} + \frac{53.28}{2} = 89.9 \text{ kN (20210 lbf.)}$$

The test specimen, as illustrated in Figure 6, allows a simple end axial loading to obtain the maximum combined loads in the center of the curved section. A compromise was required to obtain the following:

    (a)   Maximum compression cap load.
    (b)   Maximum moment for web crushing.
    (c)   Maintain a constant twenty-inch section
            beyond the curved portion of the frame.
    (d)   Assure fracture will occur in the curved
            portion.

The solution resulted in a load offset (e) of 16.0 cm (6.3 in.). The results are as follows:

Load		Curved Portion (Section AA Figure 6)	Constant Section at Ends (Section B-B Figure 6)
P. Applied Design Test Load		47.37 kN (10,650 lbf.)	47.37 kN (10,650 lbf.)
Cap Axial Load	Inner	90.16 kN (20,270 lbf. Comp.)	32.69 kN (7350 lbf. Tens.)
	Outer	42.78 kN (9620 lbf. Tens.)	72.28 kN (16,250 lbf. Comp.)
Maximum Bending Moment (Ref. Figure 6)		7.59 kNm (67,270 in. lbf.)	6.08 kNm (53,820 in. lbf.)
Axial Load (Ref. Figure 6)		47.37 kN (10,650 lbf.)	41.01 kN (9220 lbf.)

Both caps are sized based on the 90.16 kN compression load. This assured fracture in the curved portion. The maximum moment in the curved portion (affecting web crushing) is within 5 percent of BLACK HAWK Design Loads. The "exact" cap peak compression load in the curved portion was obtained.

2.4 Material Properties

The material properties for unidirectional and woven graphite epoxy are contained in Table II of Reference 4. The room temperature dry (RTD) typical properties are used to determine the response of the test structure. The "B" properties at 125°F and 68% RH would be used in design for crash loads. The cured thickness per ply for these materials is 0.304 mm (0.012 in.) for unidirectional graphite-epoxy and 0.355 mm (0.014 in.) for woven graphite-epoxy.

2.5 Design Concepts

Seven design concepts were investigated in this study. The selected design was a bead stiffened web which was assessed as a best solution for near constant web shear strength and weight/cost projection.

15

The key features of the selected design, concept 1, are illustrated in Figure 8. The web is of woven graphite/epoxy and consists of two back-to-back channels, each have three plies of woven material oriented at 45 degrees. The web is also beaded and 0, 0/90 plies are used to increase the radial crush strength and stability. The 0 degree plies are of graphite/epoxy tape. The frame caps (flanges) are also graphite/epoxy using tape and woven material. The flange ply layup is shown in Figure 8. The initial design, 8A, was the result of using preliminary analysis methods. The finite element analysis (Section 4.0) indicated higher stresses from flange transverse bending (curling). This curling is the distortion of the flange from the induced radial loads and results in increased axial stresses and transverse bending stresses. The design was modified to that shown in Figure 8B and used for specimen fabrication. As a result of the tests, (Section 5.0), additional reinforcements were added to the flange web intersection as shown in Figure 8C.

Concept 2 (Figure 9)

Channels laid up by slitting or darting flanges to allow for stretch or overlap. Reinforcing channels laid up over silicon rubber blocks and inserted into beam channel. Unigraphite rolled and molded into fillets.

Silicon Rubber blocks will apply bagging pressure to channels and beam.

Concept 3 (Figure 9)

Channel laid up from each side from 45° woven material. Butts staggered at center of bend. Doubler plys of 0/90 woven material staggered on bend. Doubler strips of Unigraphite added at center of bend to take compression.

Concept 4 (Figure 9)

Channels laid up from 45° woven material with darts in webs at 15° intervals. Darts staggered for each ply of web. Two 0/90 doublers added, one 60° wide over whole curved section, the other 30° wide in center. Two 90° Unigraphite doublers at center.

Concept 5 (Figure 10)

The channels are formed continuously with woven graphite/epoxy materials with a ±45 degree orientation. The web is split radially and overlapped to provide structural continuity around the

curve. Radial stiffeners of unidirectional strips are laid over the lapped web areas. The channels in the curved section of the frame, are bonded to a structural foam sheet (density of 70.9 kg/m³, 4.4 lbs/ft³). Thus the web becomes a sandwich structure to provide additional stability.

Concept 6 (Figure 10)

The channels are formed in segments with woven graphite/epoxy materials with a ±45 degree orientation. The segments are over-lapped and staggered to provide the structural continuity. Structural foam strips are placed under the overlap regions. Unidirectional strips are placed on the outsides of the overlap regions to provide additional reinforcement as radial stiffeners.

Concept 7 (Figure 10)

Unidirectional tape is wound over a mandrel. The direction of winding, as illustrated in Figure 10, concept 7, provides the orientations for an equivalent ±45°/90° layup. The resulting closed section is then cut along the centerline to form two channels. The channels are subsequently bonded back to back to form an I-section frame. The procedure is also adaptable for filament winding.
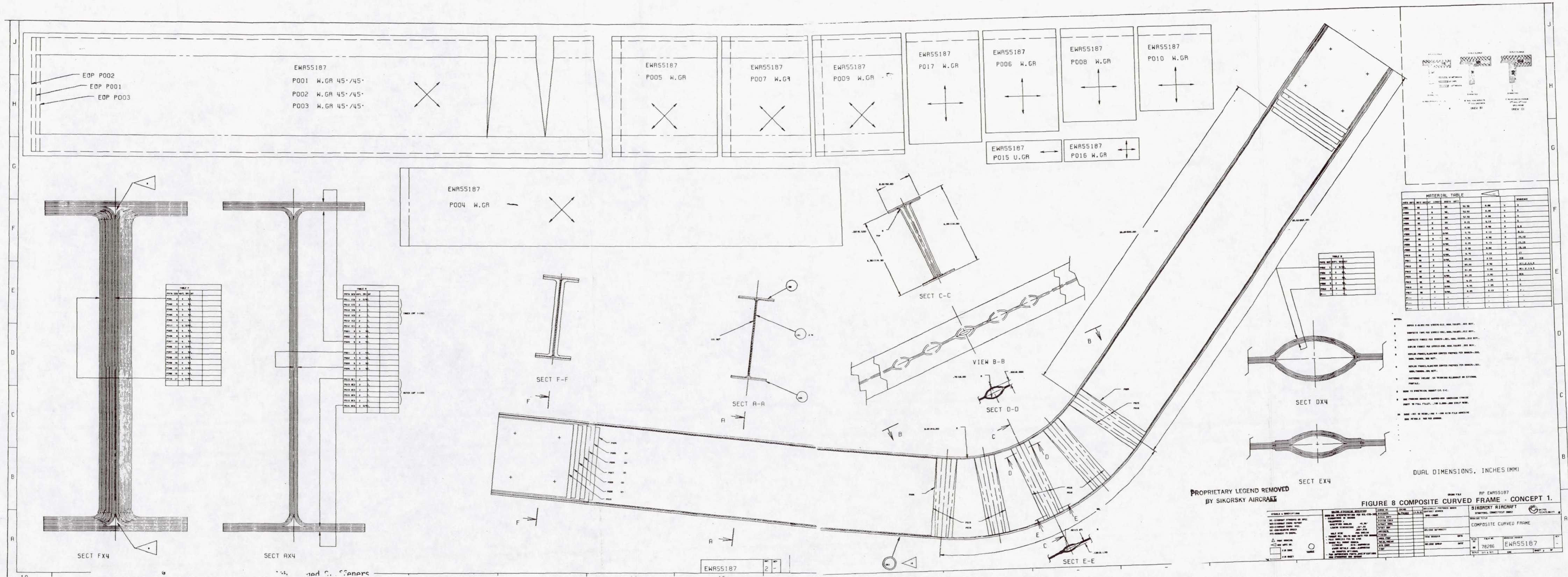
Figure 8.   Composite Curved Frame - Concept 1

19

Page intentionally left blank

SECTION G-G

1PLT W.GR, 2PLT U.GR
3PLT W.GR 45°
1PLT W.GR, 2PLT U.GR

STRAIGHT PORTION OF BEAM
4PLY 45° W.GR TIPICAL EACH SIDE.

2PLY 0/90° W.GR STIFFENER
COCURED WITH CHANNELS

BUTTJOINTS OF CHANNEL PLIES

3PLT 45° W.GR CHANNEL
EACH SIDE

SECTION H-H

SECTION H-H

FRAME CONCEPT 2

SECTION J-J

1PLT W.GR, 2PLT U.GR
3PLT W.GR 45°
1PLT W.GR, 2PLT U.GR

1PLY 90° U.GR STIFFENER

STRAIGHT PORTION OF BEAM
4PLY 45° W.GR TIPICAL EACH SIDE.

1PLY 0/90° W.GR DOUBLER

45°

45°

BUTTJOINTS OF CHANNEL PLIES
CHANNELS 3PLT W.GR 45°

SECTION K-K
(PLT THICKNESS SHOWN X2 SCALE
IN THIS SECTION FOR CLARITY.)

FRAME CONCEPT 3

EWR55187 3 -

SECTION L-L

1PLT W.GR 0/90°, 2PLT U.GR
3PLT W.GR 45°
2PLY 0/90° W.GR
2PL U.GR, 1PLY 0/90° W.GR

1PLY 90° U.GR STIFFENER

STRAIGHT PORTION OF BEAM
4PLY 45° W.GR TIPICAL EACH SIDE.

WEB AND INNER FLANGE OF
CHANNELS DARTED IN X PLACES
DARTING STAGGERED FOR EACH PLY.
CHANNELS 3PLT W.GR 45°

1PLY 0/90° W.GR DOUBLER

SECTION M-M
(PLT THICKNESS SHOWN X2 SCALE
IN THIS SECTION FOR CLARITY.)

FRAME CONCEPT 4

FIGURE 9 COMPOSITE
CURVED FRAMES
CONCEPTS 2,3, AND 4

CRIOS FILE RF EWR55187-4

SIKORSKY AIRCRAFT

COMPOSITE CURVED FRAME

NAS1-16826

78286 EWR55187

Figure 9. Composite Curved Frame Concepts 2, 3, and 4

21

Page intentionally left blank

SECTION N-N

SECTION U-U

1PLY W.GR 0/90°, 2PL U.GR
3PLY W.GR 45°
2L U.GR,1PLY W.GR 0/90°

STRAIGHT PORTION OF BEAM CHANNELS
4PLY W.GR 45° EACH SIDE TYPICAL.

1PLY 90° U.GR DOUBLER

WEB AND INNER FLANGE OF
FLAT PATTERN SLIT RADIALY
AND ALLOWED TO OVERLAP,
SLIT STAGGERED IN EACH PLY.

CHANNEL WEB AND FLANGES
3PLY 45° W.GR EACH SIDE

HIGH TEMP. STRUCTURAL FOAM

SECTION P-P
(PLY THICKNESS SHOWN X2 SCALE
IN THIS SECTION FOR CLARITY.)

FRAME CONCEPT 5

SECTION Q-Q

SECTION V-V

1PLT W.GR 0/90°, 2PL U.GR
3PLY W.GR 45°
2L U.GR,1PLT W.GR 0/90°

STIFFENERS LAID UP ON .125 THICK
HIGH TEMPERATURE STRUCTURAL FOAM.

STRAIGHT PORTION OF BEAM CHANNELS
4PLY W.GR 45° EACH SIDE TYPICAL.

1PLT 90° U.GR DOUBLER

WEB FLAT PATTERNS CUT INTO
SHORT SECTIONS AND OVERLAPPED
IN STAGGERED FORM AS SHOWN.

CHANNEL WEB AND FLANGES
3PLT 45° W.GR EACH SIDE

SECTION R-R
(PLY THICKNESS SHOWN X2 SCALE
IN THIS SECTION FOR CLARITY.)

FRAME CONCEPT 6

SECTION S-S

1PLY W.GR, 2PLY U.GR
TYPICAL

2PLY U.GR, 1PLY W.GR
TYPICAL

EXTENT OF 90° STIFFENER TAPES
TYPICAL

CHANNELS LAID UP FROM
U.GR TAPE 6 PLIES AS
SHOWN. LAYUP WOULD BE
REVERSED IF A MALE MANDREL
IS USED.

SECTION T-T

FRAME CONCEPT 7

LAYUP 1,4 & 8

LAYUP 2,5 & 7

LAYUP 3,6 & 9

45°

39°

FIGURE 10 COMPOSITE
CURVED FRAMES
CONCEPTS 5,6, AND 7

CAIDS FILE RF EWR55187-4

SIKORSKY AIRCRAFT

COMPOSITE CURVED FRAME

NAS1-16828

EWR55187

EWR55187

Figure 10.   Composite Curved Frame Concepts 5, 6, and 7

23

Page intentionally left blank

2.6 Preliminary Analysis (Calculated in the U.S. System of Units)

2.6.1 Load Introduction Section - Reinforced Ends - All Concepts
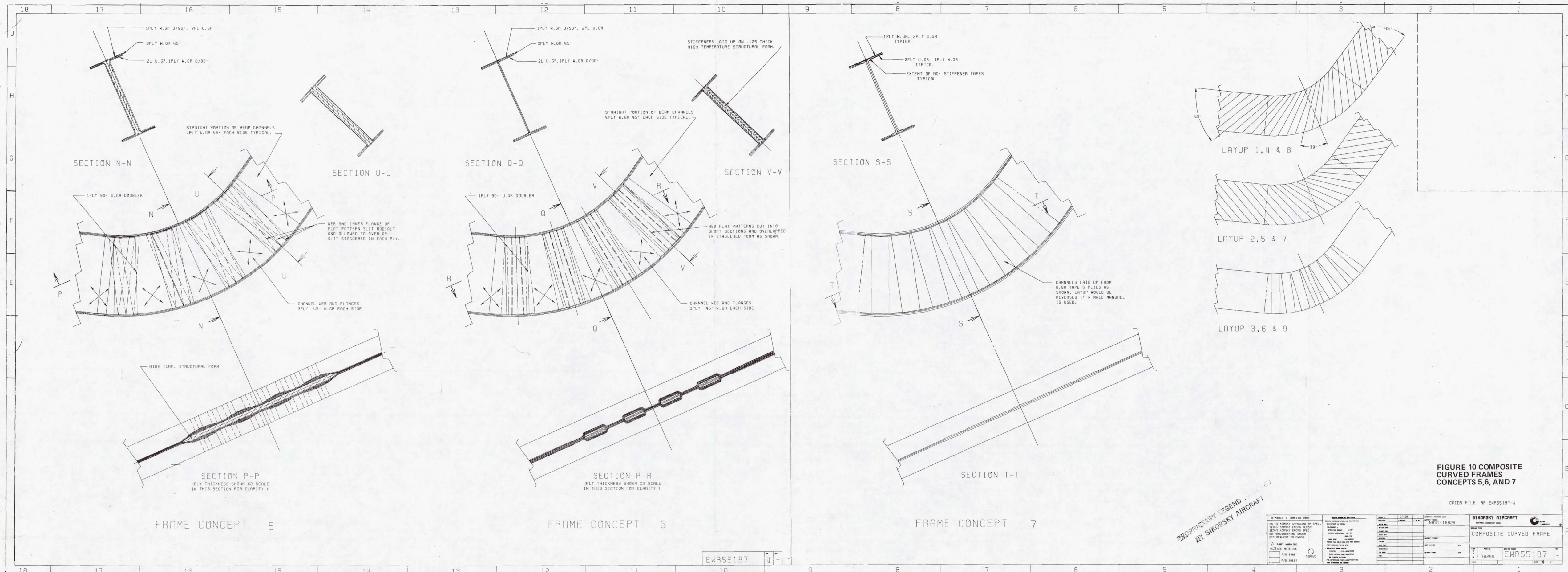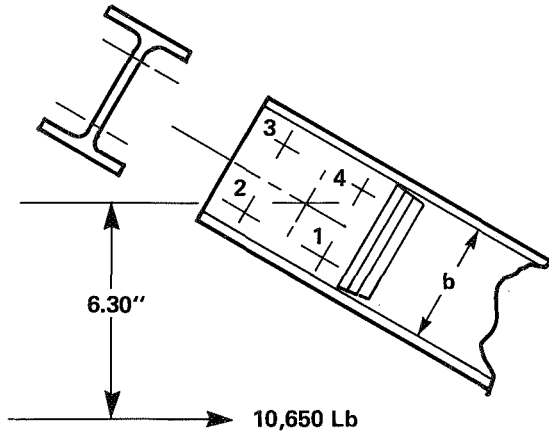

Maximum Load, Applied to Bolt No. 1, is 54176 N(12180 lb.)

For a 5/8" lockbolt, single shear allowable is 29150 lb. (Ref.5)

double shear is 2 x 29150 = 58300 lb.

F.S. = 58300/12180 = 4.8

Bearing web (32 ply total) 56% ± 45° and 44% 0°/90°

$$F_{bru} = 12180/(5/8)(32 \times .012) = 50,750 \text{ p.s.i.}$$

A bearing allowable, F_{bru}, is based on the data of Figure 20 pg 50 of "The Strength of Bolted Joints in Multi-Directional CFRP Laminates" Composites, January 1977 (Ref. (6)) and Table II of NASA-CR-159384 (Ref. (4)).

From Ref. (4) $\bar{F}_{cu}$ = 200000 p.s.i.

From Ref. (6) $\bar{F}_{cu}$ = 233000 p.s.i.

F_{cuA} = 156000 p.s.i.

Assuming 100% ± 45° graphite as the worst case, $\bar{F}_{BU}$ = 120000 p.s.i. (Ref. (4))

For design, a strength factor is used.

$$\text{Strength Factor} = \frac{\bar{F}_{cu} \text{ (Ref. (6))}}{F_{cu} \text{ (Ref. (4))}} = \frac{233000}{200000} = 1.165$$

The design bearing allowable is:

$$F_{BRU\ Design} = F_{BU} \times \text{Strength Factor} \times \frac{F_{CU_A}}{F_{CU}}\ \text{(Ref. 4)}$$

$$= 120000 \times 1.165 \times 156000/233000 = 93,600\ \text{psi}.$$

M.S. = (93600/50750)-1 = 0.84 which is acceptable for preliminary design.

Frame Caps - All sections - inner and outer - all concepts.

P_C = 20,270 lb. (Ref. Page 15).

F_{cu} = 163,000 psi (Ref. 4 Table II, AS/6350 Graphite/
Epoxy Tape, "B" values for crash
condition).

Cap area required = 20270/163,000 = 0.124 in²
Cap width = 2 inches
Number of 12 mil plies = 0.124/2 x .012 = 5.2 use of 6 plies,
0° tape.

Shear Web - 20 inch straight sections - all concepts

Web thickness, t = .096 inches (8 ply ± 45° G/E Fabric)

F_{su} = 36000 psi

E = 2.1 x 10^6 psi   Ref. (4) Table II

G_{12} = 4.8 x 10^6 psi

ν_{12} = 0.77

Web allowable shear buckling load,

$$N_{xy_{cr.all.}} = (2/b)^2 \sqrt{D_{22}\ (D_{12} + 2D_{66})}\,(11.7 + .5320 + .9380^2)$$

Ref. (7) equation 2.2.2-22 <u>Air Force Advance Composite Design Guide</u>, <u>Vol. II</u>, <u>Analysis</u>, January 1973.

$$\theta_{11} = D_{11} D_{22}/D_{12} + 2D_{66}$$

$$D_{11} = D_{22} = Et^3/12[1-v_{12}^2] = 380.3 \text{ lb. in.}$$

$$D_{12} = v_{12} D_{22} = 292.4 \text{ lb. in.}$$

$$D_{66} = Gt^3/12 = 353.9 \text{ lb. in.}$$

$$\theta = 0.38 \qquad b = 4.5 \text{ in.}$$

$$N_{xycr.all.} = 1470 \text{ lb./in.}$$

$$N_{xyapplied} = V/d = 5320*/4.5 = 1182 \text{ lb./in. (*Ref. Fig. 6)}$$

$$F_s = N_{xy \text{ applied}}/t = 1182/.096 = 12,310 \text{ psi}$$

CONCEPT 1 BEADED WEB

For the web in the beaded curved section,

b = 1.45 in. which is the average flat distance bead to bead.

Then the allowable shear buckling load is:

$$N_{xycr \text{ all.}} = 1470/(1.45/4.5)^2 = 14160 \text{ lb./in.}$$

The web pattern is cut as shown in Figure 7 to provide approximately ±45° web material in the curve.

Beads - Curved Section

Five beads are molded into each half of the web in the curved section to form five elliptical cross section stiffeners as shown in Figure 7. The stiffener at the center of the curved section is sized based on the crushing loads caused by bending the curved frame.

The bending moment M = 67,270 in. lb. (Ref. Figure 6)
Axial Load (comp.) P_c = 10,650 lb. (Ref. Figure 6)

The crushing load from the caps is;

q_{out} = M/hRo-Pc/2Ro where Ro = Radius of outer cap = 12.5 in.

$$q_{out} = \frac{67270}{(4.5)(12.5)} - \frac{10650}{2(12.5)} = 770 \text{ lb./in.}$$

q_{in} = M/hRi + Pc/2Ri where Ri = radius of inner cap = 8 in.

$$q_{in} = \frac{67270}{(4.5)(8)} + \frac{10650}{2 \ (8)} = 2530 \text{ lb./in.}$$

The center stiffener is sized for a maximum crushing load of:

P_{crush} = 2530(2.0)* = 5060 lb.

*Distance between stiffener center lines at inner cap.

The stiffener cross section was sized to prevent column buckling, local buckling (crippling) and material fracture. Each bead, making the stiffener, is 4 ply ± 45° fabric, 1 ply 0°/90° fabric and 1 ply 0° tape, cap to cap (see Figure 7).

The compression stress for the stiffener is:

$$f_{ci} = \frac{PcrushEi}{\Sigma AiEi}$$

Where $\Sigma AiEi$ = .896 x 10^6 lb.

$$f_{c(45)} = \frac{5060 \ (2.1 \times 10^6)}{.896 \times 10^6} = 11,860 \text{ psi}$$
$$(F_{cu} = 19,000 \text{ psi})$$

$$f_c(o) = \frac{5060 \ (17.6 \times 10^6)}{.896 \times 10^6} = 99,390 \text{ psi}$$
$$(F_{cu} = 163,000 \text{ psi})$$

$$f_c(0/90) = \frac{5060 \ (10.0 \times 10^6)}{.896 \times 10^6} = 56,470 \text{ psi}$$
$$(F_{cu} = 56,000 \text{ psi})$$

Column buckling and local buckling allowables are very large.

A similar preliminary analysis was conducted for the webs in the curved section of concepts 2, 3, 4, 5, 6, and 7. Each web or stiffener was checked for shear buckling, compression fracture, column buckling and local buckling.

The weight of each curved section concept and the straight section with loading pads was calculated based on the preliminary structural analysis.

2.7 WEIGHT AND COST ANALYSIS

2.7.1 The weight of each curved section studied are summarized in Table I. A detailed weight analysis of each curved concept is presented on the following pages of this section.

TABLE I

Summary of Composite Curved Frame Concept Weights

Concept	Description	Weight*	
		Grams	(lbs)
1	Beaded Stiffeners	348.7	(.769)
2	Radial Stiffeners	397.6	(.876)
3	Thick Web (Butted Web)	366.8	(.808)
4	Thick Web (Darted)	366.8	(.808)
5	Sandwich Foam	365.4	(.805)
6	Foam Stiffeners	348.1	(.767)
7	Filament Wound	316.0	(.696)

*Only the weights of the curved section of the frames are considered.

Weight of Components for Curved Frame Concepts
(Calculated in the U.S. System of Units)

	Weight (lbs)	Grams
CONCEPT 1 (Beaded Stiffeners)		

CHANNEL WEBS
     3 ply woven graphite/epoxy
         48.2 x 3 x .014 x .055 x 2   = (.223)   101.1

CHANNEL FLANGES
     3 ply woven graphite/epoxy
         21.5 x .94 x 3 x .014 x .055 x 2   = (.093)   42.2

INNER AND OUTER CAPS IN CHANNEL FLANGES
     2 ply unidirectional graphite epoxy
     1 ply woven
         21.5 x 3.9 x .038 x .055   = (.175)   79.4

STIFFENER DOUBLER
     1 ply unidirectional graphite/epoxy
     1 ply woven
         4.5 x 1.25 x 10 x .026 x .055   = (.080)   36.3

ADHESIVE
     .03 lbs./ft.^{2}
         48.3 + 21.5 x 21 x .03/144   = (.019)   8.6

INNER AND OUTER CAPS (BONDED TO CHANNEL
FLANGES)
         21.5 x 2 x 2 x .038 x .055   = (.179)   81.5

CURVED SECTION TOTAL WEIGHT   (.769)   348.7

CONCEPT 2 (Radial Stiffeners)

CHANNEL WEBS
     Same as Concept 1   = (.223)   101.1

CHANNEL FLANGES
     Same as Concept 1   = (.093)   42.2

INNER AND OUTER CAPS IN CHANNEL FLANGES
     Same as Concept 1   = (.175)   79.4

STIFFENER WEBS
     2 ply woven graphite/epoxy
         48.3 x .028 x .055   = (.074)   33.6

	Weight	
CONCEPT 2 (Radial Stiffeners Continued)	(lbs)	Grams

CONCEPT 2 (Radial Stiffeners Continued)

    STIFFENER FLANGES
       2 ply woven graphite/epoxy
          21.5 + 27 x .9 x .028 x .055   = (.067)   30.4

    STIFFENER ANGLES
       2 ply woven graphite/epoxy
          1.65 x 4.5 x 4 x .028 x .055   = (.046)   20.8

    ADHESIVE
       Same as Concept 1   = (.019)   8.6

    INNER AND OUTER CAPS (BONDED TO CHANNEL)
    FLANGES)
       Same as Concept 1   = (.179)   81.5

CURVED SECTION TOTAL WEIGHT   (.876)   397.6

CONCEPT 3 (Thick Web Butted Web)

    CHANNEL WEBS
       Same as Concept 1   = (.223)   101.1

    CHANNEL FLANGES
       Same as Concept 1   = (.093)   42.2

    INNER AND OUTER CAPS IN CHANNEL FLANGES
       Same as Concept 1   = (.175)   79.4

    DOUBLERS
       3 ply woven graphite/epoxy
          48.3 x 3 x .014 x .055   = (.112)   50.2

    CENTER DOUBLER
       2 ply unidirectional graphite/epoxy
          4.5 x 1.25 x 2 x .012 x .055   = (.007)   3.4

    ADHESIVE
       Same as Concept 1   = (.019)   8.6

    INNER AND OUTER CAPS (BONDED TO CHANNEL
    FLANGE)
       Same as Concept 1   = (.179)   81.5

CURVED SECTION TOTAL WEIGHT   (.808)   366.8

	Weight	
	(lbs)	Grams

CONCEPT 5 (Sandwich Foam)

CHANNELS
  3 ply woven graphite/epoxy
  12.5 $x\pi/3$ x 6.14 x 3 x .014 x
  .055 x 2 .... = (.371) 168.2

INNER AND OUTER CAP
  2 ply unidirectional graphite/epoxy
  1 ply woven
  12.5 x 3.65 x .038 x .055 .... = (.164) 74.4

DOUBLERS
  2 ply unidirectional graphite/epoxy
  4.5 x 1.25 x 8 x .012 x .055 .... = (.030) 13.6

FOAM CORE
  48.3 x .25 x 4.4/1728 .... = (.031) 14.1

ADHESIVE
  48.3 x 2 x 21.5 x 2 x .03/144 .... = (.030) 13.6

INNER AND OUTER CAPS (BONDED TO CHANNEL
FLANGES)
  Same as Concept 1 .... = <u>(.179)</u> <u>81.5</u>

CURVED SECTION TOTAL WEIGHT   (.805) 365.4

CONCEPT 6 (Foam Stiffeners)

CHANNELS
  3 ply woven graphite/epoxy
  19.54 x 24 x .014 x .055 .... = (.361) 163.7

INNER AND OUTER CAPS
  Same as Concept 5 .... = (.164) 74.4

FOAM STIFFENERS
  4.5 x 1.25 x 25 x 4 x 4.4/1728 .... = (.014) 6.3

	Weight (lbs)	Grams
<u>CONCEPT 6 (Foam Stiffeners Continued)</u>		
STIFFENER DOUBLES Same as Concept 5	= (.030)	13.6
ADHESIVE Same as Concept 1	= (.019)	8.6
INNER AND OUTER CAP (BONDED TO CHANNEL FLANGES) Same as Concept 1	= <u>(.179)</u>	<u>81.5</u>
CURVED SECTION TOTAL WEIGHT	(.767)	348.1

<u>CONCEPT 7 (Filiment Wound)</u>

	Weight (lbs)	Grams

CHANNEL
    12.5 x /3 x 6.14 x 6 x .005 x
    .005 x 2
	= (.265)	120.2

STIFFENING 5 x 7 x 6 x .005 x .005	= (.058)	26.3
INNER AND OUTER CAP IN CHANNEL FLANGES Same as Concept 1	= (.175)	79.4
ADHESIVE Same as Concept 1	= (.019)	8.6
INNER AND OUTER CAPS (BONDED TO CHANNEL FLANGES) Same as Concept 1	= <u>(.179)</u>	<u>81.5</u>
CURVED SECTION TOTAL WEIGHT	(.696)	316.0

ESTIMATE WEIGHT OF COMPLETE COMPOSITE CURVED FRAME SPECIMEN

<u>20" Straight Sections</u>

```
CHANNEL WEBS
    4 Ply Woven graphite/epoxy
        4.8 x 20 x .014 x 4 x .055 x 2      = .590
                        Two Sections                        1.180

CHANNEL FLANGES
    3 Ply Woven graphite/epoxy
        20 x 2 x 1.0 x 3 x .014 x .055 x 2 = .188
                        Two Sections        .                .370

INNER AND OUTER CAPT IN CHANNEL FLANGES
    2 Uni, 1 Woven graphite/epoxy
        20 x 2 x .90 x 2 x .038 x .055      = .150
                        Two Sections                         .300

INNER AND OUTER CAP
    20 x 2 x 2 x .038 x .055                = .167
                        Two Sections                         .334

ADHESIVE                                                     .114

                                                           2.298
```

TABLE II   COMPOSITE FRAME WEIGHT (LBS.)

CONCEPT	1	2	3	4	5	6	7
Curve Wt (Ref. Table 1)	.769	.876	.808	.808	.805	.767	.696
Straight Section	2.298	2.298	2.298	2.298	2.298	2.298	2.298
Sub Total	3.067	3.174	3.106	3.106	3.103	3.065	3.994
5" Exten.	.570	.570	.570	.570	.570	.570	.570
Prod. Wt.	3.637	3.744	3.676	3.676	3.673	3.635	3.564
Pads	.96	.96	.96	.96	.96	.96	.96
TOTAL WT.	4.597	4.704	4.636	4.636	4.633	4.595	4.524
CAP REINFORCED	.363	.363	.363	.363	.363	.363	.363
TEST SPECIMEN	4.960	6.067	4.999	4.999	4.996	4.958	4.887

A preliminary analysis was conducted to develop the weight of a baseline aluminum frame. The resulting aluminum gages were comparable to the frame at Station 379 shown in Figure 2.

ESTIMATE OF ALUMINUM CURVED FRAME
(U.S. System of Units)

Caps P = 20,270 lbs. (Ref. Page 15)

F_{cy} = 75,000 p.s.i. (7075-T6 Extru.) ("B" Value) (Ref. 5)

A = 20,270/75,000 = .270 in^2

$$t = .270/3 = .090$$

$$b/t = (1-.045)/.090 = 10.6 \quad F_{cc} = 67120 \text{ p.s.i}$$

with 1" .040 web A = .270 + .040 = .310 f_c = 65390 p.s.i.

Web

q = N_{xy} = 1182 lb./in. F_{su} = 44000 p.s.i. (7075 clad "B")

t = 1182/44000 (.75)   = .035 use .040

Stiffeners (assume 5)

Pcrush = 5060 lb. (Ref. Page 24)

Use Extrusions

A = 5060/75000 = .067 in.^{2}

Try 3/4 x 3/4 x .050 = .075 in.^{2} + 1" Web = .075 + .040 = .110 in.2
$$f_c = 46000 \text{ p.s.i.}$$

1. b/t = .75/.050   = .15 F_{cc} = 41000 p.s.i.

2. b/t = .75/.050 + .020 = 10.4
$$F_{cc} = 51000 \text{ p.s.i.}$$

$$F_{cc} = \frac{51000 \,(.75 \times .090) + 41000 \,(.75 \times .050)}{.75 \times .75 \times .050} = 4980/.105 = 47430 \text{ p.s.i.}$$

ESTIMATE OF ALUMINUM CURVED FRAME

1) Web

$$4.25 \times (\frac{12.5 + 8}{2}) \times .040 \times .1 = .18 \text{ lbs.}$$

2) Stiffeners

$$5 \times 4.25 \times (1.5 \times .050)(.1) = .16 \text{ lbs.}$$

3) Caps

$$2 \times (\frac{12.5 + 8}{2}) \times 3 \times .090 \times .1 = .54 \text{ lbs.}$$

Rivets   3/4 pitch
$$L = 12.5 + 8 + 5(4) = 40.5" \text{ In.}$$
$$40.5/.75 = 54 \text{ rivets}$$

Assume   AD-5 (5/32) = .00078#/Rivet
$$54 (.00078) = .04 \text{ lbs.}$$

TOTAL ESTIMATED CURVE WEIGHT   = .92 lbs.

2-25 in. straight sections

Stiff. 8/5 (.16)		.28
Webs 4.25 x 50 x .04 x .1	=	.85
Caps 50 x 3 x 090 x .1 x 2	=	2.16
Rivets		.08
		3.37
Curve Weight		.92
TOTAL WEIGHT		4.29 lbs.

2.7.2 COMPOSITE CURVED FRAME COST STUDY

Prototype cost targets for the composite curved frame study are derived from the one-thousand unit (T-1000) labor hour value and then applied to an improvement curve to arrive at the one unit (T-1) cost target. The one-thousand unit labor value is based upon using semi-automated production techniques such as preplied broadgoods, and automatic knife cutting of the ply patterns. The prototype labor hour value is based on conventional manual production methods. Material cost has been priced out in 1982 dollars. A 30% scrap factor allowance has been included in the material cost estimate. Labor costs, including overhead and general administration costs are at $33/Hour. Material at $50 per pound.

The cost of a baseline aluminum frame is based on 5.3 labor hours per pound of cabin structure and $3.10 per pound of aluminum material.

TABLE III. COMPOSITE CURVED FRAME COST STUDY

CONCEPT 1

	Production Unit T-1000 Labor Hours	T-1 Prototype Labor Hrs.	Material Dollars
Inner Channel	3.55	25.1	107
Outer Channel	3.55	25.1	107
Inner Cap	1.22	8.1	50
Outer Cap	1.32	8.5	54
Bonded Assembly	1.62	8.2	10
Loading Pad Plys	(-)	10.4	50
TOTALS	11.26	85.4	$ 378

CONCEPT 2

	Production Unit T-1000 Labor Hours	T-1 Prototype Labor Hrs.	Material Dollars
Inner Channel	3.85	27.2	119
Outer Channel	3.85	27.2	119
Inner Cap	1.22	8.1	50
Outer Cap	1.22	8.5	54
Bonded Assy.	1.76	8.4	10
Loading Pads	(-)	10.4	50
TOTALS	11.90	89.8	$ 402

TABLE III (Cont'd)

CONCEPT 3

	Production Unit T-1000 Labor Hours	T-1 Prototype Labor Hrs.	Material Dollars
Inner Channel	3.59	25.4	108
Outer Channel	3.59	25.4	108
Inner Cap	1.22	8.1	50
Outer Cap	1.32	8.5	54
Bonded Assy.	1.62	8.2	10
Loading Pads	(-)	10.4	50
TOTALS	11.34	86.0	$ 380

CONCEPT 4

	Production Unit T-1000 Labor Hours	T-1 Prototype Labor Hrs.	Material Dollars
Inner Channel	3.80	26.8	108
Outer Channel	3.80	26.8	108
Inner Cap	1.22	8.1	50
Outer Cap	1.32	8.5	54
Bonded Assy.	1.62	8.2	10
Loading Pads	(-)	10.4	50
TOTALS	11.34	86.0	$ 380

TABLE III (Cont'd)

CONCEPT 5

	Production Unit T-1000 Labor Hours	T-1 Prototype Labor Hrs	Material Dollars
Inner Channel	3.6	25.1	110
Outer Channel	3.6	25.1	110
Inner Cap	1.2	8.1	50
Outer Cap	1.2	8.1	50
Precast Foam	2.8	14.1	10
Bonded Assembly	1.9	9.6	20
Loading Pads	(-)	10.4	50
TOTALS	14.3	100.5	$ 400

CONCEPT 6

	Production Unit T-1000 Labor Hours	T-1 Prototype Labor Hrs	Material Dollars
Inner Channel	3.7	26.2	108
Outer Channel	3.7	26.2	108
Inner Cap	1.2	8.1	50
Outer Cap	1.2	8.1	50
Precast Foam	1.6	8.0	10
Bonded Assembly	1.9	9.6	20
Loading Pads	(-)	10.4	400
TOTALS	13.3	96.6	$ 390

40

TABLE III (Cont'd)

FRAME CONCEPT 7

	Production Unit T-1000 Labor Hours	T-1 Prototype Labor Hrs	Material Dollars
Inner Channel) Outer Channel)	10.0	70.2	318
Inner Cap) Outer Cap)	2.4	16.2	100
Bonding	1.9	9.6	19
Loading Pads	-	10.4	50
TOTALS	14.3	106.4	$ 487

2.8   SELECTED DESIGN FOR FABRICATION AND TEST

Concept number 1 (beaded stiffener) was selected for detailed analysis and fabrication based on the data presented in Table IV. This concept resulted in a best cost/weight reduction over the aluminum baseline frame.

TABLE IV

Selection Of Composite Curved Frame Concept

	Production Cost ($)	Production Weight (lbs)	Δ Cost * ($)	Δ Wt. * (lbs.)	Δ Cost/Δ Wt. ($/lbs.)	Remarks
Baseline Aluminum	764	4.290				
Concepts 1	699	3.637	-65	+.653	-99.54	Cost savings, Low Manufacturing Risk.
3 and 4	704	3.676	-60	+.614	-97.72	Lower Cost Savings, Low Risk.
2	745	3.744	-19	+.546	-34.79	Lowest Cost Savings, Low Risk.
6	778	3.635	+14	+.655	+21.37	Small Cost Increase, Low Risk.
5	821	3.673	+57	+.617	+92.38	Cost Increase, Low Risk.
7	954	3.564	+190	+.726	+261.70	High Manufacturing Risk & Cost Increase

* + Δ Cost is a cost increase over the baseline aluminum frame.

   + Δ Wt. is a weight savings with respect to the baseline.

3.0 FABRICATION OF FRAMES

During the initial curved frame preliminary design and analysis the frame geometry, height, cap width, overall lengths, and material lay-ups were established to allow lead time for the fabrication of molds. The molds were developed from the original frame drawing EWR 55187A (Figure 8). The mold for fabrication of the channels was constructed as an aluminum female mold with no interior protrusions for beads (Concept 1), or provisions for foam core (Concept 5 and 6). Based on the selected design, aluminum inserts would be fastened into the mold to produce the desired channel web contours. The mold for the channels is shown in Figure 11.

A single aluminum mold, fabricated to the outer contours of the channel flanges, was used to produce the inner and outer frame caps. The cap mold is sketched in Figure 12.

The frame components, two channels and the caps were laid-up on the molds as required and cured. The components were then assembled with film adhesive, vacuum bagged and the adhesive cured. A completed frame is shown in Figure 13.

Six frames were fabricated under this study. The first frame was used for tool try-out only. Five frames were statically loaded to fracture. Each frame was weighed after the components were bonded. The weight of each frame is given in Table V.

TABLE V
Composite Curved Frame Weight after Bonding

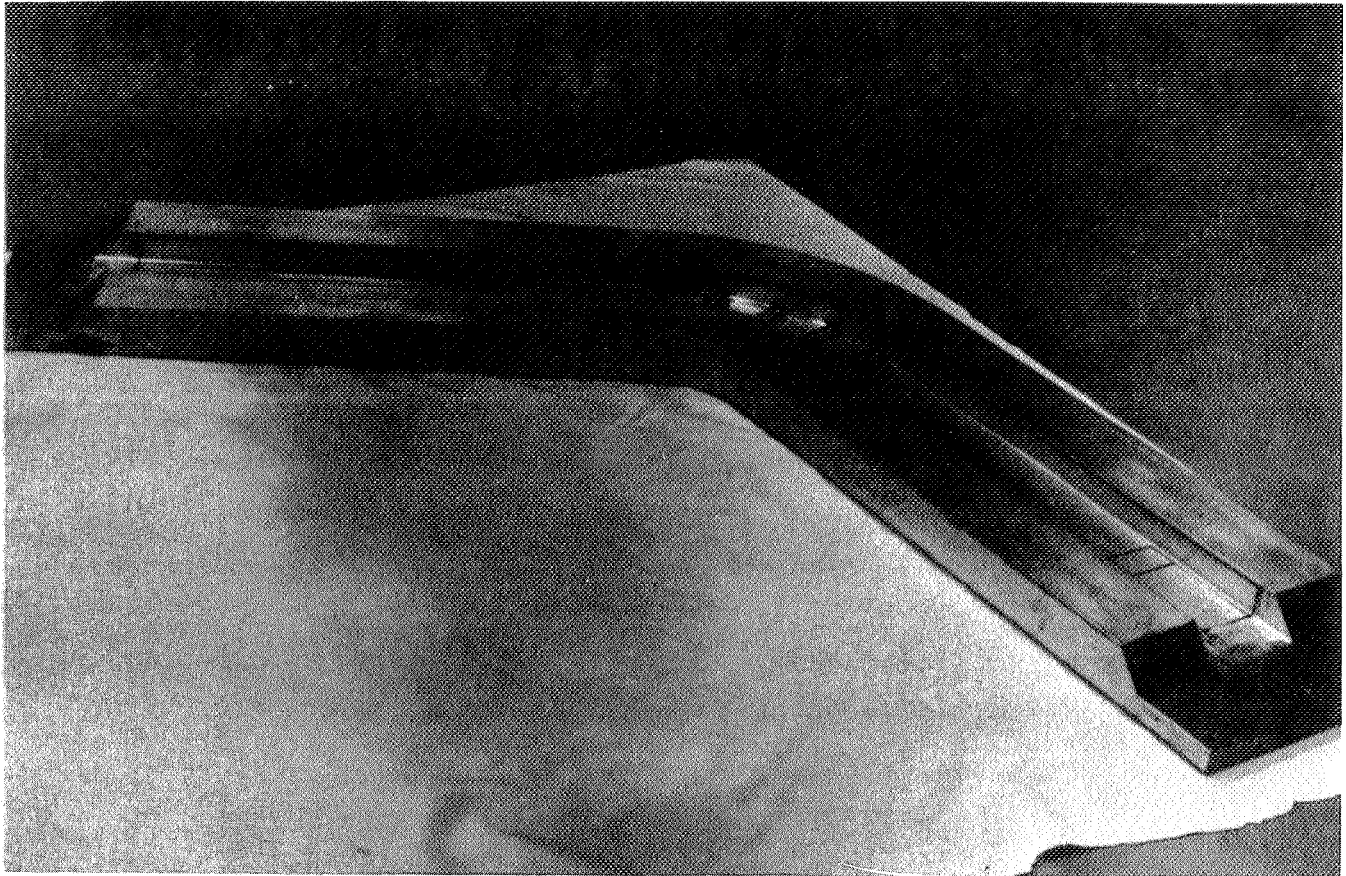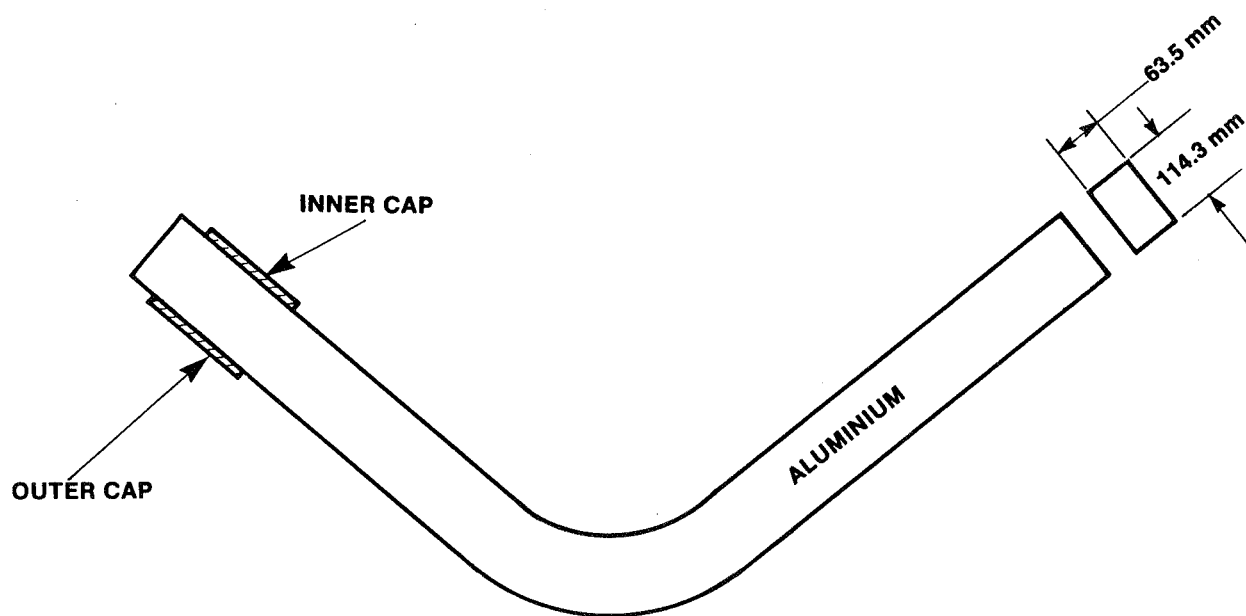| Frame	Weight Grams	(Pounds)
Tool Try Out	2287.65	5.050
Test Specimen No. 1	2298.98	5.075
Test Specimen No. 2	2310.30	5.100
Test Specimen No. 3	2303.51	5.085
Test Specimen No. 4	2242.35	4.950
Test Specimen No. 5	2332.95	5.150
Average Weight	2295.80	5.068
Calculated	2246.88	4.960 (Ref. Table II)

43

Figure 11.   Composite Curved Frame Channel Mold

Figure 12. Composite Curved Frame Inner and Outer Cap Mold
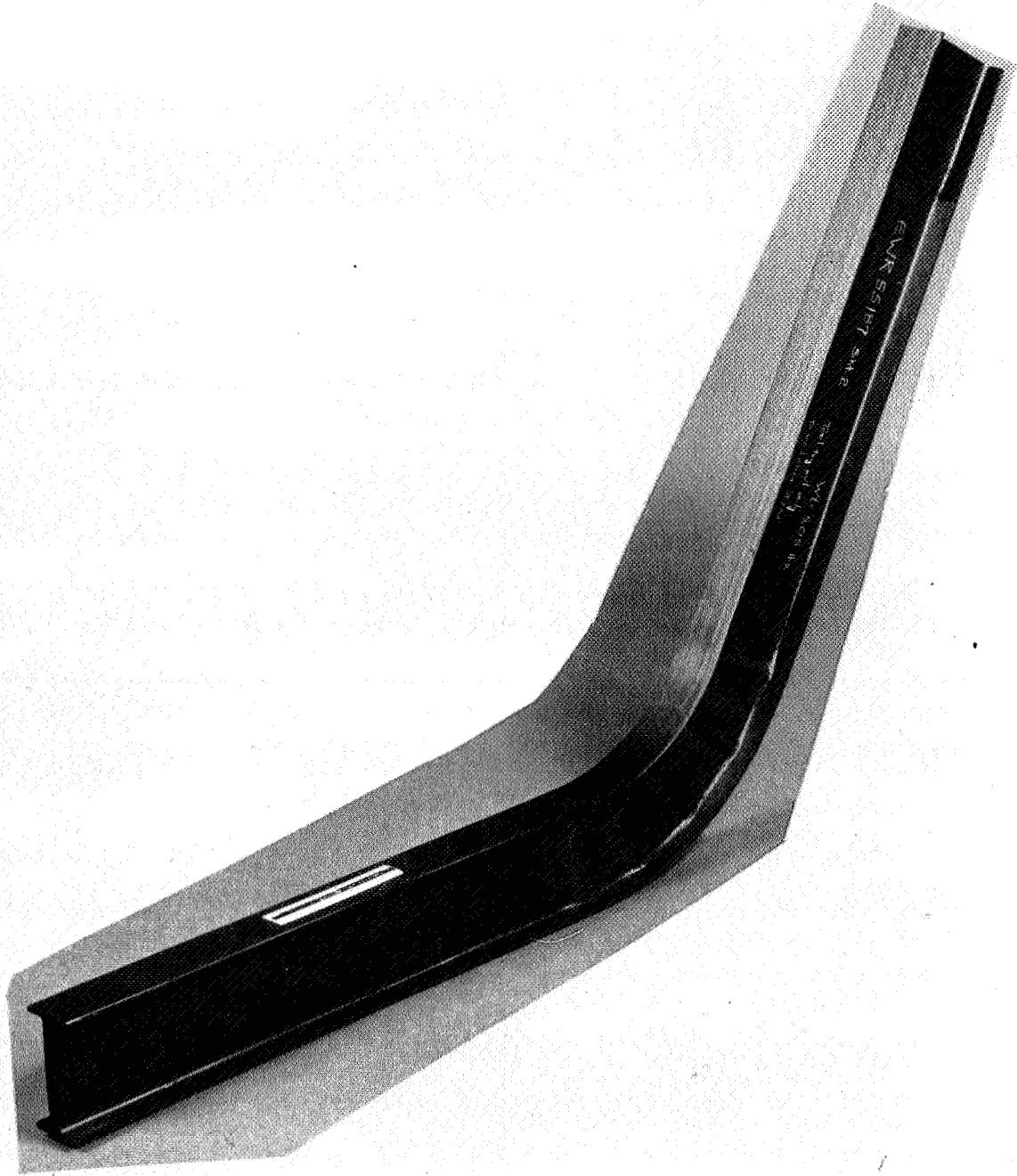(Sketch)

Figure 13. Composite Curved Frame

4.0 DETAILED ANALYSIS OF THE TEST FRAME

4.1 Finite Element Analysis

A finite element model of the graphite/epoxy curved frame was developed as shown in Figure 14. Quadilateral and triangular elements with combined membrane and bending stiffness were used to obtain strain distributions in the test specimen curved region. Strain contour plots for the inner cap, and the outer cap are shown in Figures 15 and 16. Maximum compressive strains on the inner cap occur at the center of the curve at section A-A, Figure 15. Maximum tensile strains on the outer cap occur at the center of the curve at section B-B, Figure 16. Predicted deformed shapes for the inner and outer caps in the curved region are shown in Figure 17. These shapes indicate that the free edges of the inner and outer cap bend towards each other. The axial and transverse magnitudes and distributions for the inner cap, over the center bead, indicated an anticlastic behavior of the cap.

1784 NODES
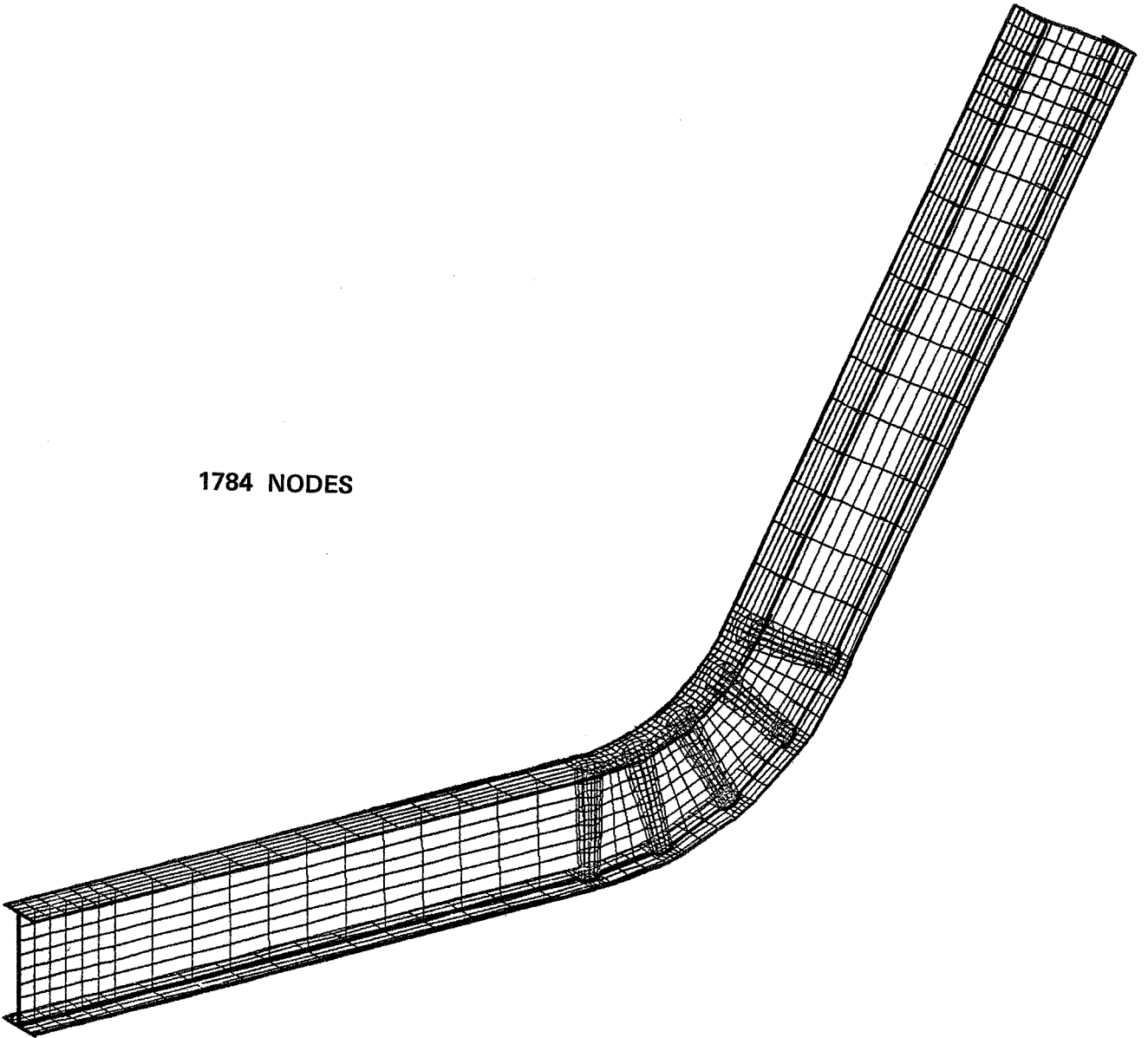
CURVED BEAM TEST

UNDEFORMED SHAPE

Figure 14.   NASTRAN Model – Beaded Curved Frame

STRAINS AT SECTION A-A

$\epsilon_1 = -.0100$

$\epsilon_2 = -.00925$

$\epsilon_3 = -.008460$

$\epsilon_4 = -.00767$

$\epsilon_5 = -.00688$

$\epsilon_6 = -.00609$

$\epsilon_7 = -.00529$

$\epsilon_8 = -.00450$

$\epsilon_9 = -.00371$

$\epsilon_{10} = -.00292$

AVG. = - .00647
(1-10)
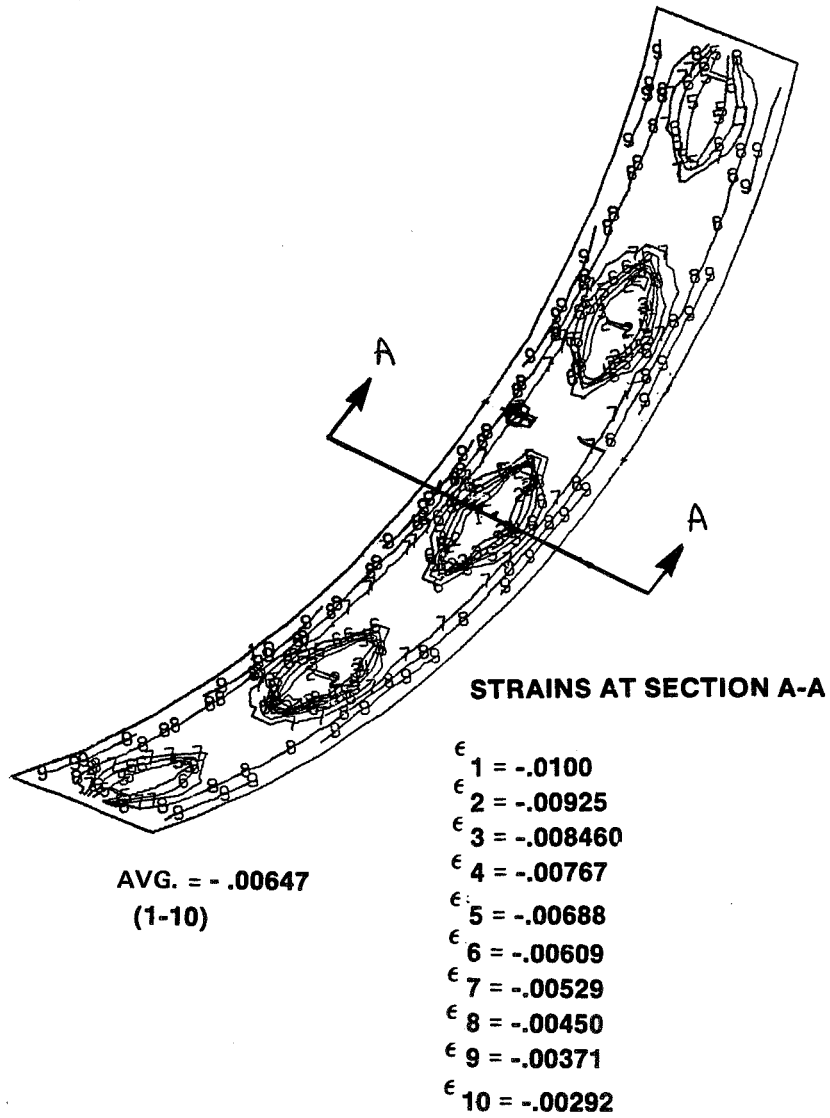
Figure 15. Strain Plots - Composite Curved Frame - Inner Cap

STRAINS AT SECTION B-B

$\epsilon_1 = .00185$

$\epsilon_2 = .00242$

$\epsilon_3 = .00299$

$\epsilon_4 = .00355$

$\epsilon_5 = .00412$

$\epsilon_6 = .00469$

$\epsilon_7 = .00525$

$\epsilon_8 = .00582$

$\epsilon_9 = .00638$

$\epsilon_{10} = .00695$

ϵ AVG = .00496
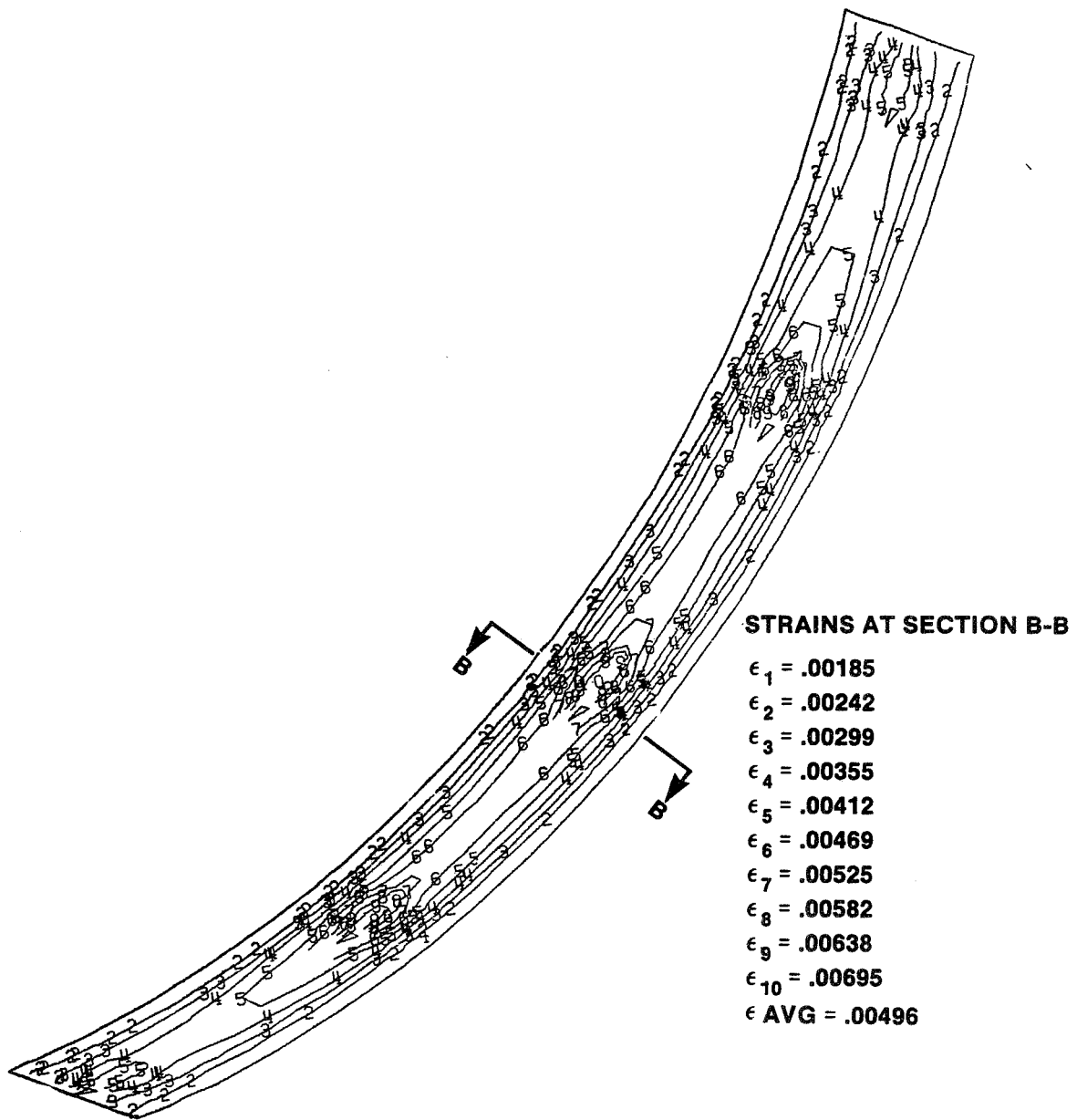
Figure 16.   Strain Plots − Composite Curved Frame − Outer Cap

50
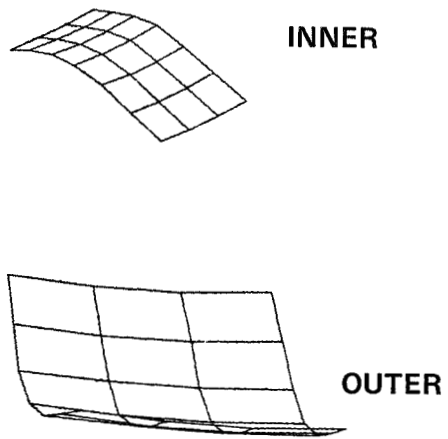
INNER

OUTER

Figure 17.   Static Deformation – Inner and Outer Cap –
             Composite Curve Frame

5.0 STATIC TEST

5.1 Test Facilities

The composite frames were tested as shown in Figure 18. For safety reasons, the specimens were tested in a prone position. The test load was applied as shown in Figure 18 which duplicated frame bending, shear and axial forces with a single point load application. The test facility was capable of applying a single load of 88.96 kN (20,000 lbs) in incremental loads.

The test specimens were not directly attached to the test facility but rather free standing with the hydraulic cylinder. The test specimens were supported by the load horns and associated hardware.

Under test conditions, i.e., frame bending, the frame structure would tend to warp out of plane. It is therefore necessary to restrict any deflection by sandwiching the frames between horizontal beams and the floor as shown in Figure 18. In the unloaded condition there was no contact between the specimen and facility.

The purpose of these tests was to demonstrate the structural integrity of a curved composite fuselage frame utilizing improved design and fabrication methodology.

5.2 Strain Gaging

The composite test frames were strain gaged similarly to that shown in Figures 19 through 22. In addition to strain gages, load and frame deflection readings were required.

Strain gages were located on the frame caps and web as determined from the NASTRAN analysis. Axial strain gages were used for the frame caps and rosette strain gages were used on both sides of the web. The frame axial deflection was monitored with a DCDT (direct current differential transformer) as indicated in Figure 19. After the first test completion all the strain, load and deflection data were reduced to determine the bending moments, axial loads and shear loads. A plot of strains vs. test loads were plotted and compared to those predicted by NASTRAN analysis. A Hewlett Packard 9825-T desk top computer and 7225A Graphics Plotter were used for real time data acquisition and data reduction.
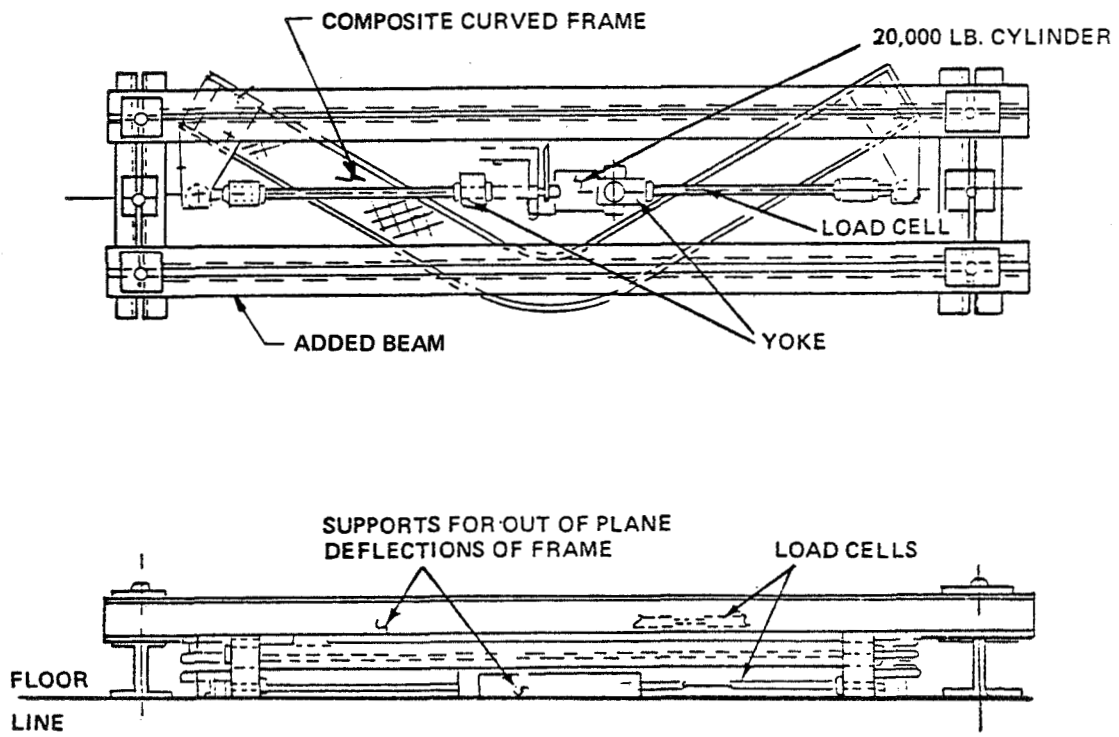
52

Figure 18. Sketch of the Loading Fixture

53

CTS
3

DIRECT CURRENT
DIFFERENTIAL TRANSFORMER

CTS

CTS 16

BTS-5

BTS—6 (OPPOSITE SIDE
OF WEB/BEAD)

WR-C

WR-A
WR-B (OPPOSITE SIDE OF WEB)

WR-A

WR-B

WR-C

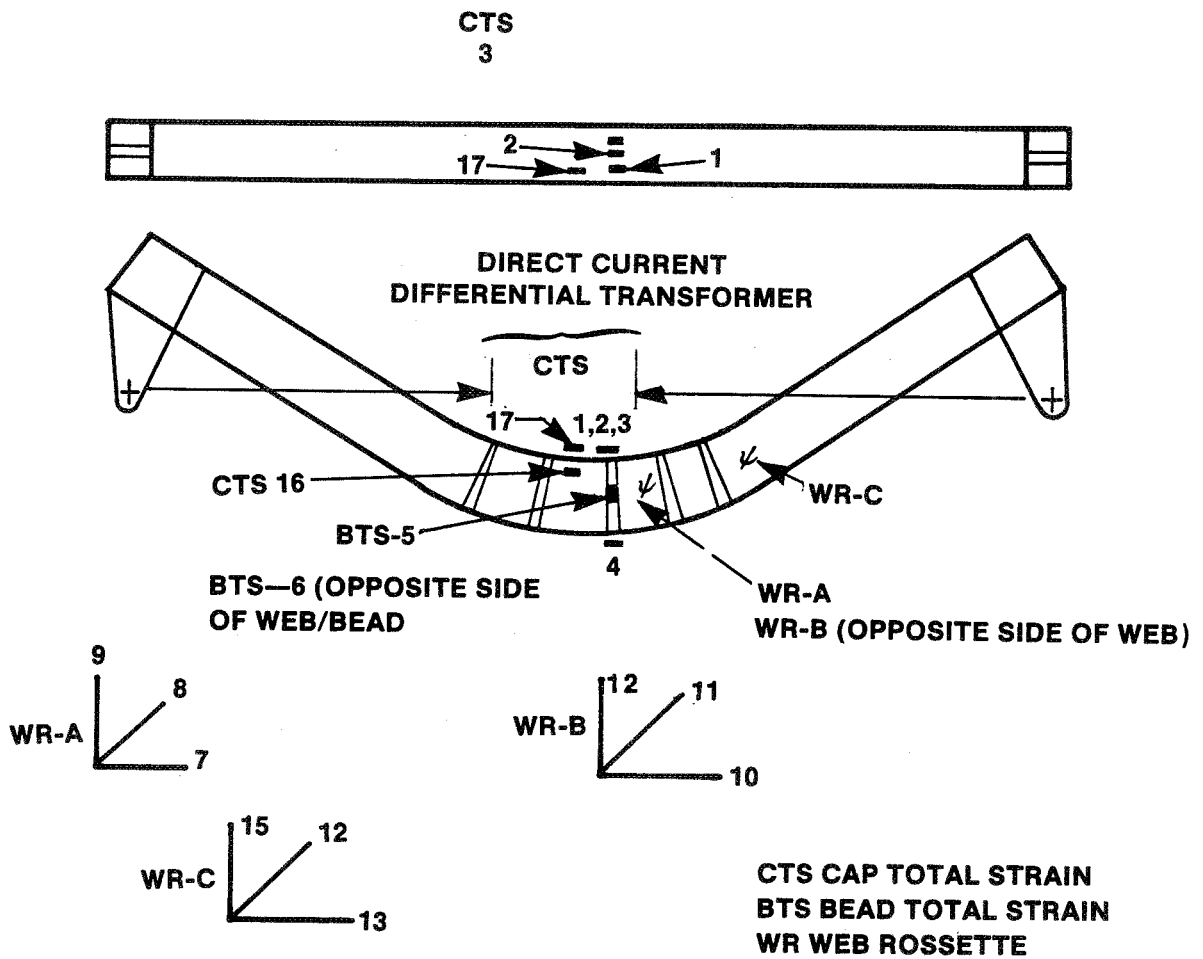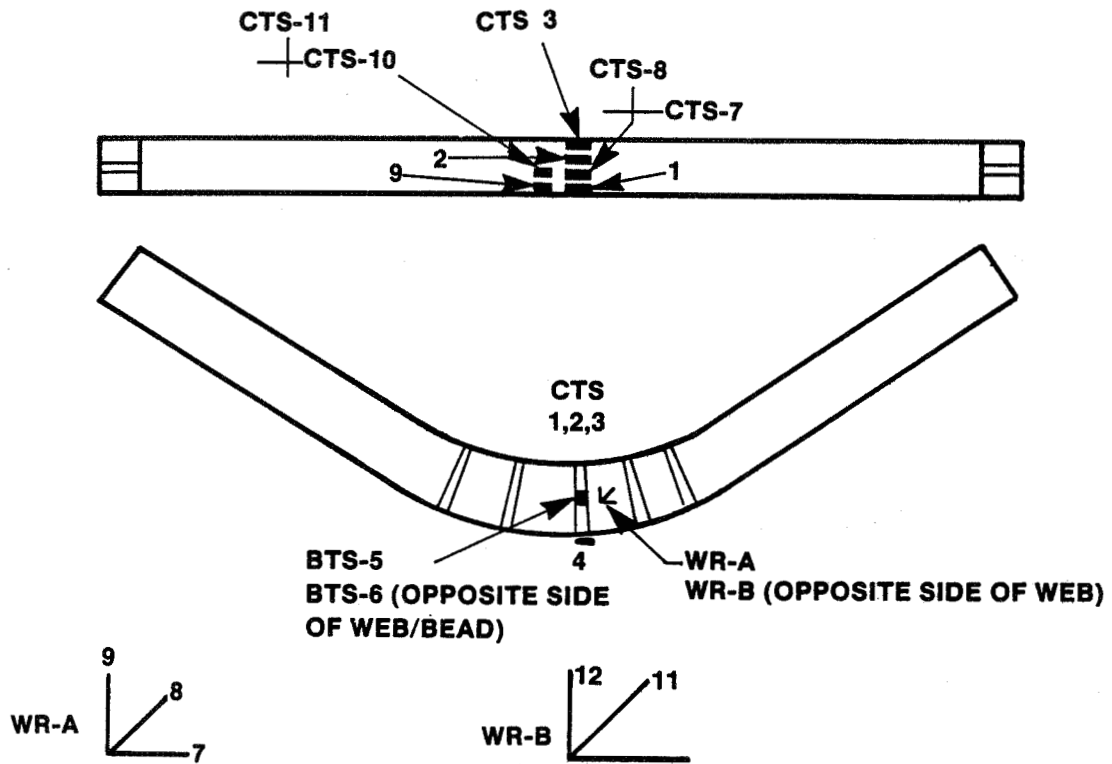CTS CAP TOTAL STRAIN
BTS BEAD TOTAL STRAIN
WR WEB ROSSETTE

Figure 19. Composite Curved Frame Strain Gage Location –
Specimen No. 1

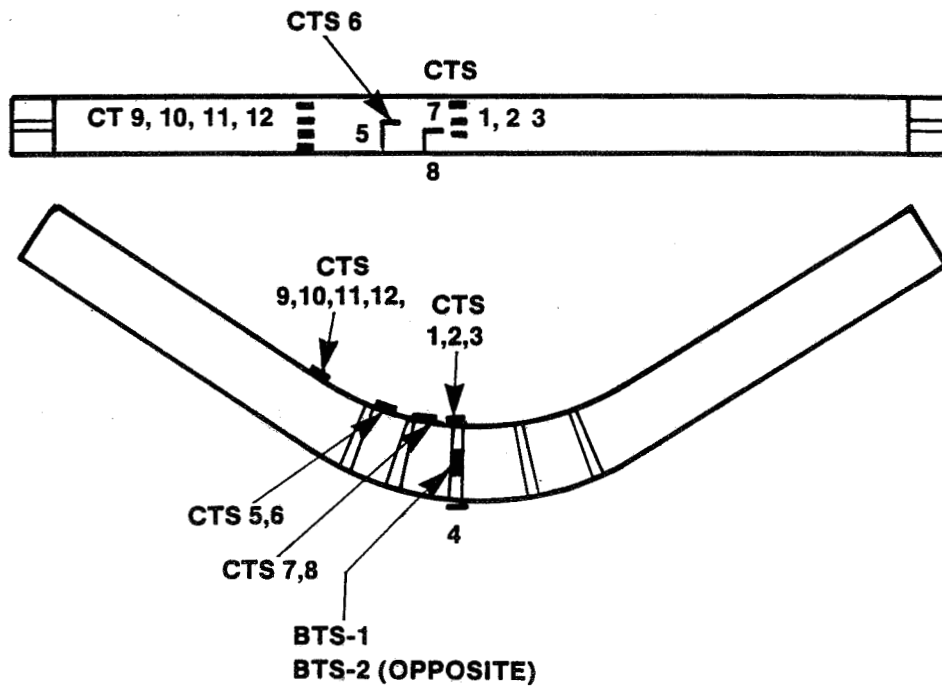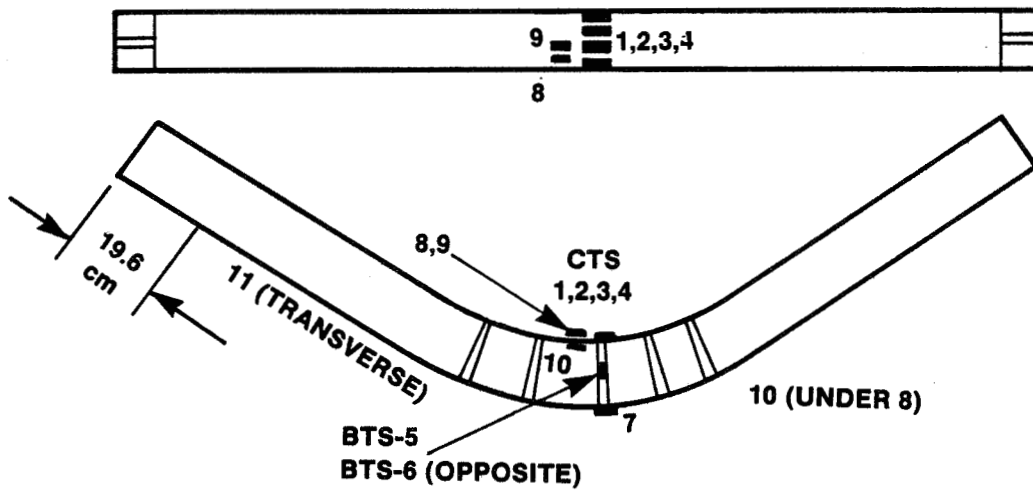Figure 20. Composite Curved Frame Strain Gage Location – Specimen No. 2

Figure 21. Composite Curved Frame Strain Gage Location – Specimen No. 3

56

Figure 22. Composite Curved Frames Strain Gage Locations - Specimens 4 and 5

5.3 Experimental Tests

Static tests were performed to demonstrate the structural integrity of the curved composite fuselage frames.

An initial phase consisted of incrementally loading the test specimen to 40% of the 10650 lb design load. During this phase the test results were compared to those predicted by NASTRAN analysis. The load was then released.

The final phase consisted of incrementally loading the test specimen until fracture. At 40% of the design crash load, a comparison was made with the initial loading.

The test load was designed to simulate crash bending moments, axial loads and shear loads.

Strain gages located along the webs, caps and stiffeners were analyzed at all test levels with a Hewlett Packard 9825-T desk top computer. One gage located at the predicted fracture site was monitored to warn test personnel of impending fracture.

The test results were plotted as axial deflection vs. load and strain vs. load for each of the gage locations. As a cross-check, the frame bending, axial load and shear load at 40% and 100% design crash load, were determined.

The results were compared to those predicted by NASTRAN and were used as a data base for any design changes.

5.4 Static Test of the First Specimen

The loading was made with the test specimen held in the fixture supports.

Strain gage data was obtained at each 500 lb. load increment. The gage data, as shown in Figure 23, 24, 25 and 26, showed that the strains were close to the NASTRAN predictions.

No problems were encountered at the 8000 lb (75% design load) level and the data of Figure 24 shows that gage CTS 2, cap compression total strain, was linear with loads. When attempting to go to 8500 lb. (80% design load) the frame twisted torsionally in the fixture and the test was stopped.

The specimen was removed from the test fixture and visually inspected. No damage could be observed and it was decided to retest with minor modifications. The modification was a balance check of the load cells. An unbalance of the load cells induced a torsion on the specimen. Supports were added to the test fixture to prevent torsional rotation of the frame specimen.

The static retest was conducted using the modified fixture and checking the load cell balance. As for the first test, the strain data was obtained at each 500 lb. load increment up to 7500 lb. The load-strain stayed linear for gages CTS 1, 2 and 3 (locations shown in Figure 19). As illustrated in Figure 24, the CTS 2 gage readings were identical with the first loading results. When attempting to go to the 8000 lb. load level the inner cap fractured in compression. Location of fracture was under gages CTS 1, 2, and 3.

It was suspected that some damage had been induced from the twisting action that was caused in the first loading.

Strain gage data for the first and second loadings were compared. It was found that the strain gage readings of the stiffener, BTS 5 and 6, were the only ones that differed in the first and second loadings, as shown in Figure 27. The beaded stiffener gages are linear with load and nearly of the same values as in the first loading. For the second loading these gages begin to deviate from linearity after 2000 lbs. Thereafter the gages showed that the stiffener was becoming unstable.

The interpretation was that the first loading damaged the stiffener and that initial fracture was due to column buckling of the stiffener. The result was that the compression cap became unsupported and the induced additional stresses lead to fracture.

Based on the results of the strain gage survey it was decided to test the second frame test specimen without modification.

5.5   Static Test of the Second Specimen

The loading was made with the specimen held in the test fixture.

Strain gage data was obtained at each 500 lb. load increment. The gage data, as shown in Figure 28, showed that the strains were again close to the NASTRAN predictions and the data of the first test specimen.

Testing was stopped at approximately the 9500 lb. load level when it was observed that the two gages on the beaded stiffener (Gages BTS 1 and 2) began to deviate as shown in Figure 30. The deviation was interpreted as the beginning of an instability caused by weakening of the layup in the radius between the stiffener and the compression cap.

The drawing for the composite curved frame was revised (Revision C) to reinforce the bead to cap radius area as shown in Figure 8.

The radius reinforcements were bonded to specimens 2 and 3.

Reinforced frame specimen No. 2 (Rev. C) was statically loaded to fracture. At 101% design load, the frame fractured in the straight constant section near the loading pads. A photograph of the fracture is shown in Figure 31. The fracture, in the constant section, was thought to be a crippling type of fracture.

Strain data, in the curved section of the frame (Ref. Figure 29), indicated that no damage had been done to that section. The strain gages on the beaded stiffener (gages BTS 1 and BTS 2) did not deviate, compared to the previous loading, as shown in Figure 30.

5.6 Static Test of the Third Specimen

Frame Specimen No. 3 was reinforced in the straight sections as shown in the drawing EWR 55187 Rev. D. The frame was loaded to fracture. At 84% design load, the frame fractured in the same manner as No. 2 (Rev. C). No damage appears to have been done to the curved section of the frame. Gages BTS 1 and BTS 2 did not deviate as shown in Figure 33.

The added reinforcement on the third frame was believed to have lowered the stresses in the straight section and prevent what was thought to be a crippling type of fracture. Since the frame straight section fractured at a lower load than frame specimen number 2, a study was conducted to investigate the behavior of frames 2 and 3.
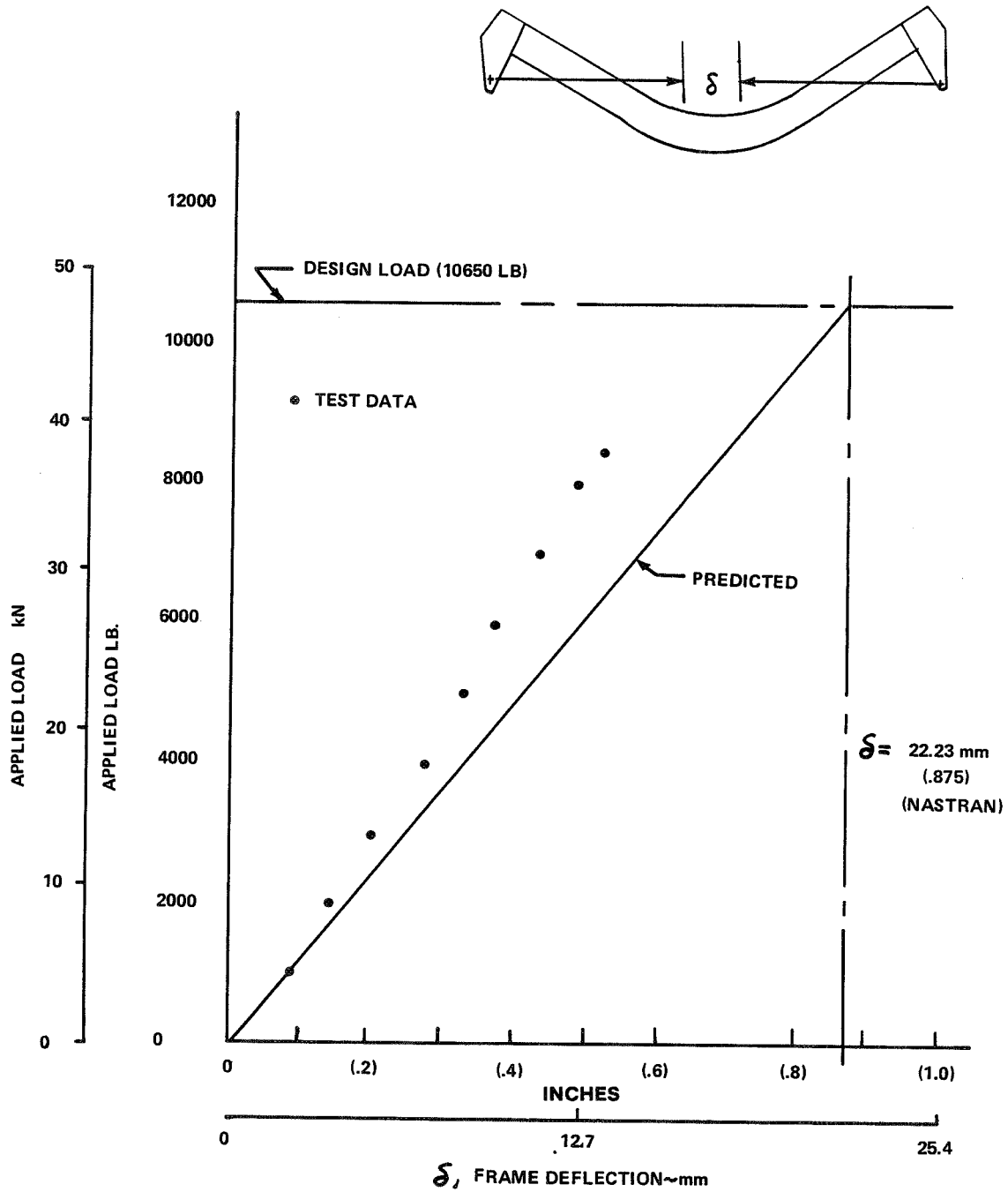
Figure 23. Deflection of Composite Curved Frame - Specimen No. 1
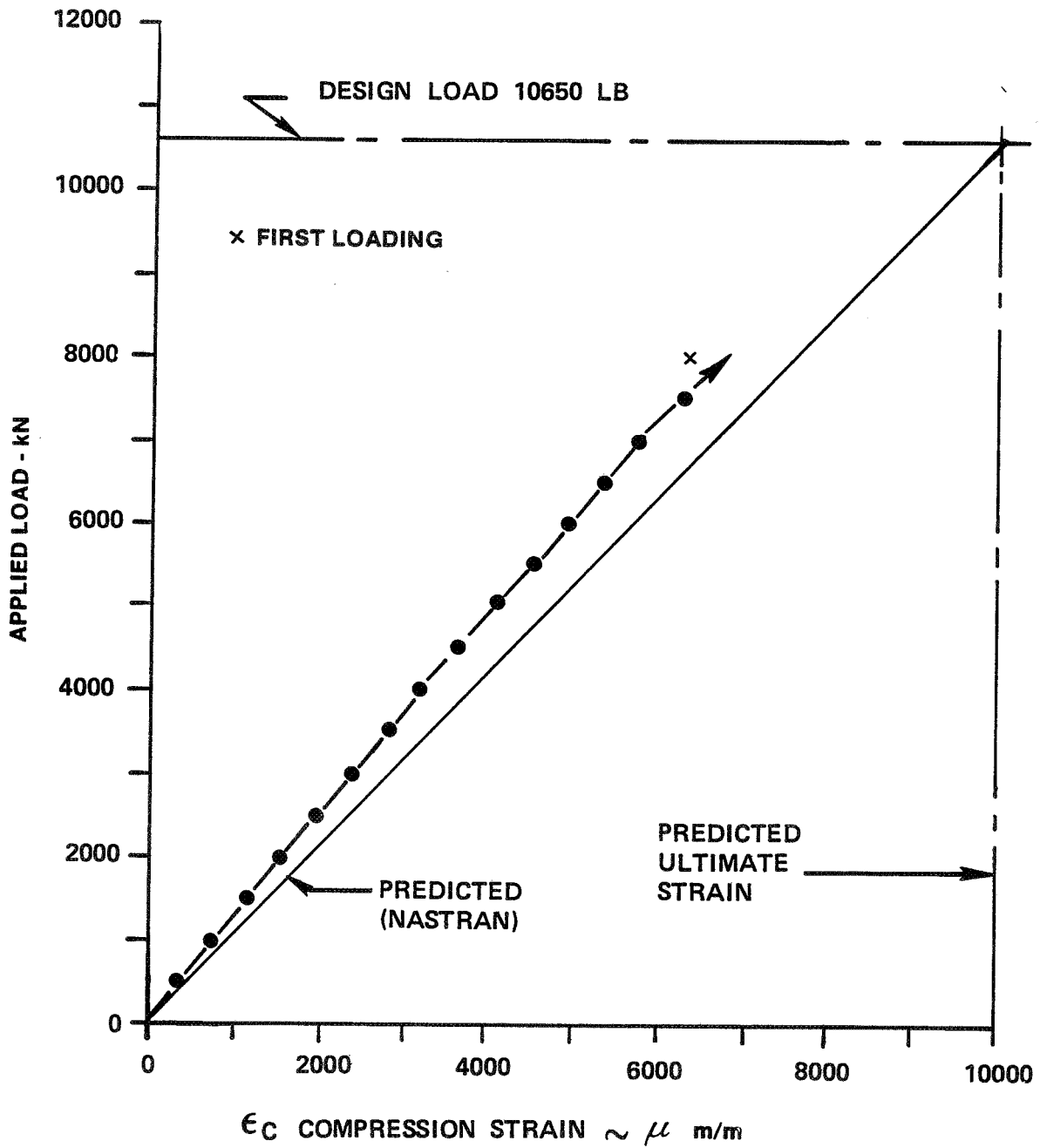
Figure 24.   CTS 2 Load-Strain Data Second Loading of
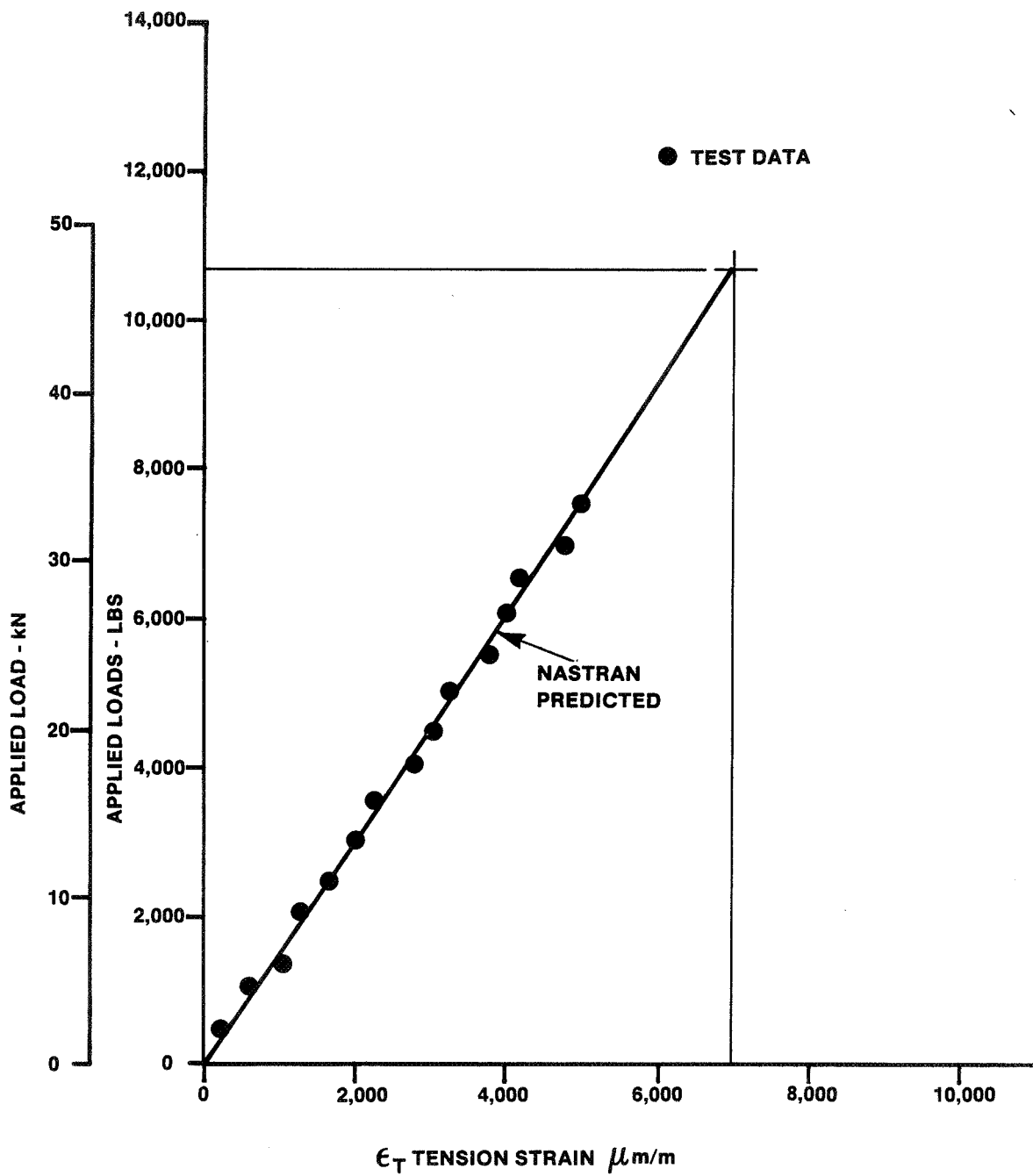Specimen No. 1

Figure 25.   Applied Load as a Function of Strain – Outer Cap –
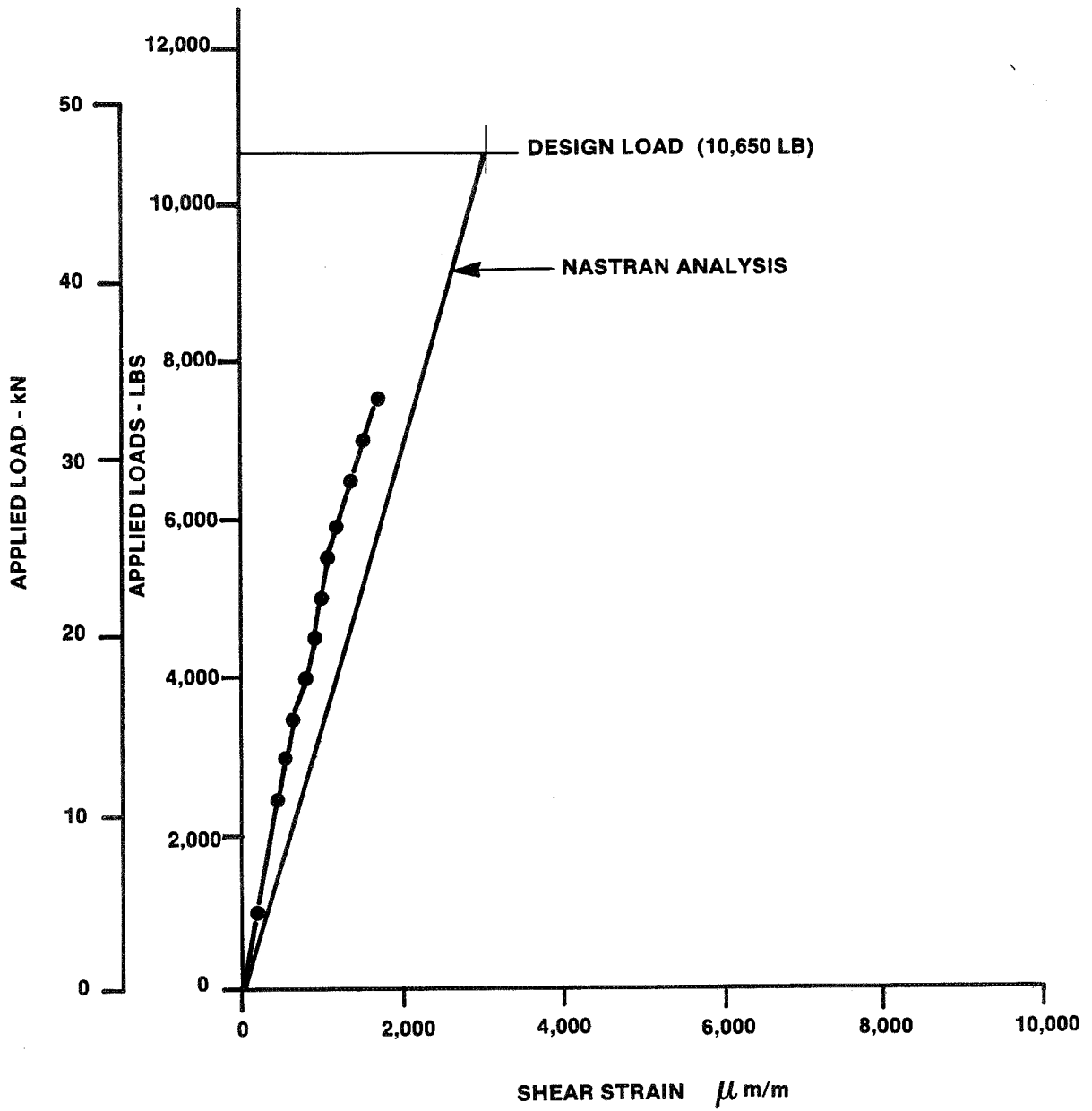Bottom of Center Bead – Gage CTS 4 Specimen No. 1

Figure 26. Applied Load as a Function of Shear Strain –
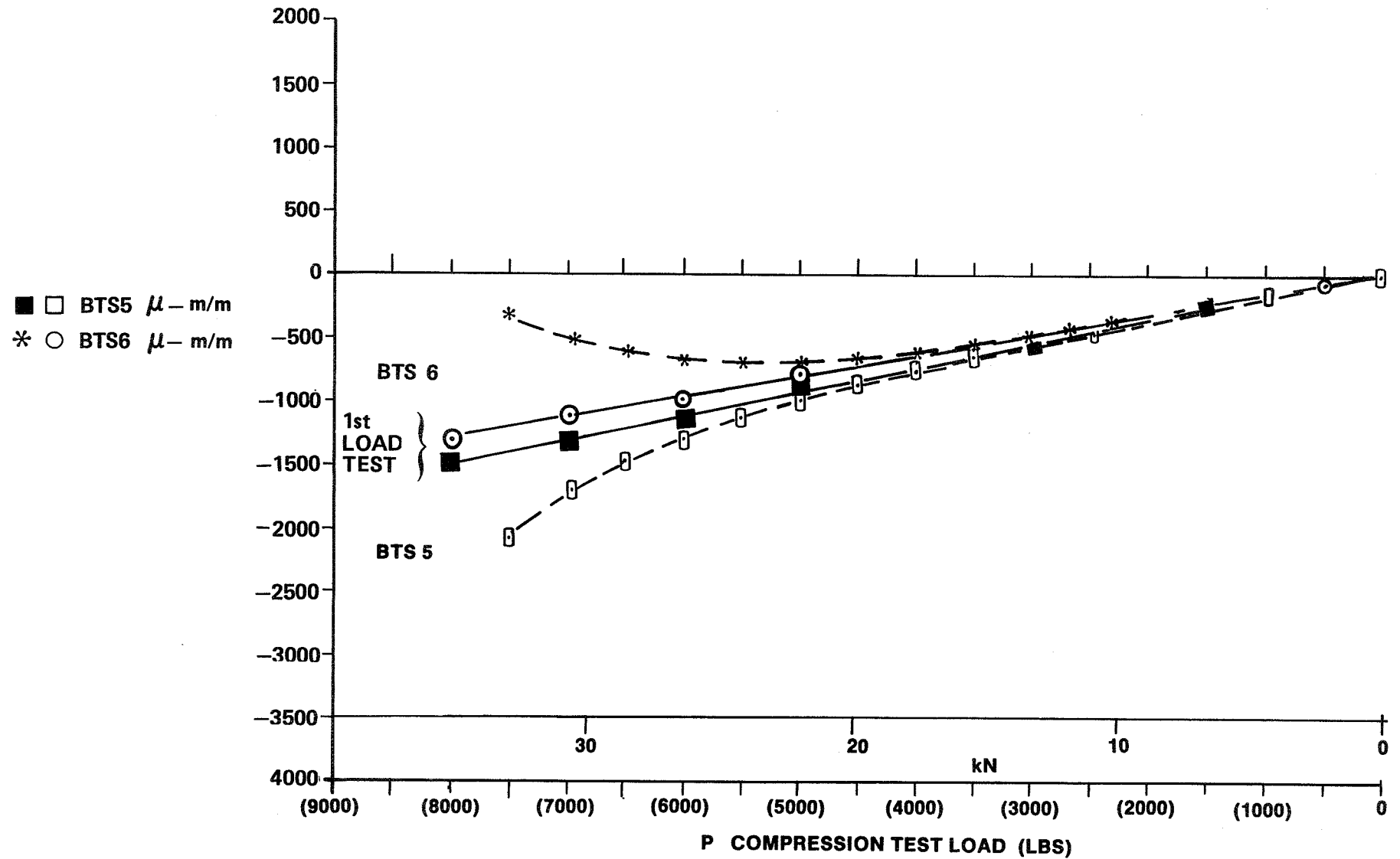Web in Constant Section – Gage No. WRC –
Specimen No. 1

Figure 27.   Specimen No. 1 Beaded Stiffener Load – Strain Data
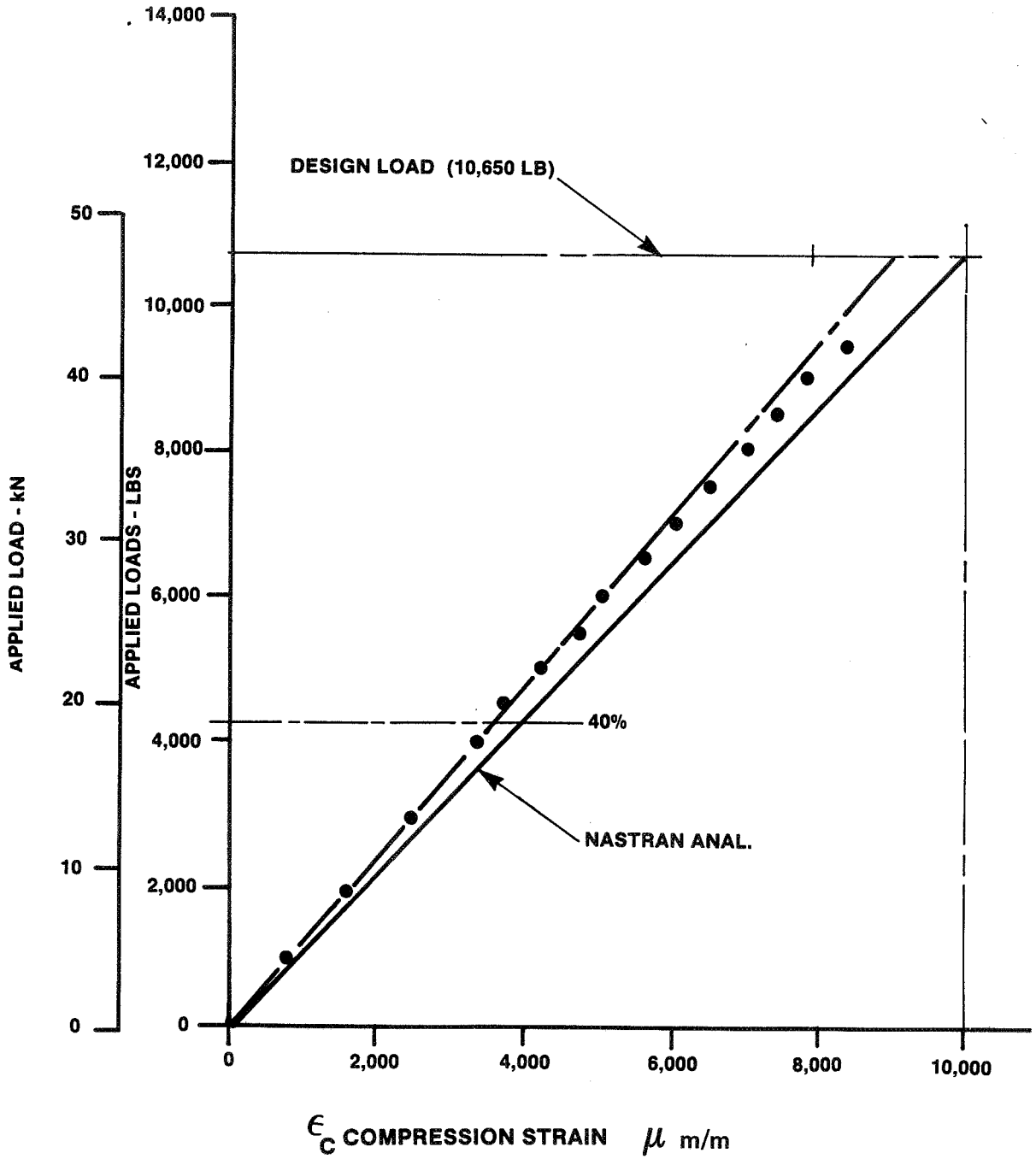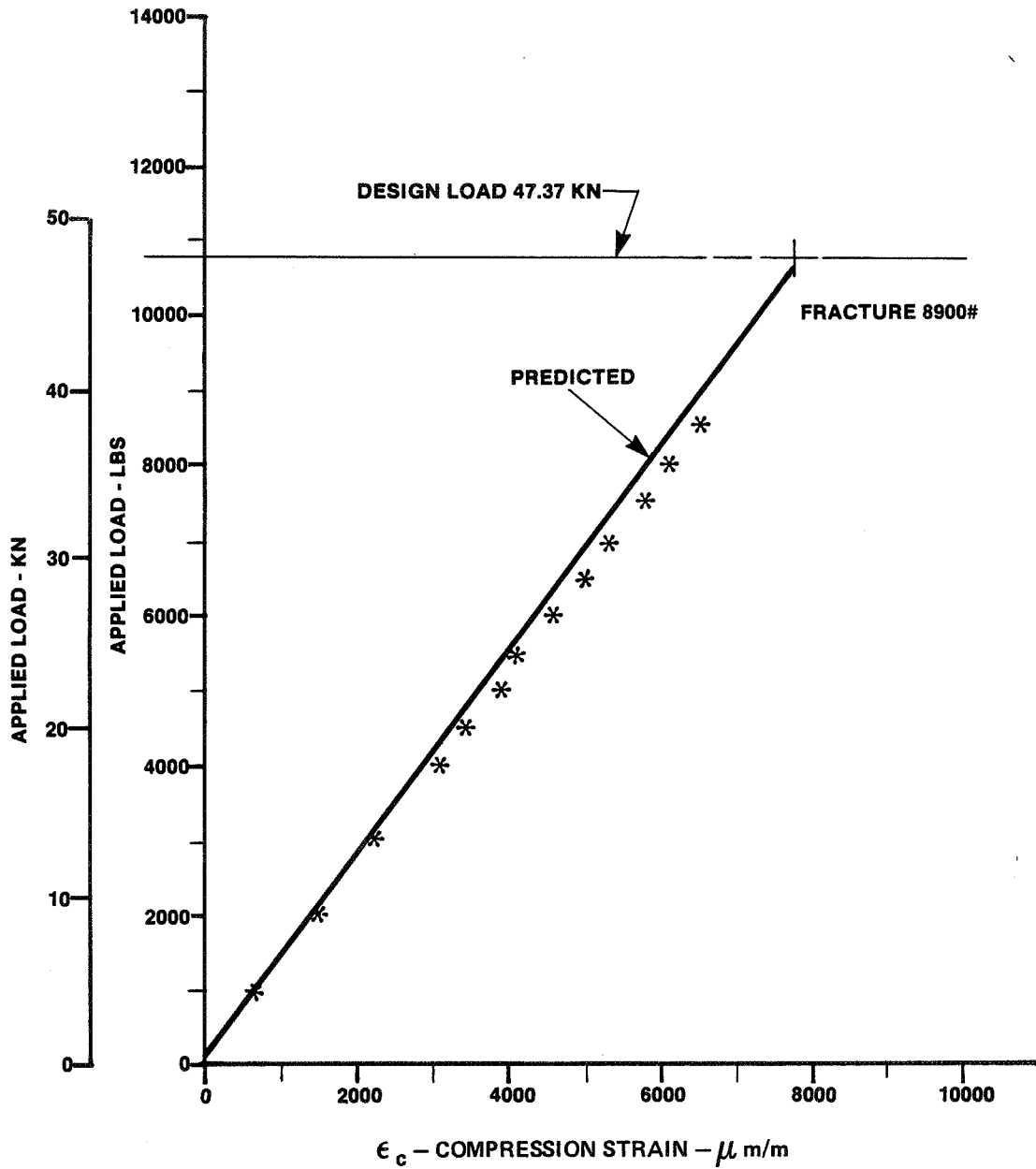(Hewlett Packard 9825-T Computer Plot)

Figure 28. Applied Load as a Function of Strain - Inner Cap -
Top of Centerline Bead - Gage No. CTS 2 -
Specimen No. 2 Rev. B
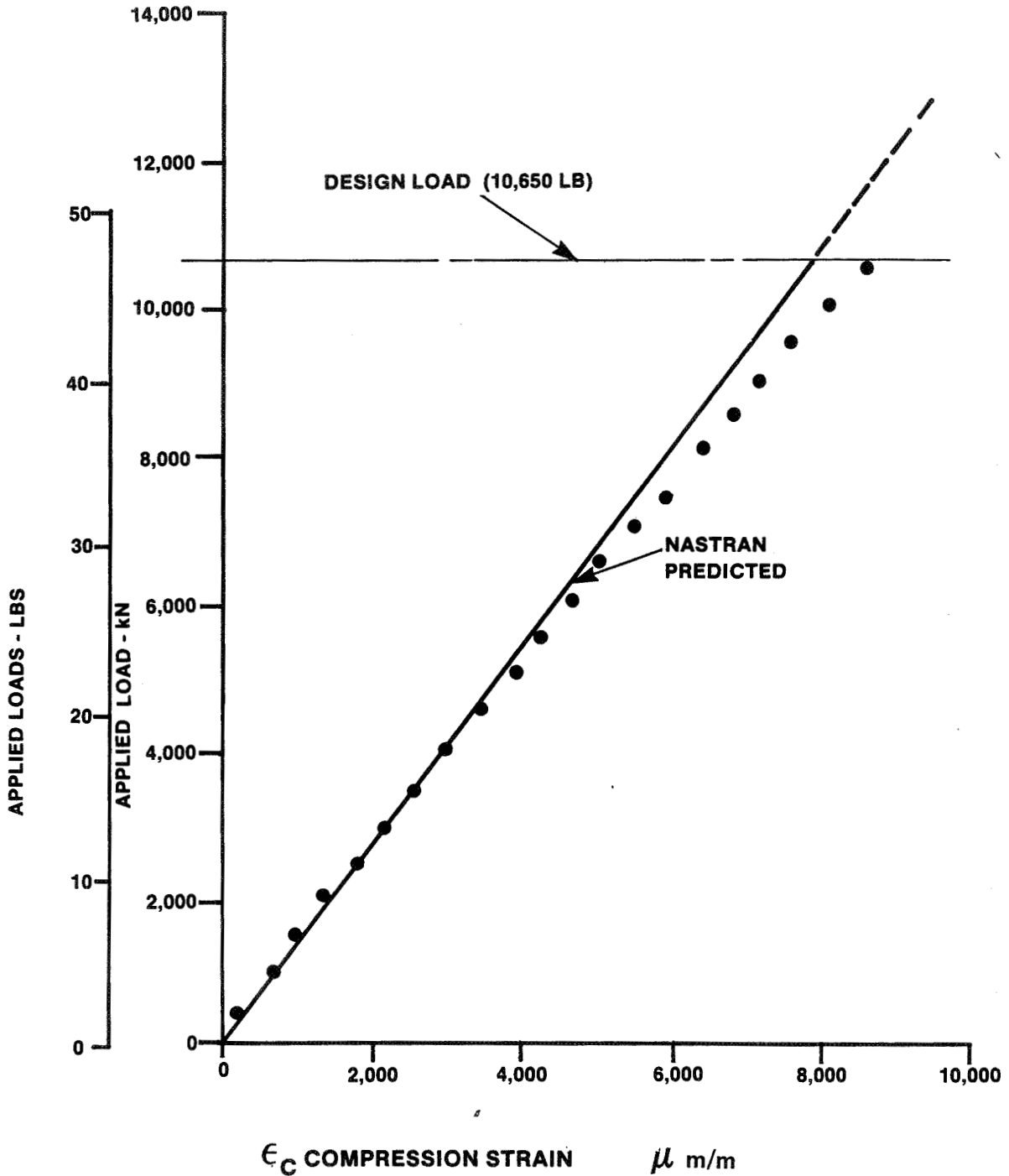
Figure 29.   Applied Load as a Function of Strain - Inner Cap -
Top of Centerline Bead - Gage No. CTS 2 -
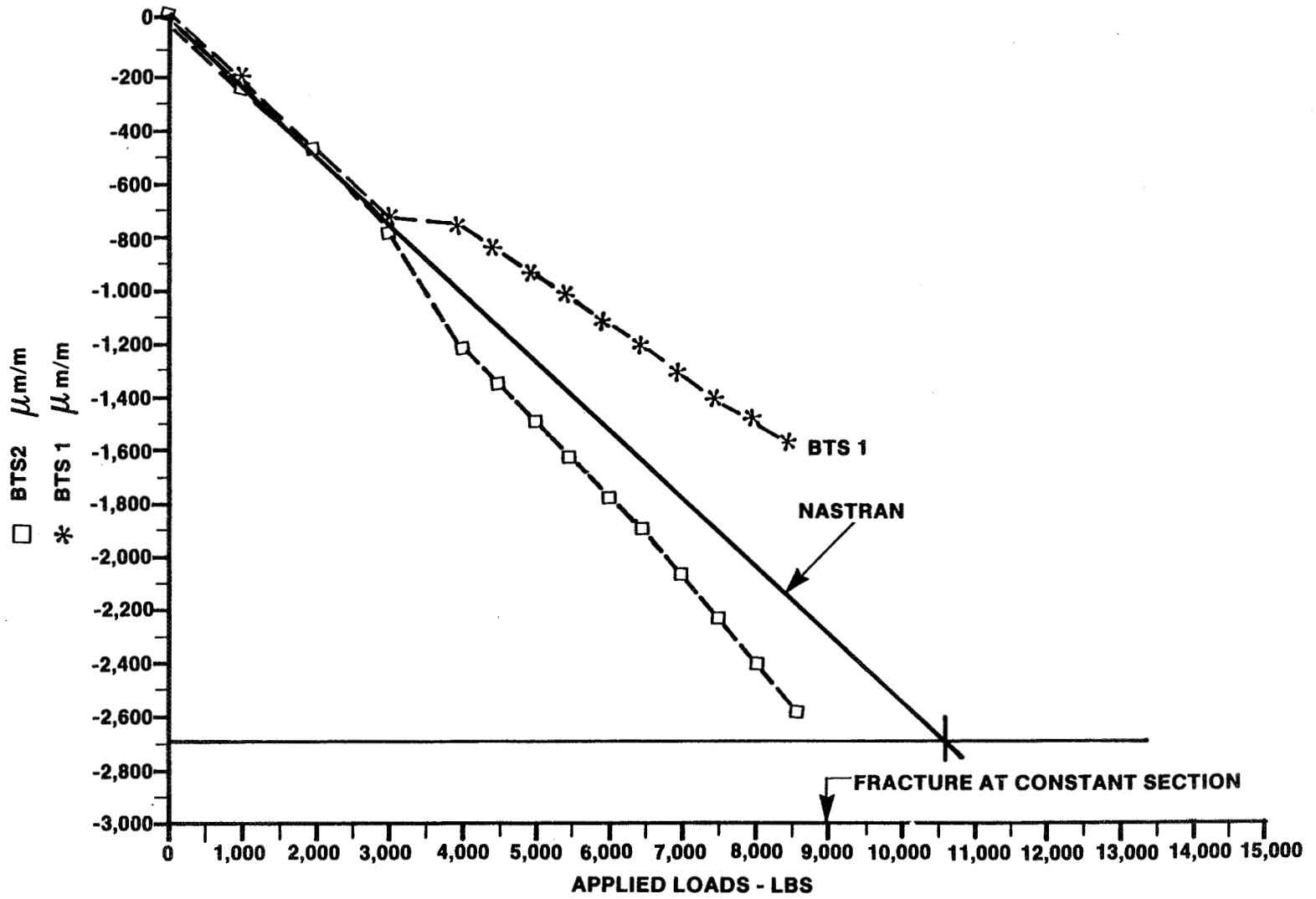Specimen No. 2 Rev. C
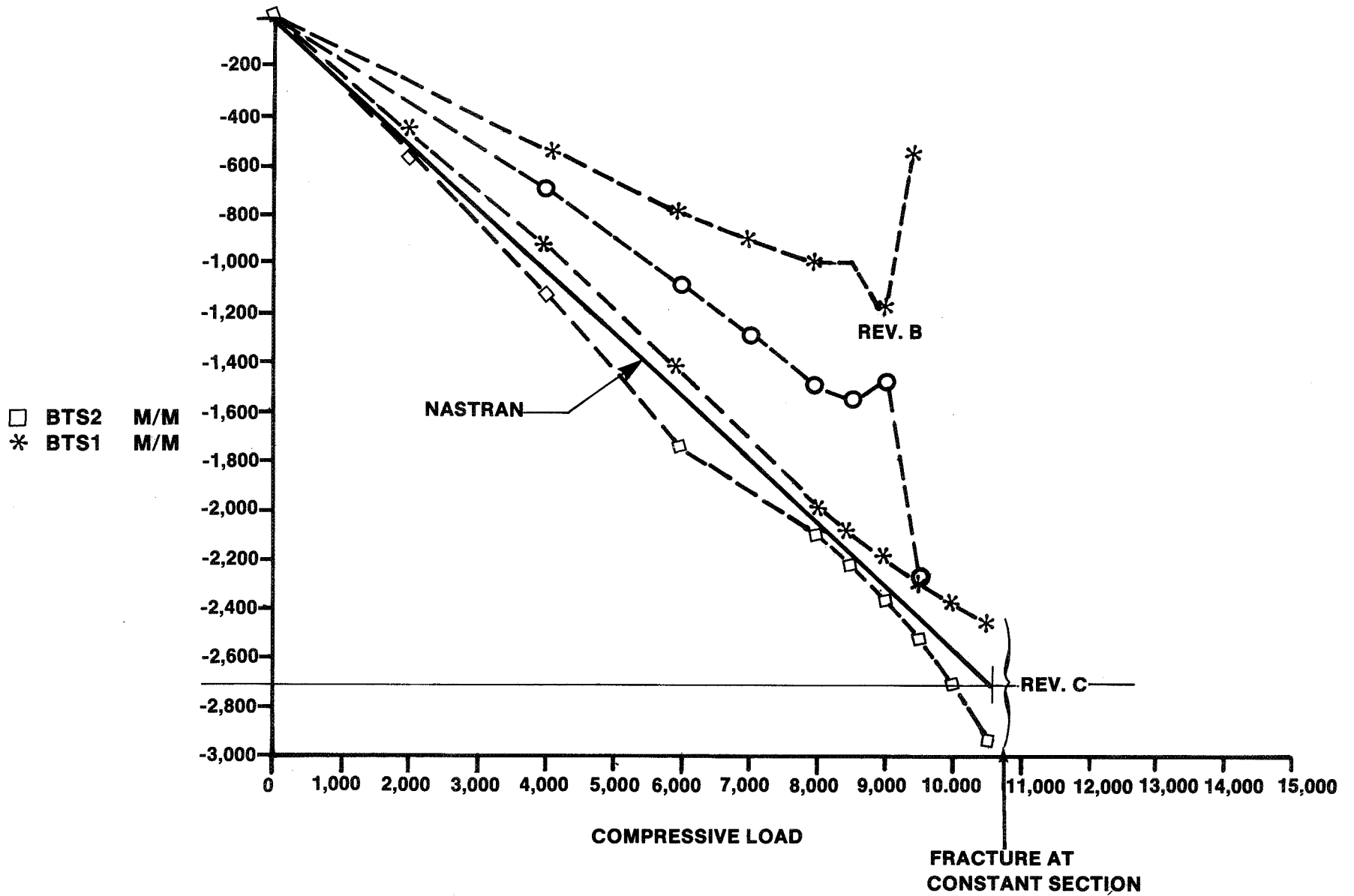
Figure 30. Specimen No. 2 – Beaded Stiffener
Load – Strain Data – Basic Frame
(Rev. B) and Reinforced (Rev. C)
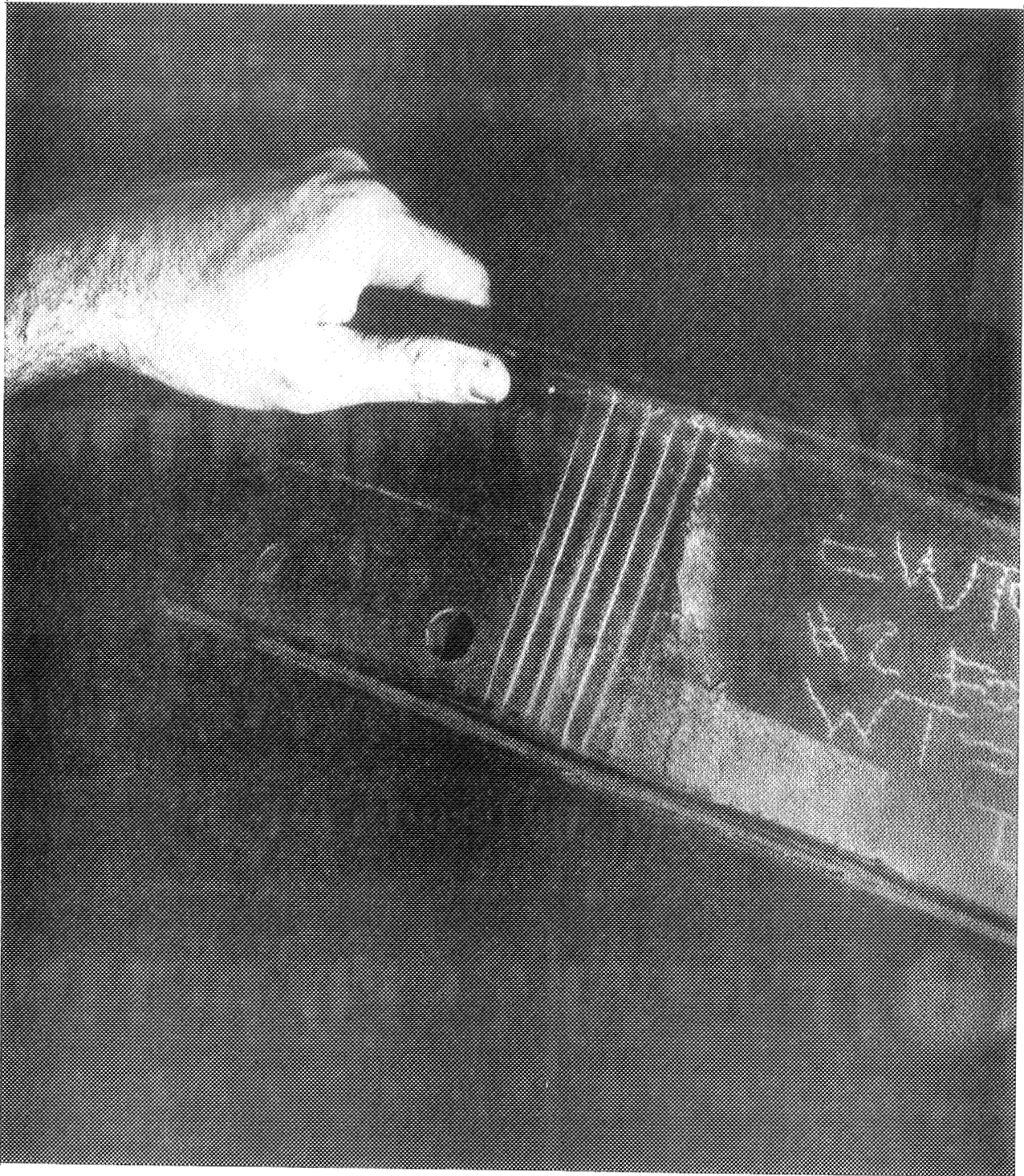
Figure 31. Fracture – Straight Section –
Composite Curved Frame –
Specimen No. 2 Rev. C

Figure 32. Applied Load as a Function of Strain -
Inner Cap - Top Center Bead - Gage No. CTS 2 -
Specimen No. 3, Rev. D

70

Figure 33. Specimen No. 3, Rev. D, Beaded Stiffener Load – Strain Data (Hewlett Packard 9825-T Computer Plot)

6.0 ELEMENT ANALYSIS, DESIGN AND TEST

6.1 BACKGROUND

The reinforcement of the straight section of frame No. 3 was accomplished by an application of a wet layup consisting of three plies of 0/90 graphite epoxy fabric and EA956 resin. The wet layup was placed directly on the outer frame cap, bagged, vacuum applied, and room temperature cured for 24 hours. The purpose of the 3 ply 0/90 graphite epoxy "fix" was to increase the cap thickness and lower the flange width to thickness ratio (b/t) thereby increasing the "allowable crippling" stress. Since the "fix" did not increase the strength of the straight section of the curved frame an IR&D program was conducted by Sikorsky to study the "crippling" problem.

6.2 CRIPPLING ANALYSIS

A three dimensional finite element model was developed to analyze the stress distribution of the frame cap in the straight section at the point of fracture. Three finite element models were analyzed. The first model represented the layup of the lower cap in the straight section of frame specimen number 2. The second model represented the layup on frame specimen number 3. The third model represented the basic layup as frame number 2 with an addition of three plies of ±45° graphite epoxy fabric. The three models are shown in Figures 34, 35 and 36.

The results of the three-dimensional (3-D) finite element analysis showed a high transverse tensile stress (peel) at the free edge of models 1 and 2 and a transverse compression stress at the free edge of model 3. The analysis results are shown in Figures 34, 35 and 36. The maximum transverse stress in each case is developed at the interface between the ±45° web plies and the 0°-0°/90° cap plies as sketched in Figure 37.

The transverse stress through the thickness of the layups is due to the Poisson effect of the plies in the layup. This effect is illustrated in Figure 37.

6.3 ELEMENT DESIGN AND TESTING

Honeycomb beams with graphite epoxy faces were designed, fabricated and tested to substantiate the results of the three dimensional finite element analysis.

Three configurations, shown in Figure 38, were designed to be loaded by four point bending. The first configuration (A) was designed with graphite/epoxy faces laid up to duplicate the tension and compression caps of the straight section of curved frames 1 and 2. The second configuration (B) was designed similar to configuration (A) except 3 plies of 0/90 graphite fabric were added to the compression face as shown in Figure 38B. The third configuration (C) was similar to configuration (A) except 1 ply of 0° graphite/epoxy tape and 2 plies of ±45° graphite/epoxy fabric were added to the compression face. Two beams of each configuration were fabricated and tested.

The ply orientation using the 0° graphite/epoxy tape and the 2 plies of ±45° graphite epoxy fabric were selected as a candidate to increase the strength of the straight portion of the frame. The 0° tape decreases the overall axial compression stress and the 2 plies of ±45° produce a transverse compression stress through the thickness of the frame cap.

A prediction of the axial compression strain (ε_c) and the transverse tensile strain (ε_T) on the thin edge of the graphite/epoxy face was made for configuration A prior to strain gaging each honeycomb beam and testing. At a load P, of 3000 lbs., the bending moment M, in the 4 inch test section (see Figure 39) is (3000/2) x 8.5 = 12,750 in. lbs. The compression load is:

$$P_c = \frac{M}{d} = \frac{12750}{1.125} = 11333 \text{ lbs.}$$

The compression stress is:

$$f_s = P/A = 11333/2.0 \ (.118) = 48,021 \text{ psi}$$

The effective axial modulus E_A of this layup was 10.1 X 10^6 psi.

The axial strain, ε_c = 48021/10.1 X 10^6 = 4754 μ in./in.

The transverse tensile stress in the epoxy at the overall axial compression stress of 48,021 psi, was estimated to be 8000 psi, based on the 3-D analysis. Assuming a modulus of 1.5 X 10^6 psi for the epoxy resin, the strain ε_T, would be 8000/1.5 X 10^6 = 5330μ in./in. The predicted strains are shown in Figure 39.

73

Two small strain gages were bonded to the edge of the compression face of the honeycomb beams as shown in Figure 39. Each gage had a gage length of .79 mm (0.031 inches). All beams were loaded by four point bending to fracture.

6.4 TEST RESULTS

The strain gage data for each honeycomb beam configuration is shown in Figure 39. The transverse gage substantiated the 3-D finite element analysis.

A fracture in the compression face was obtained, as shown in the photo of Figure 40, for configuration B. The fracture was similar to the frame fracture shown in Figure 30.

6.5 CONCLUSIONS FROM HONEYCOMB BEAM TESTING

1) A combined axial and transverse strain caused the fractures in the straight sections of frames 2 and 3.

2) The 3-D finite element analysis predicted transverse strains at the free edge. The test data substantiated the analysis.

3) The use of ±45° graphite/epoxy fabric reduced the transverse tensile strain and eliminates the splitting problem.
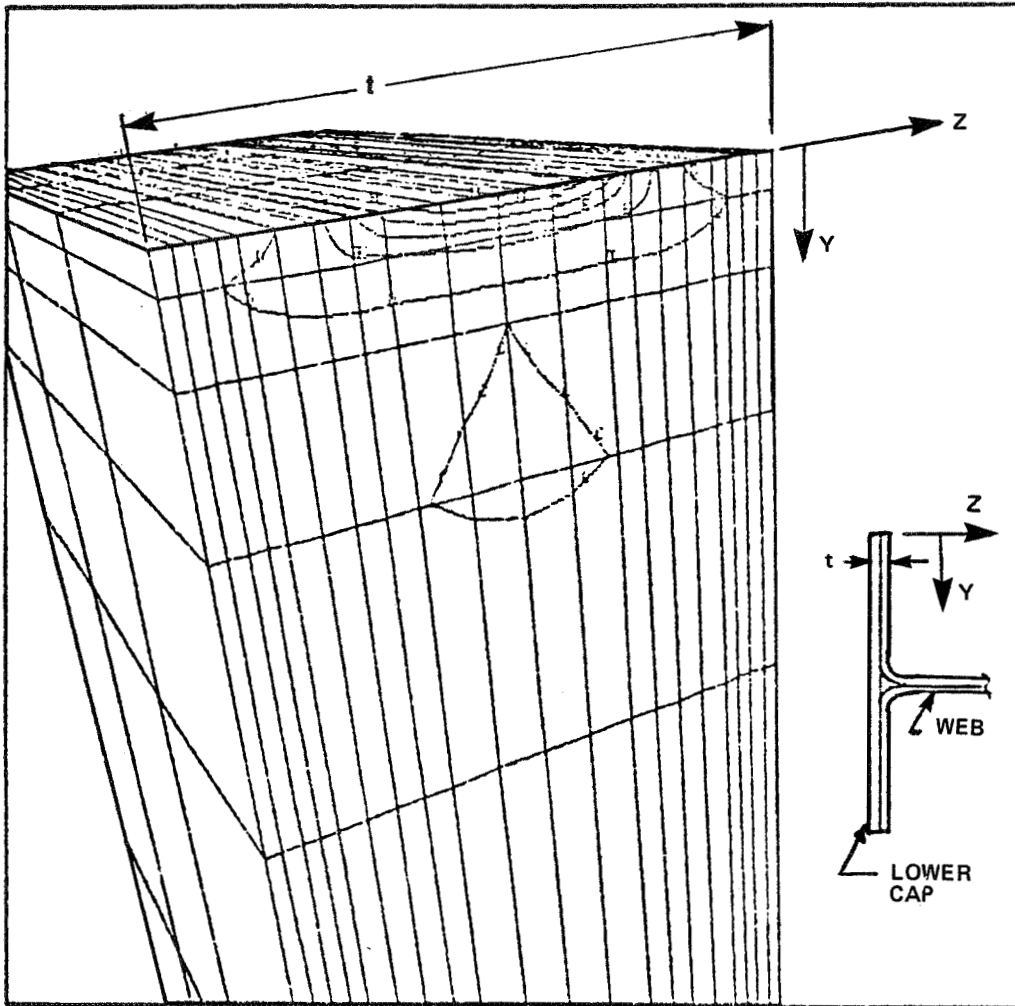
MAX σ_Z = 11,315 PSI

@ ϵ_X = .010 IN/IN

Figure 34.   Transverse Stress Contours through
Flange Thickness (Basic Lay-up)
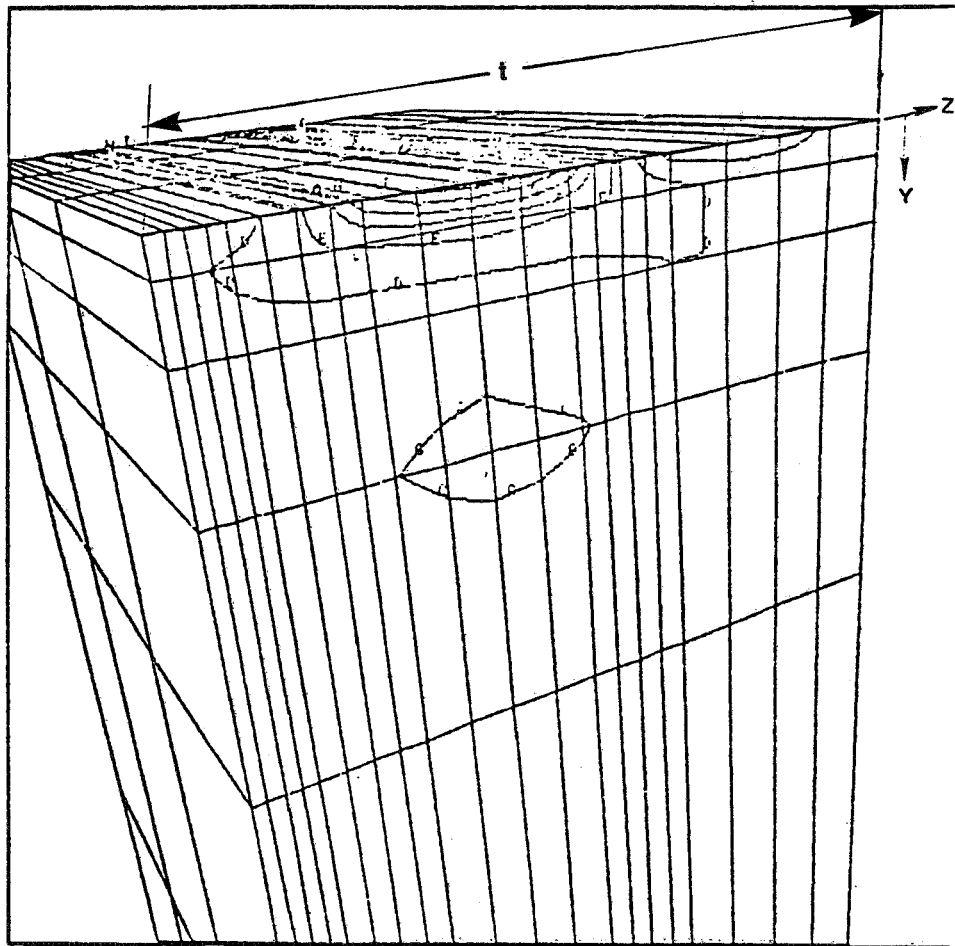
MAX σ_Z = 11,986 PSI
@ ϵ_X = .010 IN/IN

Figure 35.   Transverse Stress Contours Through Flange Thickness
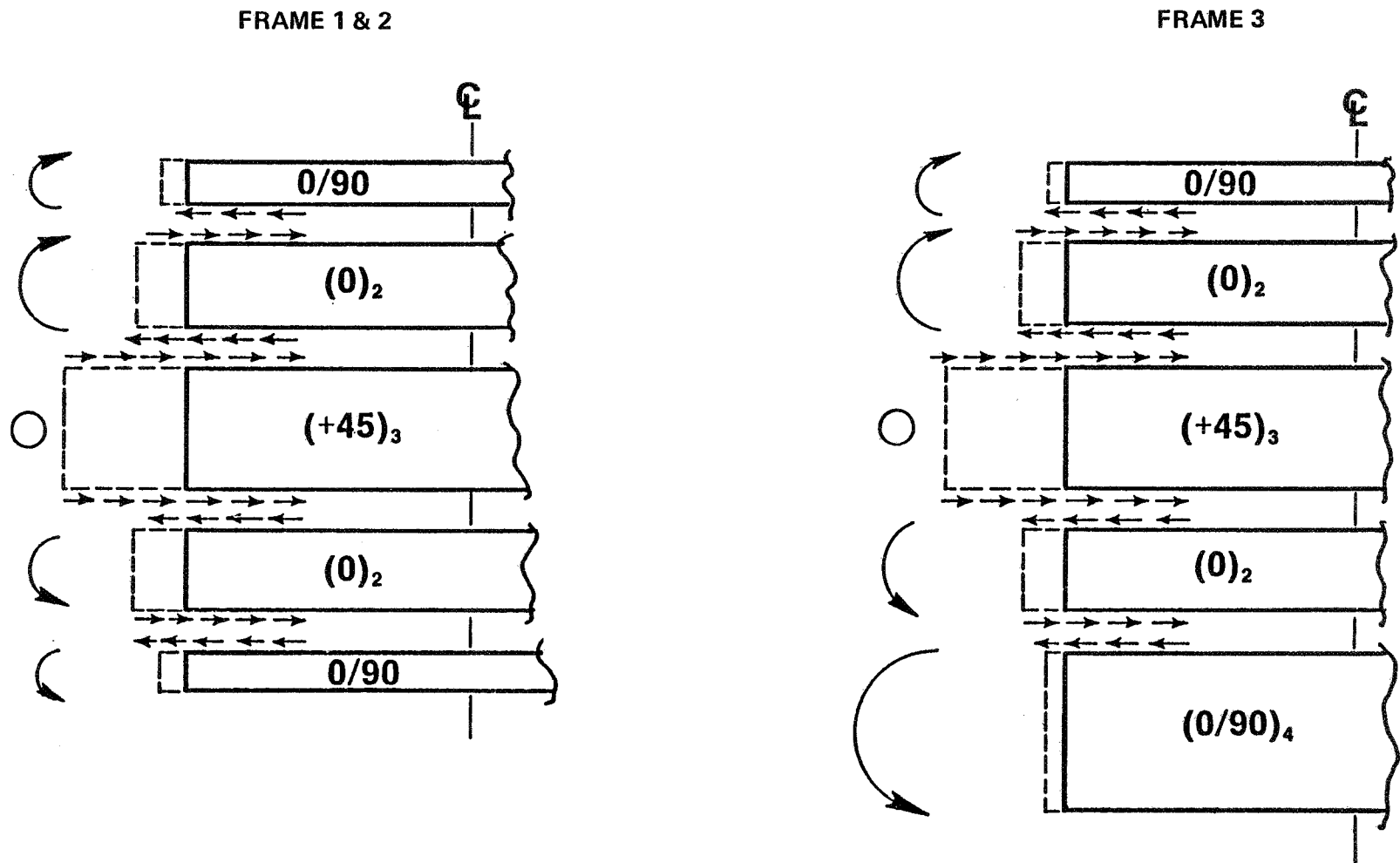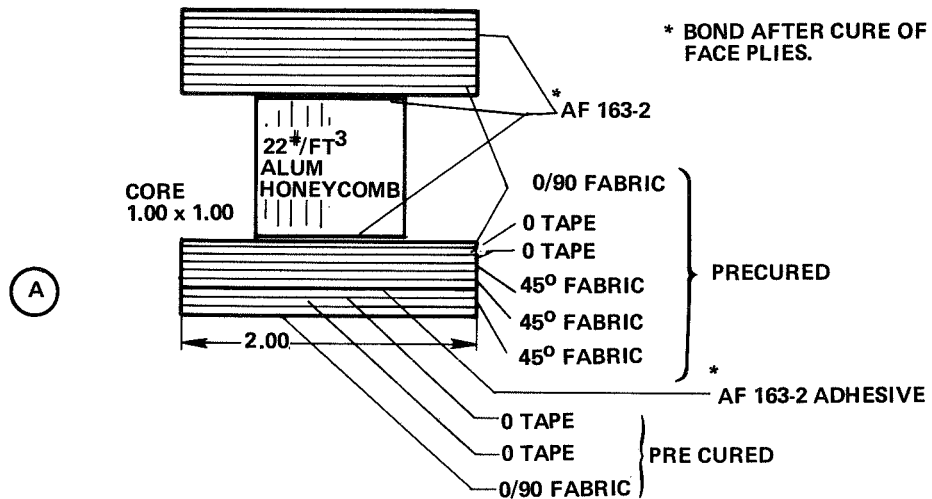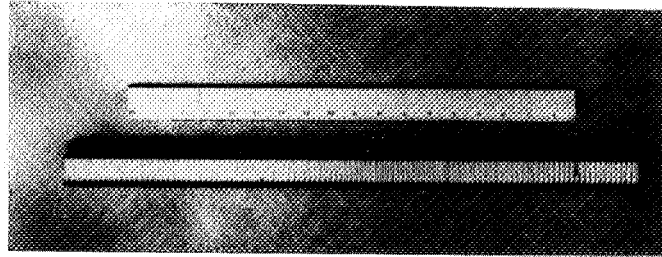   Thickness (Basic Lay-up plus 3 plies 0/90° Graphite)
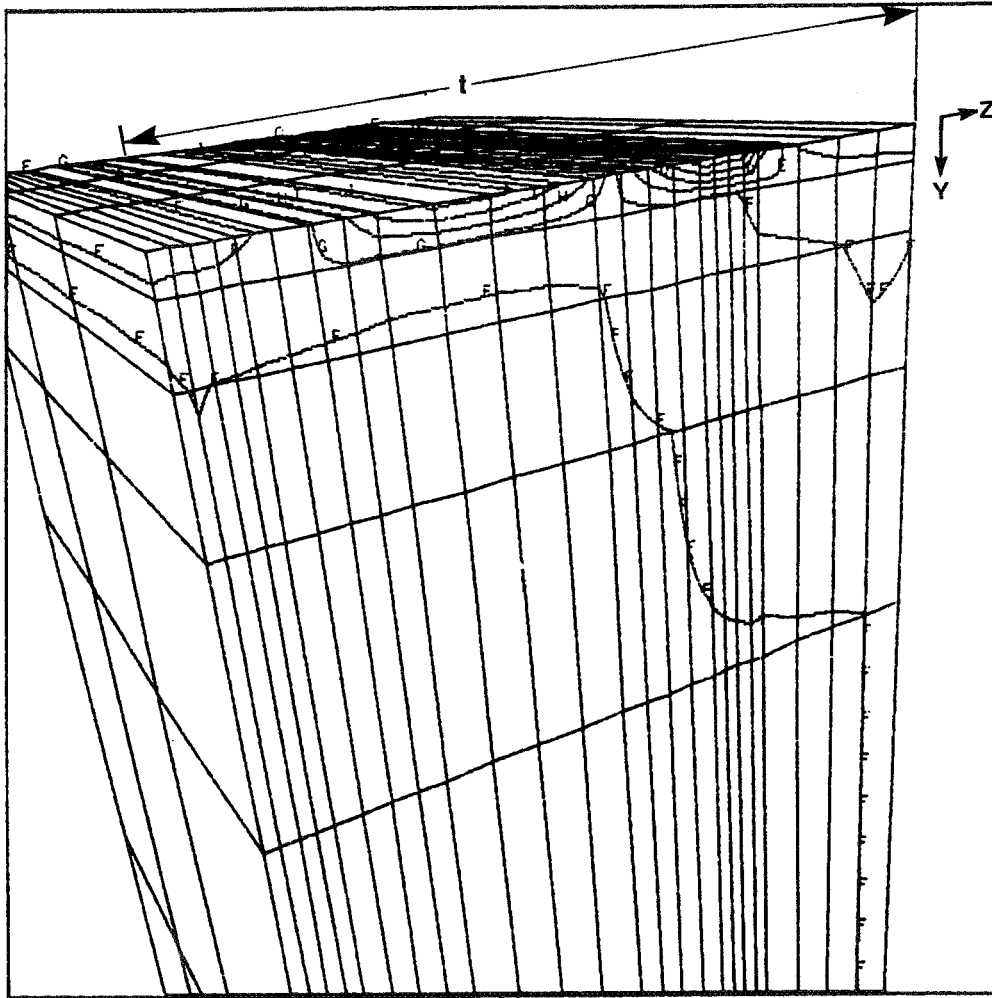
MAX σ_Z = −11352 PSI
@ ϵ_X = .010 IN/IN

Figure 36. Transverse Stress Contours Through Flange Thickness
(Basic Lay-up Plus 3 Plies 45° Graphic Fabric)

FRAME 1 & 2

FRAME 3

0/90

(0)₂

(+45)₃

(0)₂

0/90

0/90

(0)₂

(+45)₃

(0)₂

(0/90)₄

Figure 37.   Poisson Effect Induces Edge Peel Stresses

* BOND AFTER CURE OF
FACE PLIES.

AF 163-2

22 #/FT^3
ALUM
HONEYCOMB

CORE
1.00 x 1.00

0/90 FABRIC ⎫
0 TAPE
0 TAPE
45° FABRIC ⎬ PRECURED
45° FABRIC
45° FABRIC ⎭

A

2.00

* AF 163-2 ADHESIVE

0 TAPE ⎫
0 TAPE ⎬ PRE CURED
0/90 FABRIC ⎭

3 PLY 0/90 G./E FABRIC DRY, EA956 RESIN, ROOM
TEMP. CURE & BAG TO ASSEMBLED BEAM (24 HOUR ROOM
TEMP. CURE)

45° ⎫ MAT'L.
45° ⎬ FABRIC
0° ⎭ TAPE

B

C
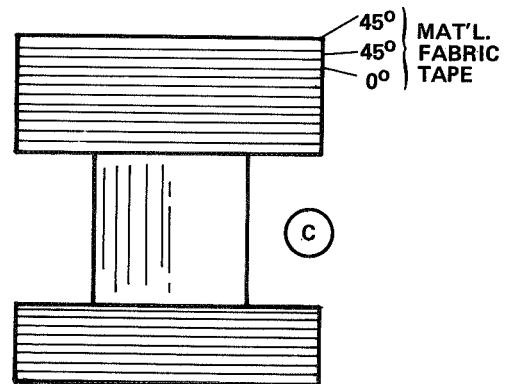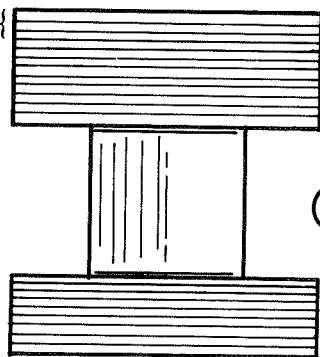
Figure 38. Honeycomb Test Beam Elements

79
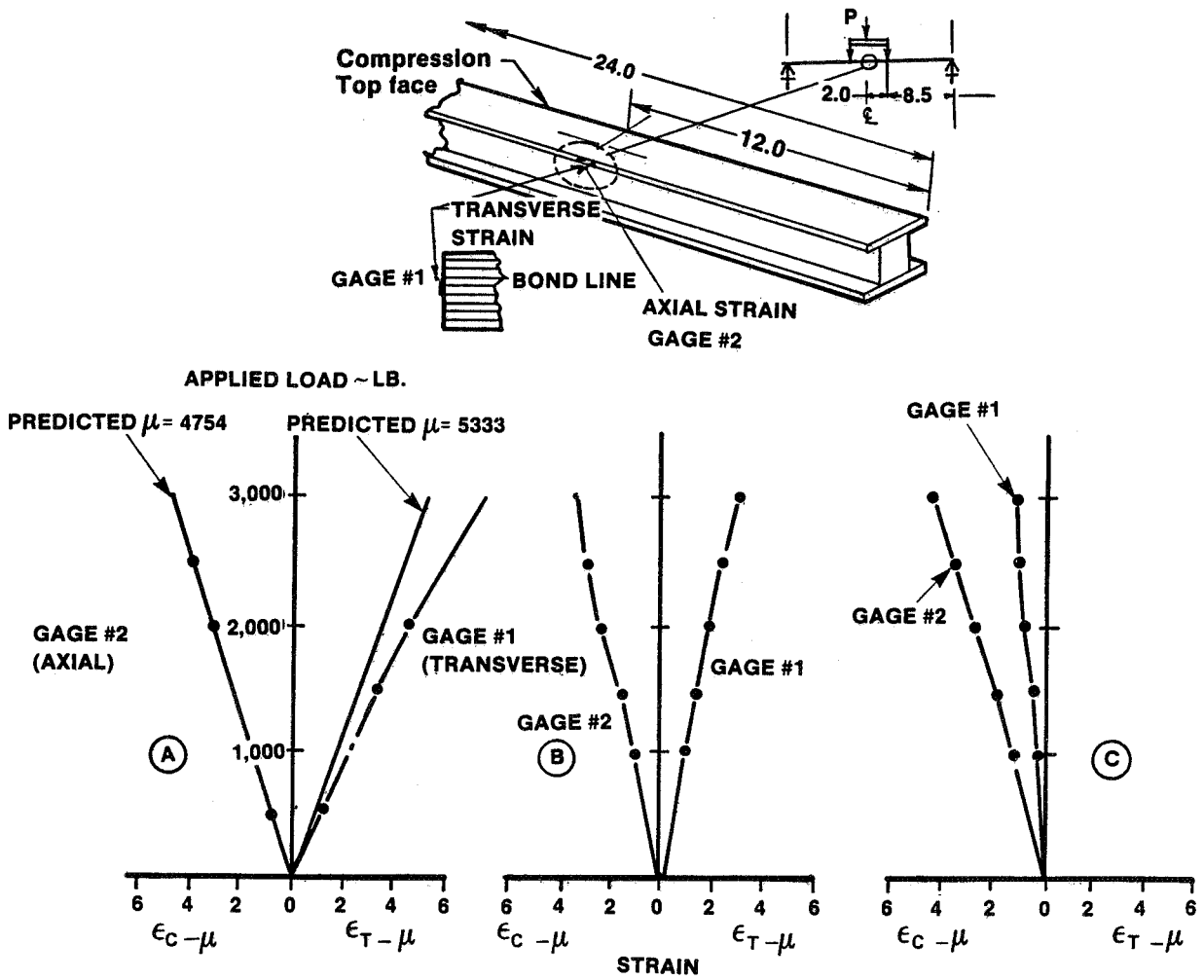
Figure 39. Element Test Results Confirm Edge (Peel) Effects
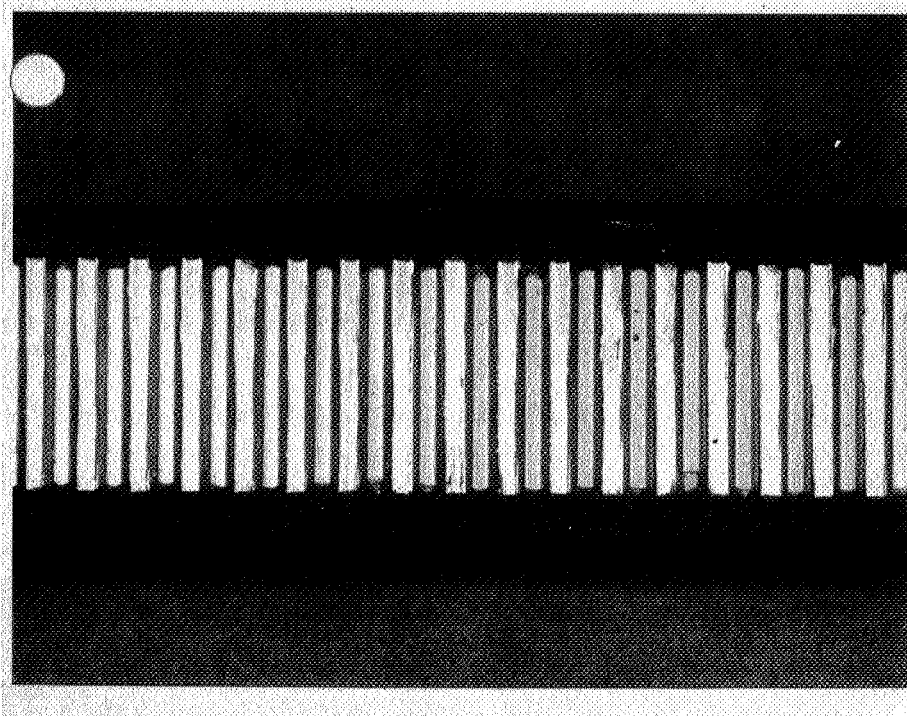
Figure 40.   Fractured Compression Face of Honeycomb
             Beam Configuration B

7.0 COMPOSITE FRAMES REINFORCED IN THE STRAIGHT SECTION

Two composite curved frames (frame numbers 4 and 5) were fabricated per drawing EWR55187 Revision E, based on the results of the data from the honeycomb beams. Strain gages were installed as shown in Figure 22.

Each frame was statically loaded to fracture. Both frames fractured in the curved section. Frame No. 4 fractured at an applied load of 33.3 kN (7600 lbs) or 71% of design load. Frame No. 5 fractured at an applied load of 37.8 kN (8500 lbs) or 80% of design load. A preliminary review of the strain data plotted during the tests of both frames indicates that the cause of the fracture was due to the inner (compression) cap and beaded stiffeners becoming unstable.

The instability that developed is indicated by the strain plots in Figures 41 and 42 of gages TS-2 and TS-3 on the compression caps of both frames. Gages TS-5 and TS-6 on the beaded stiffener of both frames, Figures 43 and 44 also indicated instability. These plots were developed by the Hewlett Packard 9825-T desk top computer and 7225A graphics plotter as each test was in progress.

Since the frames, numbers 4 and 5, fractured at loads lower than frame number 2, it was decided to compare the lay-up in the stiffener/web/compression cap area of each frame. Microphotographs shown in Figures 45, 46, and 47 were obtained for the radius in the transition between the stiffener/web and inner cap of each frame.

From the microphotographs there appears to be a difference in the thickness of the lay-up in the radius of each frame. If the effective modulus of the lay-up is assumed approximately equal for each frame, then the load at which the strains of each bead started to deviate would be a function of the square of the thickness through the radius. Table VI summarizes the load at strain deviation of the stiffeners and the measured thickness in the transition. Figure 48 is a plot of load at bead strain deviation as a function of the radius thickness squared.

The differences in the thickness of the stiffener/web/cap radii appear to be caused by the method of laying the ply materials into the channel mold. A teflon tongue depressor was used to position each ply into the corners of the mold. Several people, laying-up a total of twelve channels (two for each frame) would result in uneven pressure being applied with the tongue depressor to the corners of the mold.
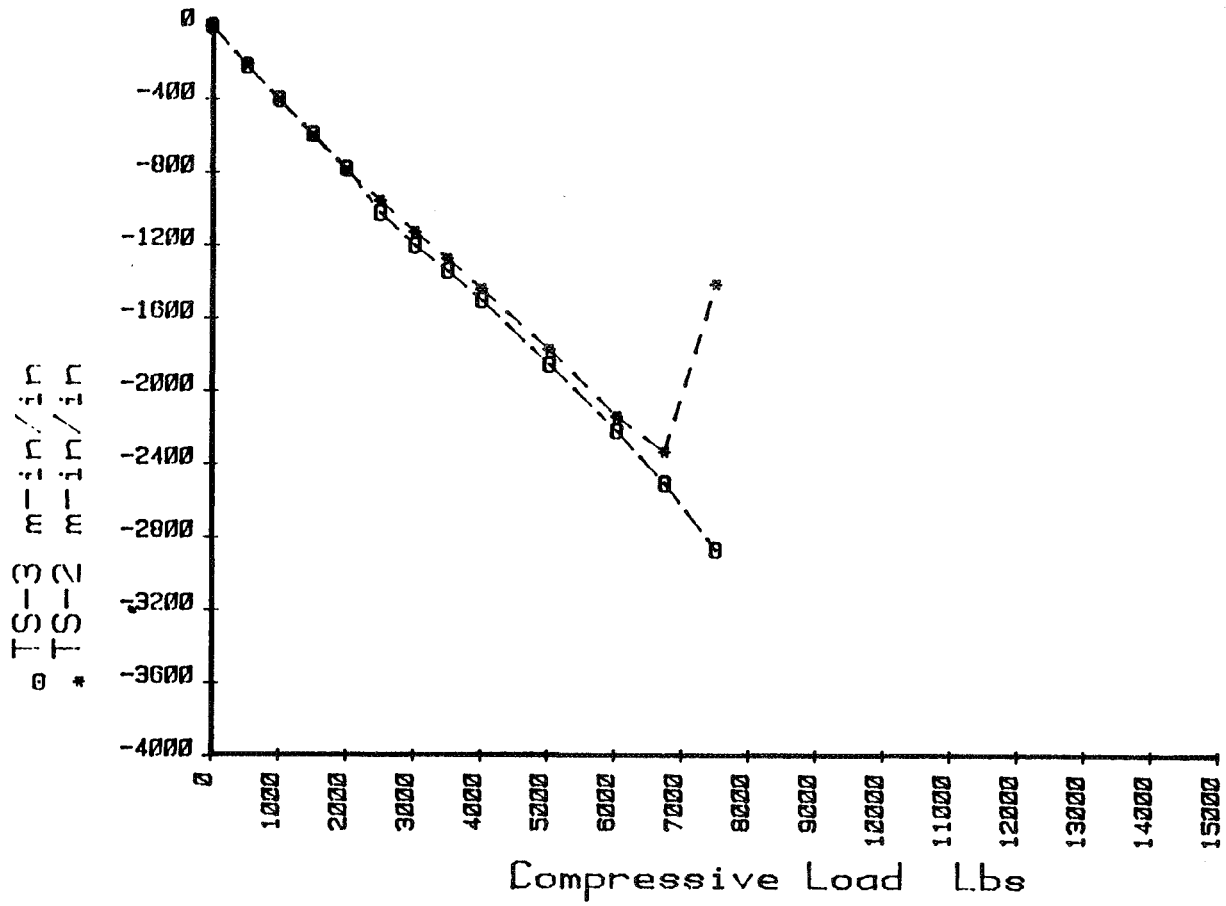
82

Figure 41 Specimen No. 4 Rev. E,
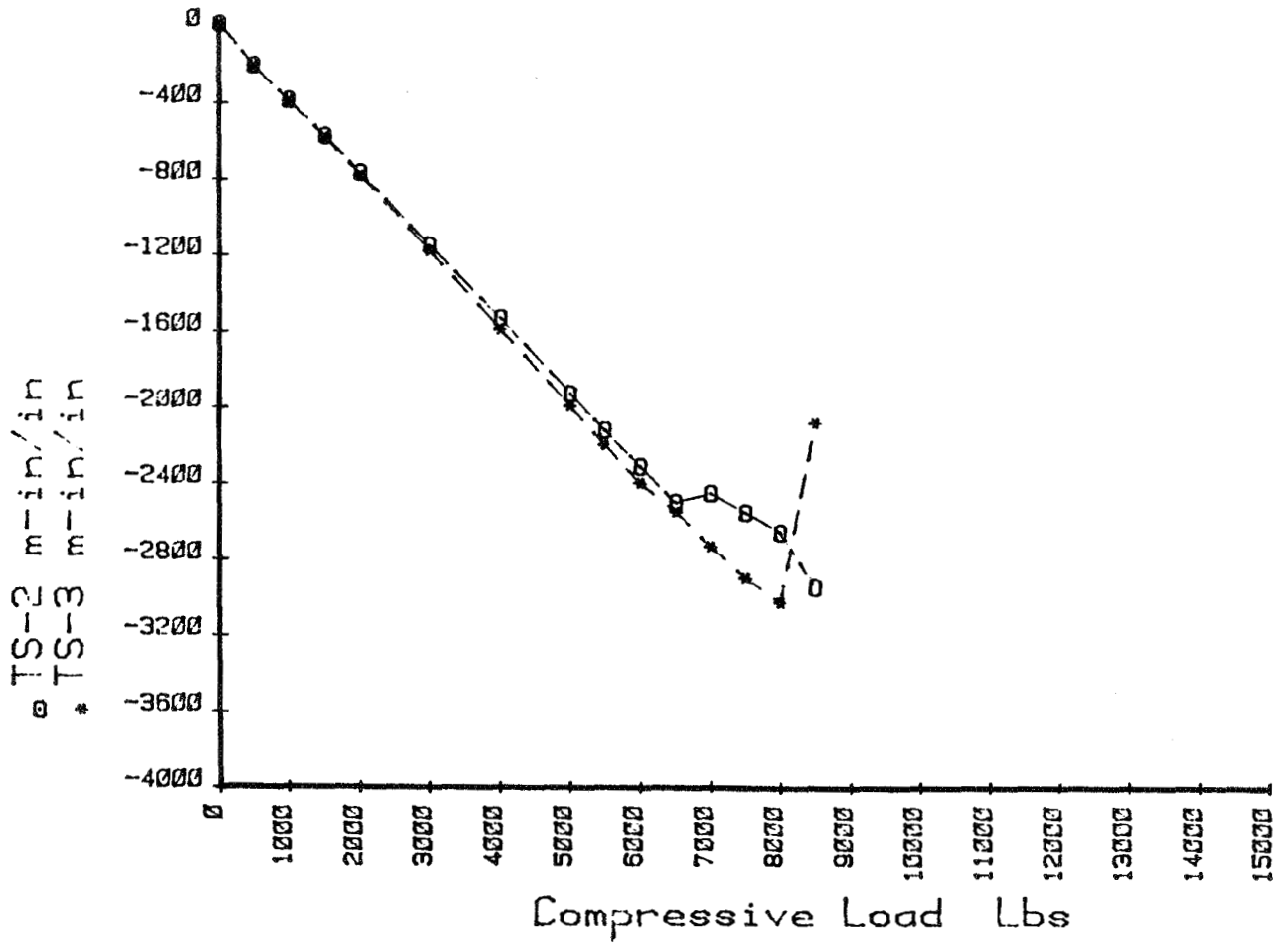Compression Cap Strains -
Gages TS-2, TS-3

83

Figure 42 Specimen No. 5 Rev. E,
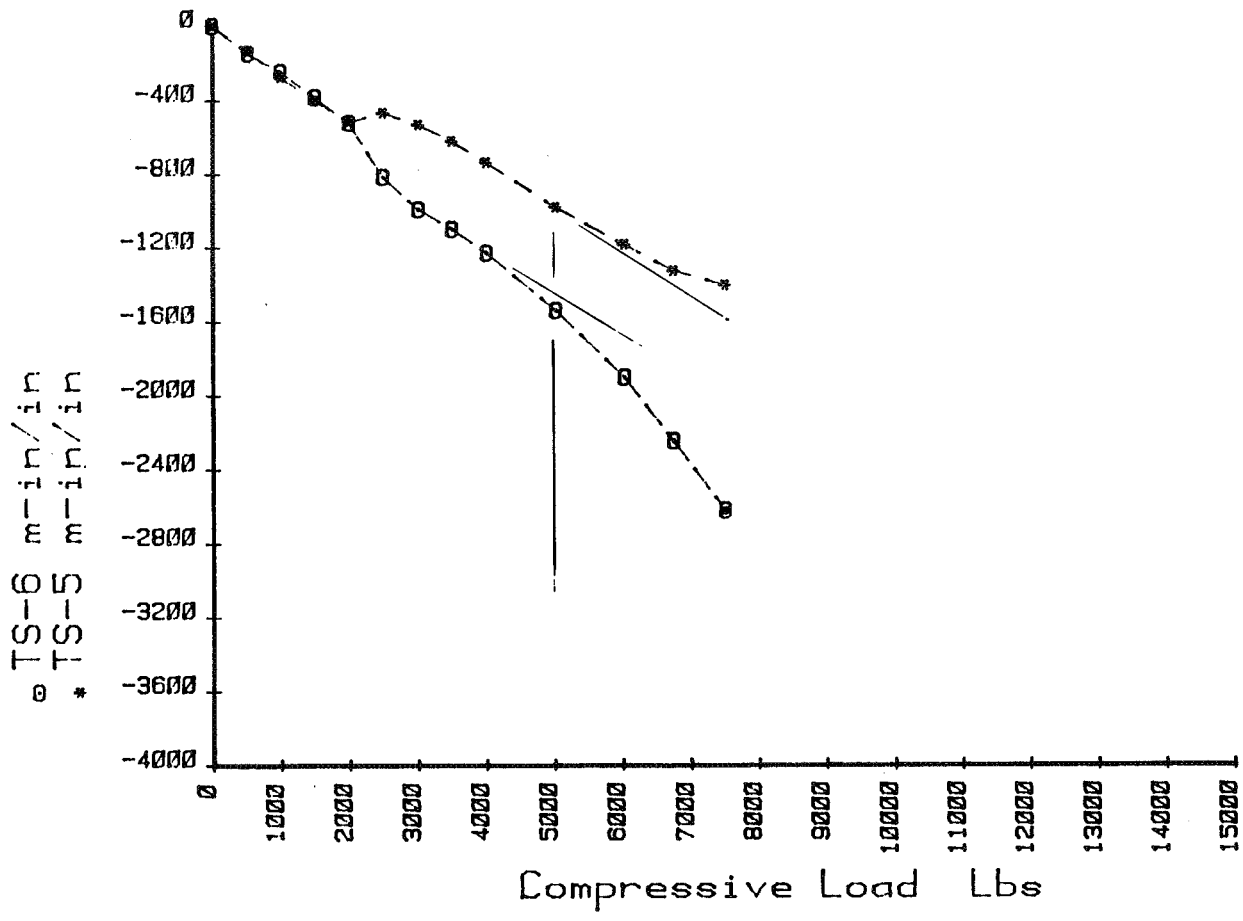Compression Cap Strains -
Gages TS-2, TS-3

84

Figure 43 Specimen No. 4 Rev. E,
Beaded Stiffener Load -
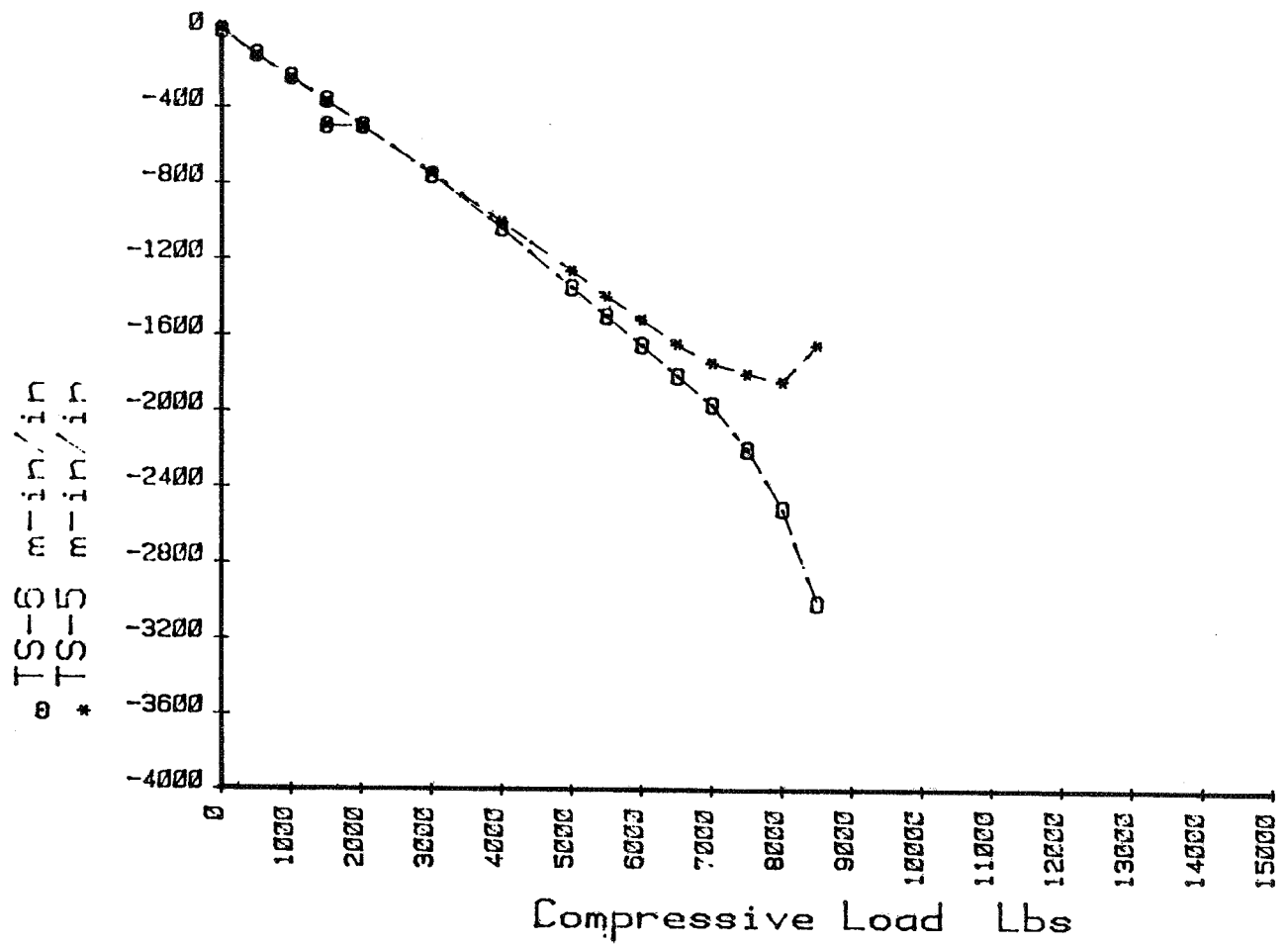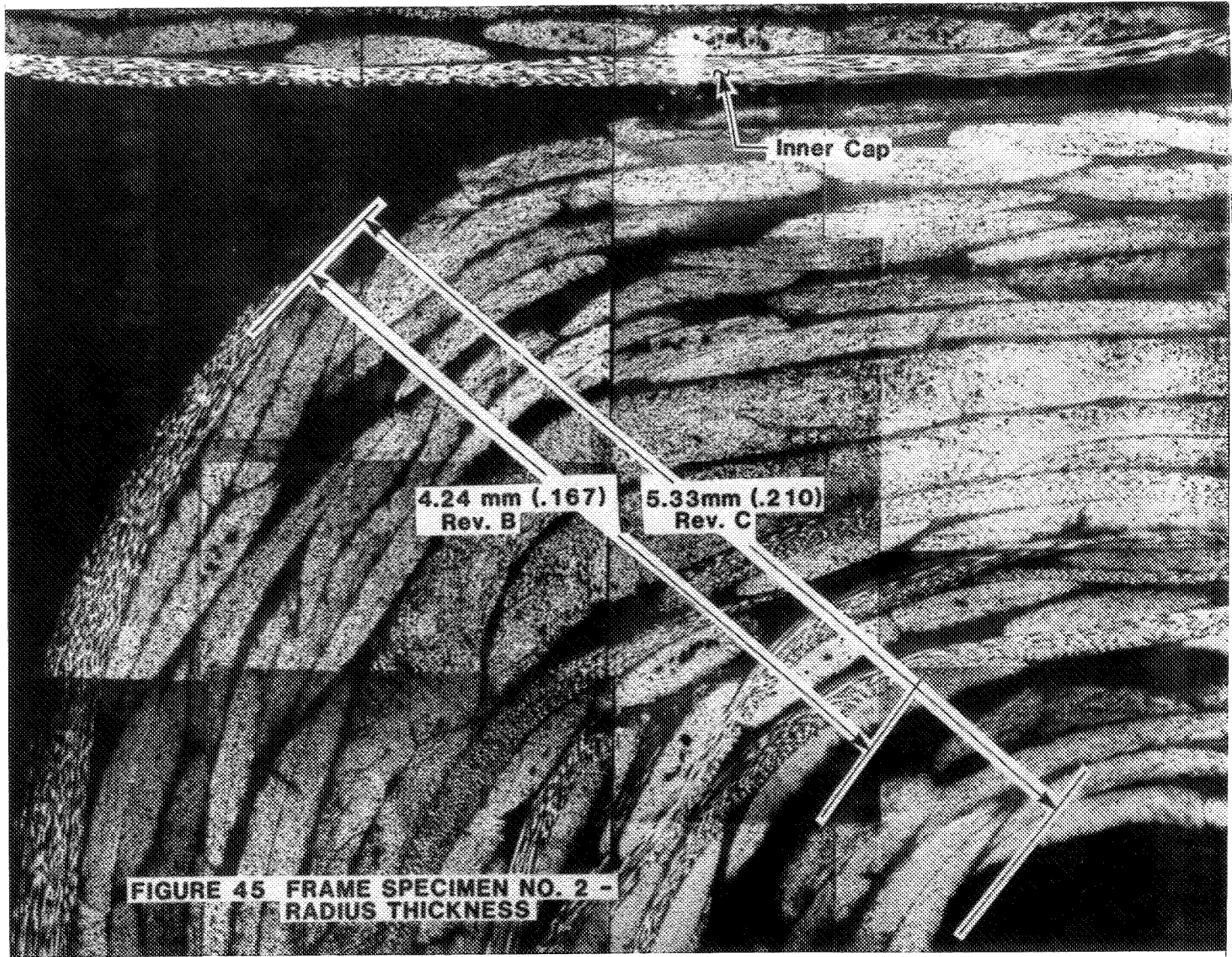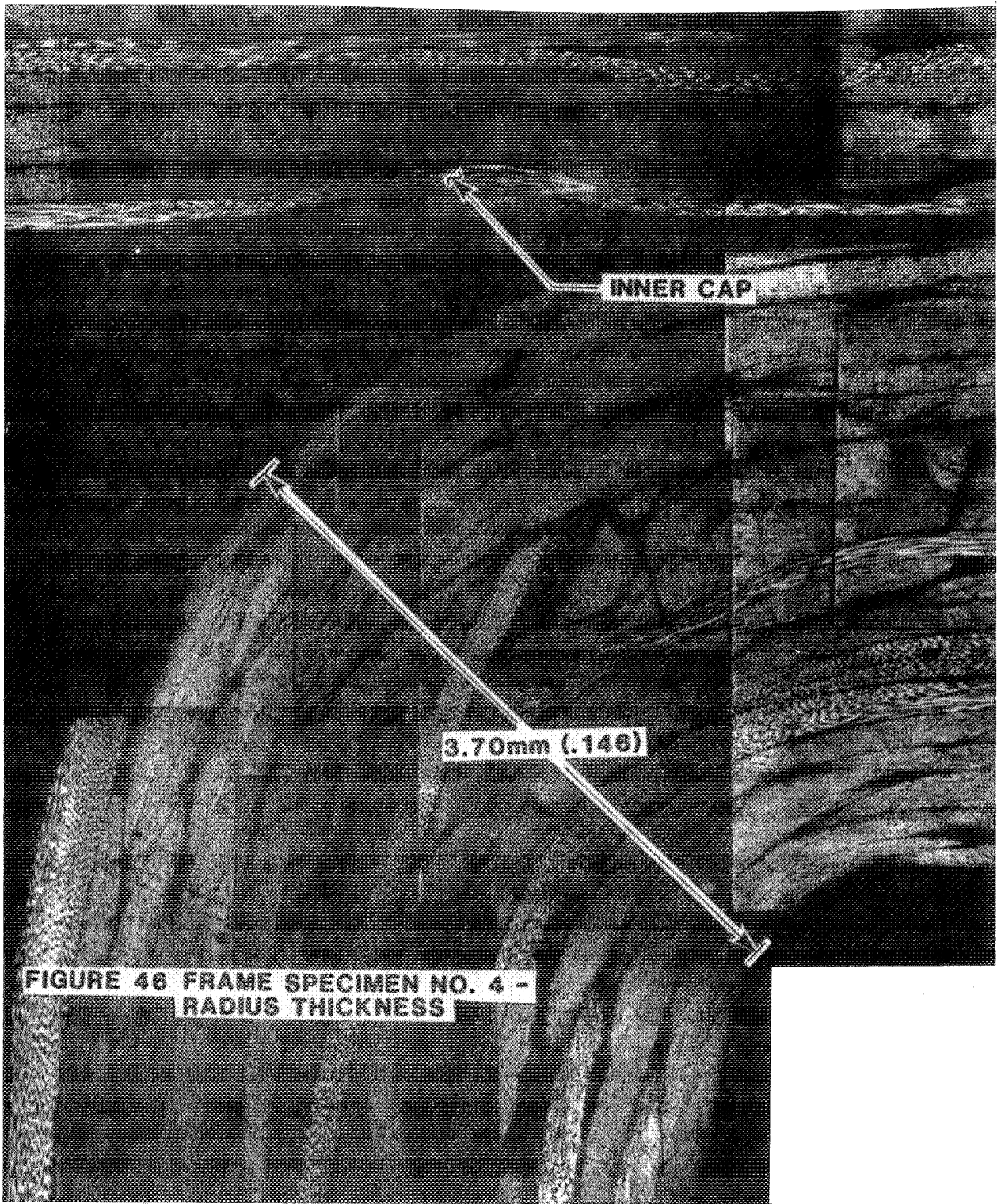Strain Data (Hewlett Packard
9825-T Computer Plot)

Figure 44 Specimen No. 5 Rev. E,
Beaded Stiffener Load -
Strain Data (Hewlett Packard
9825-T Computer Plot)

Inner Cap

4.24 mm (.167) Rev. B

5.33mm (.210) Rev. C

FIGURE 45 FRAME SPECIMEN NO. 2 –
RADIUS THICKNESS

INNER CAP

3.70mm (.146)

FIGURE 46 FRAME SPECIMEN NO. 4 - RADIUS THICKNESS
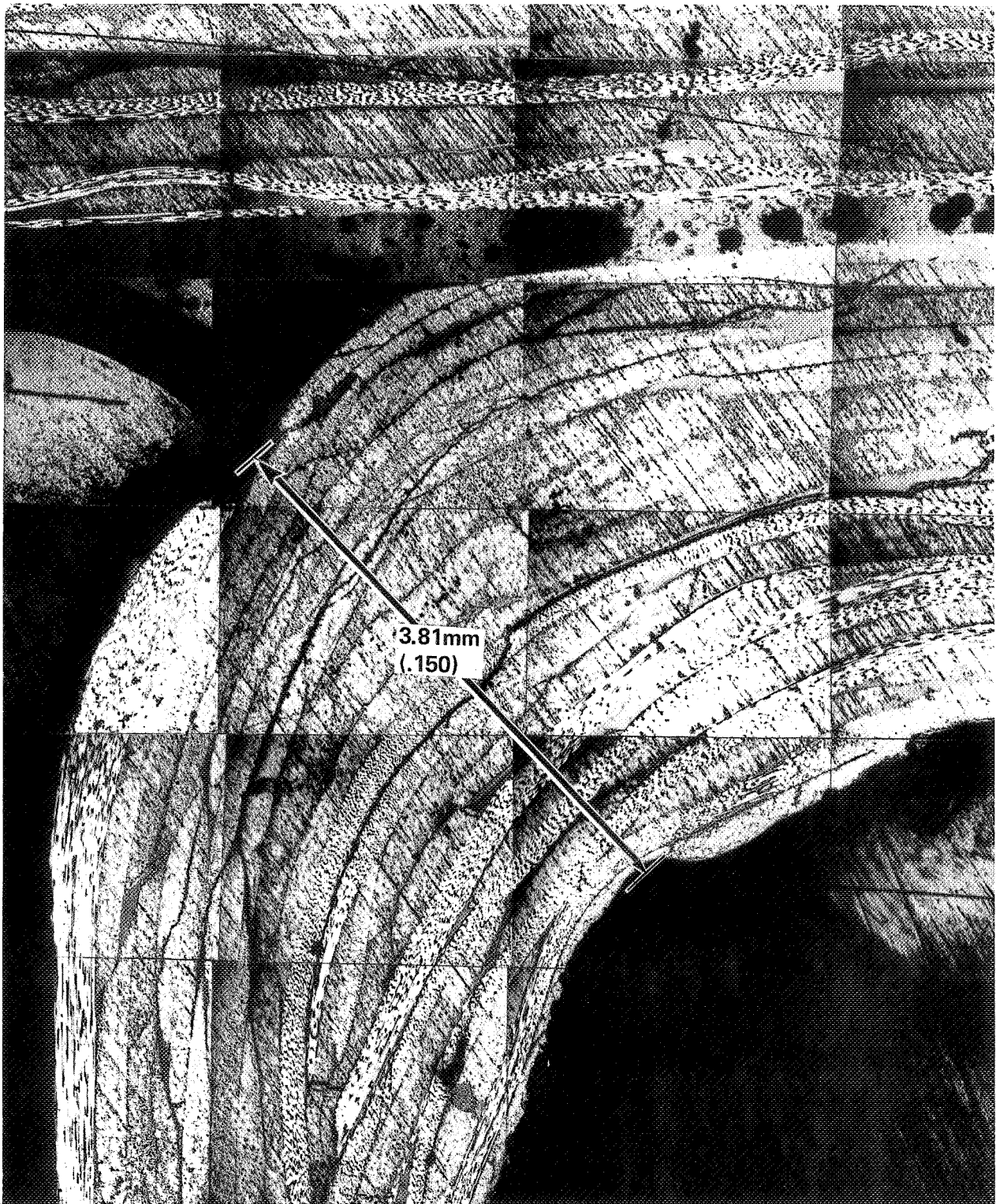
Figure 47   Frame No.5 - Radius Thickness

TABLE VI. BEADED STIFFENER DATA SUMMARY

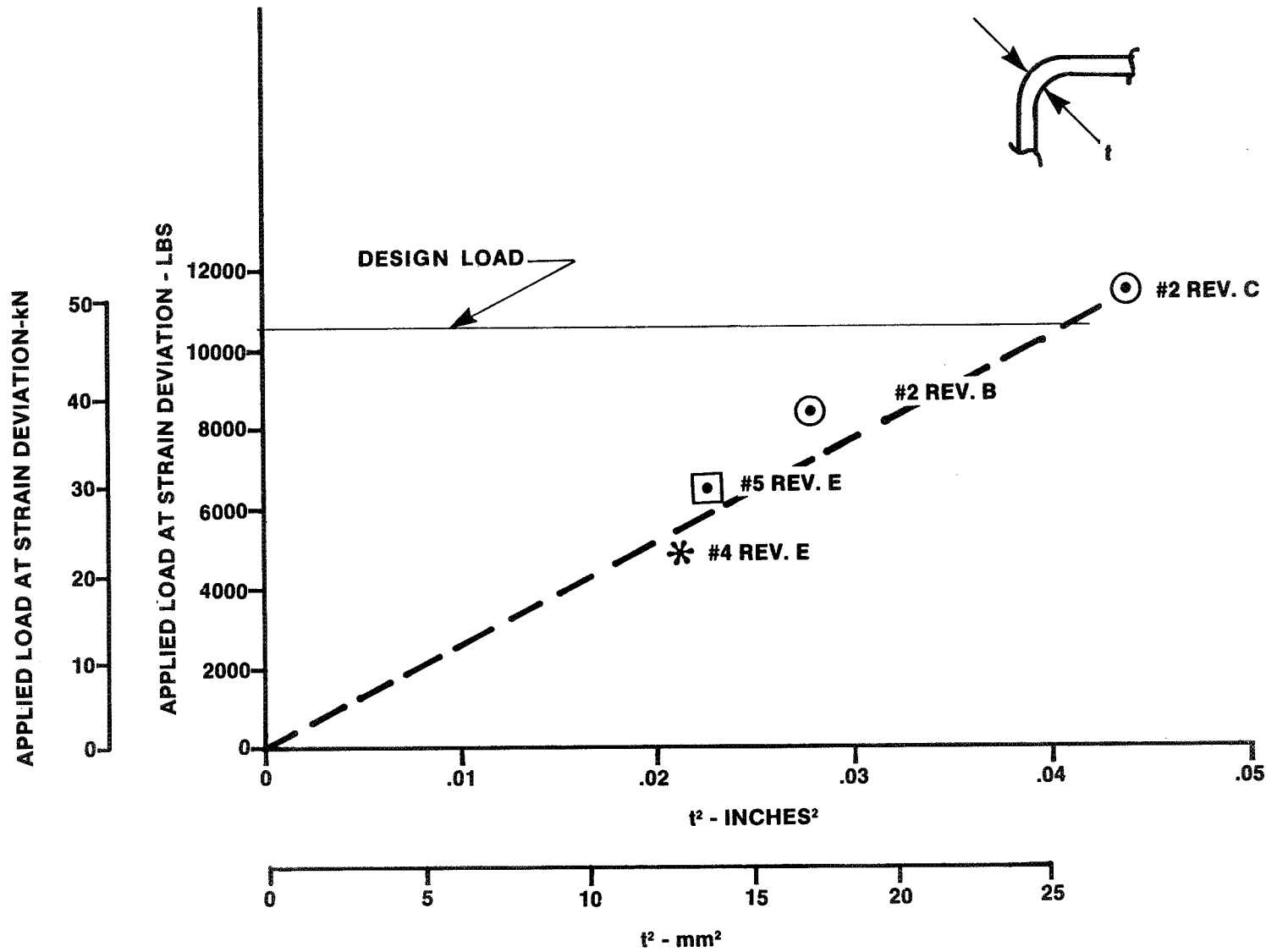| SPECIMEN	LOAD AT STRAIN DEVIATION OF BEADED STIFFENER	RADIUS t	t^2
No. 2 Rev. B	37.81 kN (Fig. 31)	4.24 mm (Fig. 45)	17.97 mm^2
No. 2 Rev. C	49.37 kN (Fig. 31)	5.33 mm (Fig. 45)	28.41 mm^2
No. 4 Rev. E	22.24 kN (Fig. 43)	3.70 mm (Fig. 46)	13.69 mm^2
No. 5 Rev. E	28.91 kN (Fig. 44)	3.81 mm (Fig. 47)	14.52 mm^2

Figure 48. Load at Bead Strain Deviation as a Function of Radius Thickness

8.0 CORRELATION OF ANALYSIS AND TEST

Prior to conducting static tests to fracture of each frame, a prediction of the maximum strain was determined based on the NASTRAN analysis. The maximum strain, from the NASTRAN analysis, was located on the inner (compression) cap, at the center line of the "I" section above the center bead. The purpose of the prediction was to monitor the performance of each frame, the loading fixture, the strain gage, and to warn test personnel of impending fracture. The strains, predicted by NASTRAN, correlated very well in the linear range, as shown in Figures 24, 28, and 32.

Axial strain distributions, across the flange, were obtained in the curved and straight sections during testing. The correlation with the NASTRAN analysis for the curved section is shown in Figure 49A. The strains in the straight section during testing are shown in Figure 49B.

There were some questions on whether the peaking of the axial stress distribution would be reduced as the load went past the nonlinear load strain region. A measure of the effect would be the ratio of the gage 1 (at the centerline) to gage 3 (most outboard) strains. These ratios are presented in Figure 50 and indicate an increase in the axial strain ratios. This increase is opposite to that which would be expected for metals where plastic relief would reduce strain ratios.

The transverse strain was measured at gage no. 7. The NASTRAN-predicted and the test-measured strains are shown in Figure 51. The analysis appears to adequately predict the induced transverse stress.

8.1 Finite Element Study

In order to assess the Bleich stress ratios a finite element analysis was conducted on the curved frame structure. The structure was transferred to aluminum with variations of the flange thickness from 1.27 mm to 7.62 mm (.05 to .30 inches). The average free flange distance, including effects of the web stiffening, was 15.24 mm (.60 inches) and used in the flange flexibility parameter calculations.

The calculated ratios of maximum axial and maximum transverse-to-nominal axial stress are plotted in Figure 52. The NASTRAN results are similar to the Bleich values shown in Figure 1. The axial ratios are almost the same, but the NASTRAN values are well below the Bleich predictions for transverse bending.

The analysis and test data (Frame No. 2, Rev. C) relate to a flange flexibility value of .225. However, it should be noted that the flange axial modulus, for the composite frame, is over twice the transverse modulus. A comparative summary of the NASTRAN analysis, Bleich analysis and Composite Curved Frame test results is presented below.

	Bleich Analysis	Aluminum Frame NASTRAN Analysis	Composite Frame NASTRAN Analysis	Composite Frame Test
$\dfrac{\sigma_{x,MAX}}{\sigma_x}$	1.03	1.03	1.34	1.25
$\dfrac{\sigma_{b,MAX}}{\sigma_x}$	.65	.56	.70	.71
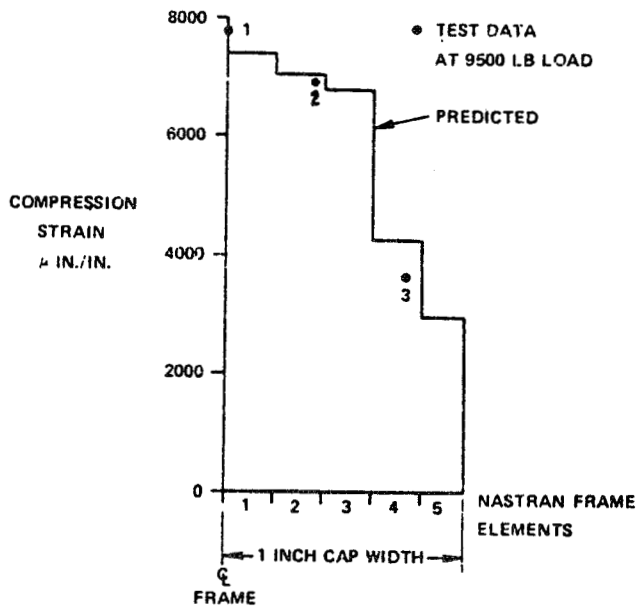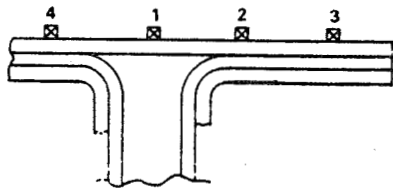
A. CURVED SECTION
NASTRAN CORRELATION
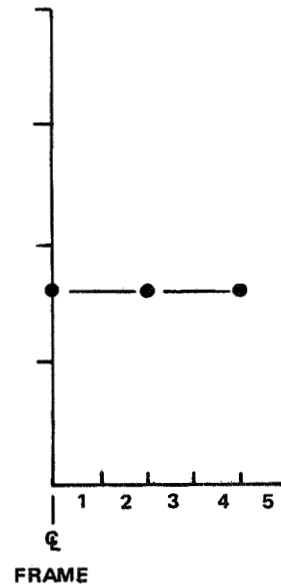
B. STRAIGHT SECTION
TEST DATA

Figure 49.   Compression Cap Strains Across Half Cap Width —
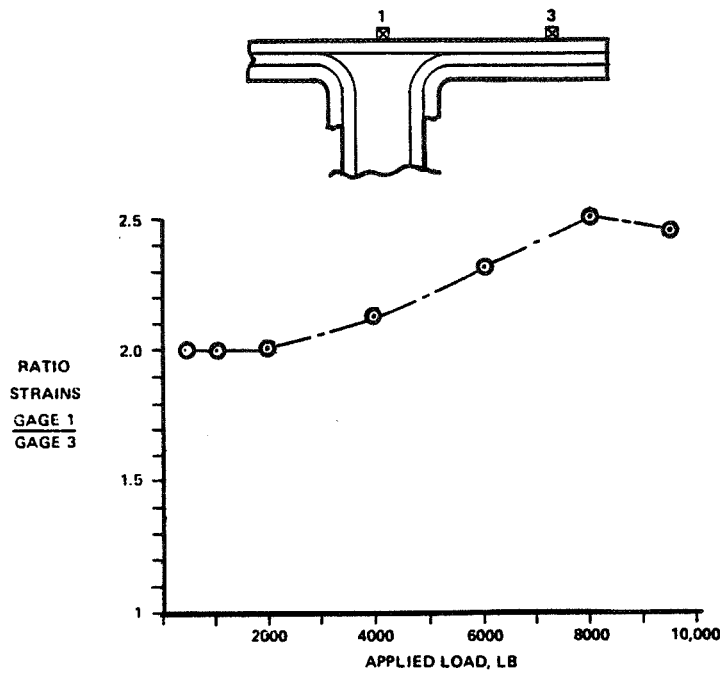Frame No. 2 Rev. C

94

Figure 50. Axial Strain Ratio Increases with Applied Load
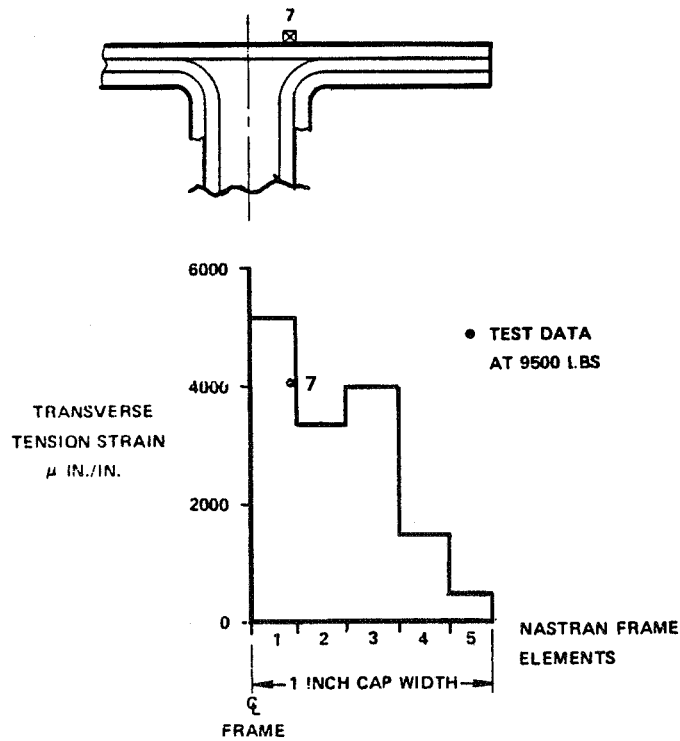

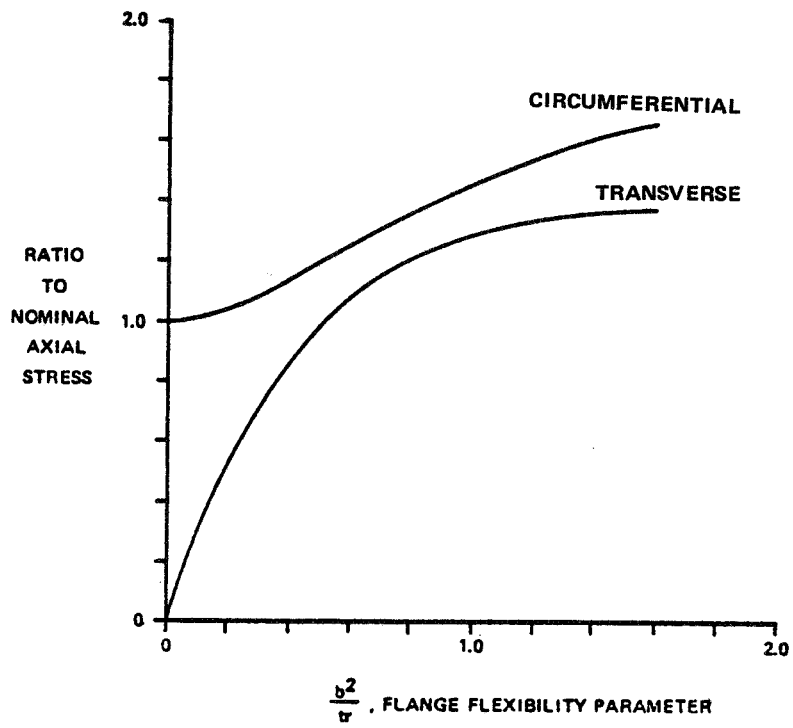Figure 51. Transverse Bending Strain
(Tension Side)

Figure 52. NASTRAN Analysis, Aluminum Frame

9.0 CONCLUSIONS

Based upon the design, analysis, fabrication and testing of the five composite curved frames the following conclusions are given:

1. The Bleich solution can be used to determine the preliminary sizing and lay-up for curved frames of composite materials.

2. The NASTRAN analysis can predict, with good accuracy, the strain distributions in the composite curved frame.

3. The fracture of Frame Specimen Number 1 (Rev. B) in the curve, was due to the beaded stiffeners becoming unstable. The stiffeners became unstable due to high stresses in the stiffener/web/cap radius interface. The compression strains in the beaded stiffeners were well below fracture strains for the materials used.

4. The beaded stiffeners of Frame Number 2, Rev. B became unstable and the testing was stopped. The radius interface was reinforced and the curved section (Rev. C) sustained a load 101% of the design load when the frame fractured in the straight section. The beaded stiffeners were stable due to the reinforcements. Bead compression strains were low.

5. The fractures of Frame Specimens Number 2, Rev. C and No. 3, Rev. D, in the straight section were not caused by crippling as originally believed. The cause of fracture was due to transverse strains through the flange thickness. The analysis, design and testing of the honeycomb beams substantiated the transverse strain effects.

6. The fractures of Frame Specimens Number 4 and 5, Rev. E, in the curve, were caused by the bead stiffeners becoming unstable. Although the lay-up in the radius was similar to Revision C requirements, the overall thickness was less or equal to Revision B requirements, and this caused the stiffener to become unstable. Stiffener strains were low.

7. The fracture of all frames tested was caused by instability from geometry and lay-up of materials. There appears to be enough material in the frames for the frames to fracture at the fracture strain of the materials, provided stability is maintained, and a 3-D analysis is performed if crippling is suspected.

97

10.0 RECOMMENDATIONS

The following studies are recommended:

1. Based on the current data, develop design/analysis data for composite curved frames.

2. Although this program concentrated on the crushing of webs and stiffeners of composite curved frames a program should be conducted to determine the effects of reverse loading on the curve. A reverse loading in the NASTRAN model would result in a sign change for all strains. No additional graphite epoxy material may be required. However the frame caps in the curve would develop a reversed edge deflection (deflecting away from the frame) and this may result in high peel strains which could separate the two cap strips from the two channel sections.

3. A study is recommended to determine criteria for the design of the interface between frame webs and caps in a curved frame structure. Also a method of fabrication is recommended to provide required thicknesses through the interface.

11.0 REFERENCES

1. Seely, F. and Smith, A., Advanced Strength of Materials, John Wiley and Sons, Inc. 1963.

2. Broughton, D., Clark, M., and Corten, H., "Tests and Theory of Elastic Stresses in Curved Beams Having I and T-Sections", Proceedings of the Society for Experimental Stress Analysis, Volume VIII, November 1, 1950.

3. Bertucio, W.: NASTRAN Model Load Analysis and Related Computer Programs, Vol. I of III, Sikorsky Engineering Report SER-70527, September 15, 1974.

4. Lowry, D.W., Kay, B.F., and Rich, M.J.: Study to Investigate Design, Fabrication and Test of Low Cost Concepts for Large Hybrid Composite Helicopter Fuselage - Phase IV, NASA Contractor Report 159384, February 1981.

5. Sikorsky Structures Manual, Revised 6/1/67.

6. Collings, T.A.: "The Strength of Bolted Joints in Multi-Directional CFRP Laminates", Composites, Volume 8, p. 43, January 1977.

7. DOD/NASA Advanced Composites Design Guide, Volume II, Analysis - Structures/Dynamics Division, Flight Dynamics Laboratory, Air Forace Wright Aeronautical Labortories, Wright-Patterson Air Force Base, Ohio, July 1983.